Tampere University

Noora Haapalainen

FUNCTIONALIZATION OF SYNTHETIC BONE SUBSTITUTE MATERIAL WITH COLLAGEN NETWORK AND BIOACTIVE MOLECULES

Master of Science Thesis
Faculty of Medicine and Health
Prof. Minna Kellomäki
Ariane Kuhnla
June 2021

Tampere University

ABSTRACT

Noora Haapalainen: Functionalization of synthetic bone substitute material with collagen network and bioactive molecules
Master of Science Thesis
Tampere University
Biotechnology and Biomedical Engineering
June 2021

There is an increasing need for bone transplants in bone related diseases, trauma, and tumours. At present time, autologous bone grafts, harvested from the patient's own body, have been considered as the "gold standard" for bone regeneration. However, autografts bear an increased risk because of the need for second surgery and the donor site morbidity. Therefore, the need for innovative solutions that support the bone regeneration and provide an ideal environment for bone tissue regeneration is high. To overcome challenges related to conventional bone grafts, a field of science, namely bone tissue engineering, aims to create three-dimensional porous scaffolds to integrate with the host tissue without harmful reactions.

The aim of the thesis was to enhance the stability, the regenerative potential and the overall performance of a synthetic bone substitute material, calcium phosphate ceramic, composed of hydroxyapatite and β-tricalcium phosphate. This material already possesses good osteoconductive and resorbable properties, but to ensure controlled bone regeneration, the material was functionalized with a collagen network. Later, bioactive molecules, such as hyaluronic acid and chitosan were incorporated to the structure to enhance the antimicrobial properties. Both materials possess self-healing capacity which helps during the implantation to improve the safety and the lifetime of the scaffold. The performance of the scaffold material was assessed *in vitro* with degradation in Hank's Balanced Salts Solution (HBSS) which simulated the environment of body fluids with stable pH and osmolality. The performance was also evaluated in hydrated stage to simulate a near application stage situation where dentist would hydrate the material before placing it to the defect site. More focus was also drawn to the collagen material which properties were assessed *in vitro* by enzymatic degradation due to collagenase.

Functionalization was shown to enhance the overall performance of a synthetic bone substitute material. The best performance was seen for a composite scaffold made from synthetic bone substitute material, collagen network and hyaluronic acid, when the scaffold had been frozen with dry ice down to -80 °C. These scaffolds had desirable degradation rates in HBSS and the best performance in hydrated stage. Additionally, the properties of collagen network were evaluated separately from the synthetic bone substitute material, which showed that collagen samples that were frozen with dry ice experienced the smallest mass loss due to enzymatic degradation by collagenase *in vitro*.

Keywords: functionalization, calcium phosphate ceramics, bone tissue engineering, collagen, bioactive molecule, bone substitute material.

TIIVISTELMÄ

Noora Haapalainen: Synteettisen luun korvikemateriaalin toiminnallistaminen kollageeniverkon ja bioaktiivisten molekuulien avulla
Diplomityö
Tampereen yliopisto
Bioteknologia ja Biolääketieteen Tekniikka
Kesäkuu 2021

Luusiirtojen tarve lisääntyy jatkuvasti luustoon liittyvien sairauksien, traumojen ja syöpäkasvaimien hoidossa. Tällä hetkellä autologiset luusiirteet, joissa siirteenä käytetään potilaan omia soluja, on pidetty luun uudistumisen kannalta parhaana valintana. Autologisiin luusiirteisiin eli autografteihin liittyy kuitenkin lisääntynyt riski toisen vaadittavan leikkauksen vuoksi sekä luovuttajakohdan mahdollinen sairastuminen. Tämän vuoksi tarvitaan uusia innovatiivisia ratkaisuja, jotka tukevat luun uudistumista ja tarjoavat ihanteellisen ympäristön luusoluille. Luukudostekniikka pyrkii vastaamaan haasteisiin kehittämällä kolmiulotteisia huokoisia materiaaleja, jotka kykenevät integroitumaan isäntäkudokseen ilman haitallisia sivuvaikutuksia.

Opinnäytetyön tavoitteena oli parantaa hydroksiapatiitista ja β-trikalsiumfosfaatista koostuvan synteettisen luun korvikemateriaalin stabiiliutta, regeneratiivista potentiaalia sekä yleistä suorituskykyä. Kyseisellä luun korvikemateriaalilla on jo entuudestaan hyvät osteokonduktiiviset ja resorboituvat ominaisuudet, mutta hallitun luun regeneroitumisen varmistamiseksi, materiaali funktionalisoitiin kollageeniverkon avulla. Myöhemmin materiaaliin lisättiin bioaktiivisia molekyylejä, kuten hyaluronihappoa ja kitosaania, jotka tunnetusti parantavat materiaalien antimikrobisia ominaisuuksia. Molemmilla bioaktiivisilla molekyyleillä on itsekorjautumiskyky, joka auttaa implantaation aikana parantamaan materiaalin turvallisuutta ja käyttöikää. Funktionalisoidun materiaalin suorituskykyä arvioitiin *in vitro* hajoamisella Hankin tasapainotetussa suolaliuoksessa (HBSS), joka simuloi kehon nesteitä pitämällä pH:n ja osmoottisen paineen vakaana. Lisäksi materiaalin ominaisuuksia arvioitiin nestemäisessä ympäristössä, jonka tavoitteena oli simuloida materiaalia käyttäytymistä lähellä sen käyttöastetta. Myös kollageenimateriaalin ominaisuuksia tarkasteltiin *in vitro* entsymaattisella hajoamisella kollagenaasi entsyymistä johtuen.

Synteettisen luun korvikemateriaaalin funktionalistamisen huomattiin parantavan materiaalin ominaisuuksia. Paras suorituskyky saavutettiin komposiittimateriaalilla, joka oli valmistettu synteettisestä luun korvikemateriaalista, kollageeniverkosta ja hyaluronihaposta, kun materiaali oli jäädytetty kuivajäällä -80°C:seen. Kyseisillä komposiittimateriaaleilla oli ideaaleimmat hajoamisnopeudet HBSS:ssa ja stabiileimmat ominaisuudet nesteytettyinä. Kollageenimateriaalia tutkittaessa huomattin, että kuivajäällä pakastetut näytteet vastustivat parhaiten kollagenaasientsyymistä johtuvaa hajoamista.

Avainsanat: funktionalisaatio, kalsiumfosfaatti keramiikka, luukudostekniikka, kollageeni, bioaktiivinen molekyyli, luun korvikemateriaali.

PREFACE

The Master of Science thesis was performed at the junction between R&D departments of Berlin Analytix GmbH, botiss biomaterials GmbH, biotrics bioimplants AG and the project partner Natural and Medical Science institute at the University of Tübingen.

Several people have contributed to this master's thesis with support and academic guidance. I would like to give a special thank you to my supervisor Ariane Kuhnla for her excellent guidance, encouragement, and support during my thesis process. I also want to thank all the employees at botiss biomaterials for making me feel welcome and providing guidance when needed.

My supervisor at the University of Tampere, Prof. Minna Kellomäki, Faculty of Medicine and Health Technology, has been supportive and shared her wide knowledge with me.

I want to thank my family for all their support throughout my study journey and during the difficult times moving alone to Germany for my master's thesis project.

Berlin, Germany, 20 June 2021

Noora Haapalainen

CONTENTS

LIST OF SYMBOLS AND ABBREVIATIONS

3D	Three-dimensional
β-TCP	Beta-tricalcium phosphate
BCP	Biphasic calcium phosphate
BMP	Bone morphogenetic protein
BSM	Bone substitute material
BTE	Bone Tissue Engineering
Ca^{2+}	Calcium ion
$CaCl_2$	Calcium chloride
CaP	Calcium phosphate
CDU	Collagen digestion unit
CPC	Calcium phosphate cement
DM-water	Demineralized water
DSC	Differential Scanning Calorimetry
ECM	Extracellular matrix
EDC	1-Ethyl-3-(3-dimethylaminopropyl)carbodiimide
FL-NH_2	Fluoresceinamine
GAG	Glycosaminoglycan
HAp	Hydroxyapatite
HBSS	Hanks' Balanced Salt Solution
HCl	Hydrochloric acid
H_2O_2	Hydrogen peroxide
H_3PO_4	Phosphoric acid
LbL	Layer-by-layer
MES	2-(N-morpholino)ethanesulfonic acid
MMP	Matrix metalloproteinase
MSC	Mesenchymal stem cell
MW	Molecular weight
MWCO	Molecular weight cut off
Na	Sodium
NaOH	Sodium hydroxide
NHS	N-hydroxysuccinimide
OH^-	Hydroxide ion
PE	Polyelectrolyte
PEI	Poly(ethyleneinimine)
PEM	Polyelectrolyte multilayer
PMMA	Poly(methyl methacrylate)
PO_4^{3-}	Phosphate ion
rhBMP-2	recombinant human Bone Morphogenetic Protein-2
SBSM	Synthetic bone substitute material
Si	Silicon
SMAT	Surface mechanical attrition treatment
TES	N-Tris(hydroxymethyl)methyl-2-aminoethanesulfonic acid
TESCA	TES + $CaCl_2$
TNP	Tri-Sodium Phosphate
w/w	weight by weight
wt%	weight percent

1. INTRODUCTION

Bone is the second most common tissue transplanted worldwide. Current gold standard for the bone regeneration are autologous bone grafts, namely autografts, that have been harvested from the patient's own body (Roseti *et al.*, 2017). Autografts contain living cells, a variety of human growth factors and provide a place for bone cells to grow and integrate with the host tissue. They provide a low risk of immunogenic response thanks to excellent biocompatibility with the human body (Kolk *et al.,* 2012). The problems associated with autografts include risk of donor site morbidity, the need for second surgery and limited availability. Another traditional option is bone graft harvested from cadavers or living donors of the same species which removes the need of second surgery associated with autografts. These grafts are called allografts and they carry the risk of transmitting pathogens or being rejected by the body of the recipient (Roseti *et al.*, 2017).

Bone Tissue Engineering (BTE) is a promising field of science that aims to overcome the challenges of conventional treatments of bone diseases. Three-dimensional (3D) porous scaffolds have been developed to support bone regeneration and provide an ideal environment for bone tissue regeneration. These scaffolds for BTE applications include polymers, ceramics, metals, and composites. Each material group has their own benefits and limitations, but they all aim to attain the characteristics of a desirable scaffold (Turnbull *et al.,* 2017). A desirable scaffold should meet specific biological requirements, including good biocompatibility, non-toxicity and biodegradability. Additionally, scaffolds should possess bioactive properties to interact with their physical environment for new bone formation. In addition to biological requirements, scaffolds should fulfil structural features to mimic the anatomical and physiological structure of native bone extra cellular matrix (ECM) (Amini *et al.,* 2012). Scaffolds should be designed to have a unique architecture with high porosity and pore interconnections to ensure vascular ingrowth and nutrient diffusion to the scaffold. The architecture plays an important role in cell proliferation and their ability to occupy the bone defect area. The 3D structure of a scaffold is affected directly by the connections between cells and scaffold, but also, by the scaffold macrostructure where cells communicate between the nanoscale and macroscale of the ECM (Lutzweiler *et al.,* 2020).

The characteristics of an ideal scaffold mentioned above are all aiming for enhanced bone regeneration. The goal is to allow cell attachment, proliferation, and homing for restoring the physiological structure and functions of bone lost bone (Roseti *et al.,* 2017).

A widely used group of scaffolds in BTE are ceramics that include ceramic composites, amorphous glasses, and crystalline ceramics. Ceramics have the advantage of osteoconductive and osteoinductive properties which enable the stimulation of immature cells to be developed into osteogenic cells and the interaction with the host tissue. The drawback of ceramics is that they can be brittle and possess unfavorable degradation rates that decrease the mechanical properties of the material. The most common bioceramics are calcium phosphates (CaPs), which have good biocompatibility because of their chemical composition and structure close to the mineral content of native bone. Furthermore, tricalcium phosphate (TCP), hydroxyapatite (HAp) and their composite called biphasic calcium phosphate (BCP) are especially interesting in the field of orthopedics and dentistry (Turnbull *et al.,* 2017).

During the bone healing process, the bone defect experiences blood vessel ingrowth and revascularization, which enable cells to build new bone. Functionalization, or the process of adding new functions or properties to bone substitute materials (BSM), is a complex process which aims to improve bone tissue regeneration (Beger *et al.,* 2018). Various strategies have been developed to functionalize the biochemical, topographical, and morphological properties of scaffolds (Fernandez-Yague *et al.,* 2015). Biochemical properties can be altered, for example, by the addition of bioactive molecules, by changing the orientation of molecules or by crosslinking the materials. Bioactive molecules, such as proteins and glycosaminoglycans (GAGs), play a key role in bone tissue regeneration by regulating host cell migration, proliferation, and differentiation (Kim & Lee*,* 2016). As an example, collagen is the most abundant protein in the body which is commonly used for bone tissue applications. The collagen superfamily can be divided into different types, of which type I is the most plentiful in skins, tendons and the organic part of the bone tissue. As it is one of the major components of the ECM, it has excellent biocompatibility and can enhance cell adhesion. To further improve the biomimicry of collagen, it is often combined with GAGs that together enhance the osteoblastic differentiation. Topographical and morphological functionalization can be used to modify the shape and surface roughness of the material, thus affecting the cellular behavior on top of the scaffold (Fernandez-Yague *et al.,* 2015).

The continuous development of new BSMs can potentially open new ways to regenerate bone and reduce the risks associated with conventional BTE methods. The integration of bone graft into the recipient's tissue is a complex and multidimensional cascade of events. The need for new solutions is high because, despite the effort to create the "perfect" bone reconstruction material, it has still not been found. Therefore, the functionalization of BSMs is the key to improve the characteristics, such as biocompatibility, regenerative properties and the degradation rate of BSMs (Titsinides *et al*., 2019).

The aim of thesis was to enhance the stability, performance and regenerative potential of a synthetic bone substitute material, maxresorb® (botiss biomaterials, Zossen, Germany), composed of 60% slowly resorbing hydroxyapatite and 40% fast resorbing beta-tricalcium phosphate (β-TCP). This material already possesses good osteoconductivity and resorbability, but to ensure controlled bone regeneration, the material was functionalized with the incorporation of a collagen network. Additionally, bioactive molecules, such as hyaluronic acid and chitosan were incorporated to the structure to enhance the antimicrobial properties for the safety and longer lifetime of the scaffold. The performance of the scaffold material was assessed *in vitro* with degradation in Hank's Balanced Salts Solution (HBSS) which simulated the environment of body fluids with stable pH and osmolality. The performance was also evaluated in hydrated stage to simulate a near application stage situation where dentist would hydrate the material before placing it to the defect site. More focus was also drawn to the collagen material which properties were assessed *in vitro* by enzymatic degradation due to collagenase.

2. BONE TISSUE ENGINEERING

2.1 Structure of the bone

Bone is a rigid connective tissue that is being remodeled constantly. It consists of approximately 65% inorganic and 35% organic matrix. The inorganic matrix gives bone tissue stiffness and is constructed mainly of phosphate (PO_4^{3-}) and calcium (Ca^{2+}) ions that together form calcium crystalline hydroxyapatite [$Ca_3(PO_4)_3Ca(OH)_2$] with Ca/P ratio of 1.67. The organic matrix provides bone tissue tensile strength and is composed of collagenous proteins, mostly collagen type I, and non-collagenous proteins, such as bone morphogenetic proteins (BMPs) and growth factors (Chang *et al.,* 2017). Remodeling of bone happens due to the activity of four different types of cells which are osteoblasts, osteocytes, osteoclasts, and bone lining cells. Osteoblasts are cuboidal cells that are derived from mesenchymal stem cells (MSC) and are responsible for the synthesis and the mineralization of bone. Osteoblasts synthesize bone matrix in two steps: by first secreting collagen proteins, non-collagen proteins and proteoglycans to form the organic matrix and then mineralizing the bone matrix through vesicular and fibrillar phases. Osteocytes are the most abundant cells in bone tissue residing in lacunae and are surrounded by the mineralized bone. Like osteoblasts, they are also derived from MSCs. Osteoclasts originate from mononuclear cells and are responsible for the resorption of bone. Bone lining cells cover bone surfaces in areas where no bone formation or resorption occurs (Florencio-Silva *et al.,* 2015).

Bone has a hierarchical structure that is composed of different structural levels (figure 1). The macrostructure of bone is divided into cortical and cancellous bone. Cortical bone can be found on the outer parts of most bones and is rather dense with only a little porosity. It creates a protective layer around the bone and constructs most of the bone mass. Cancellous bone can be found on the inner parts of bones and has much higher porosity than the cortical bone. The microstructure is formed of lamellae which are planar arrangements of mineralized collagen fibres. The basic building block of bone is composed of the lamellae that have mineralized collagen fibrils in its nanostructure. The tiniest structure is called sub-nanostructure that is composed of collagen molecules, non-collagenous organic proteins, and minerals, such as hydroxyapatite (Eliaz *et al*., 2017).

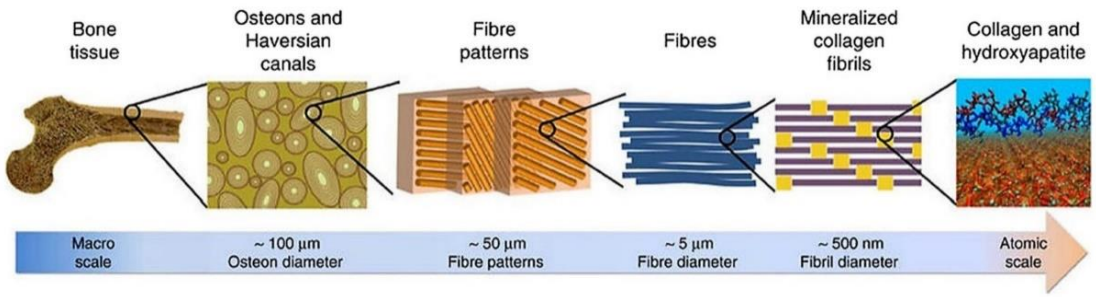

Figure 1. *Hierarchical structure of bone. (Nair et al., 2013)*

Unlike other tissues, bone tissue has an inherent ability to regenerate constantly as either part of a normal bone development, remodeling or as a result to injury. However, if the bone defect is large, the healing and repairing process will decline due to the lack of blood supply or because of an infection in the bone or surrounding tissue (Oryan *et al.,* 2014). Bone healing aims to restore its original condition through a repairing process, which includes the early inflammation phase, the proliferative phase, and the remodeling stage. Inflammation phase begins immediately after the injury and lasts between hours to days. Blood clot, a collection of blood outside blood vessels, is formed and starting a cascade of events that increase the number of macrophages, white blood cells, that release cytokines and growth factors to promote healing of the bone. During the proliferative phase, a bony callus is formed, replacing the hematoma formed during the inflammation phase. The remodeling phase forms and mineralizes the callus, resulting with mineralized bone that is being remodeled to its original shape. The remodeling phase can last up to many years (Oryan *et al.,* 2015).

In addition to the natural regeneration of bone, bone defects, or the lack of bone, can be restored with bone substitute materials. When talking about dental applications, such as implantology, periodontology, or oral and cranio-maxillofacial surgery, there are multiple indications where bone tissue engineering can be implemented. The need for bone grafts can arise from the loss of tooth, due to a tooth fracture or periodontal disease, which can lead to severe alveolar bone resorption. As a result, dental implant cannot be placed without an alveolar ridge preservation graft, where the extraction socket is filled with BSM to heal into solid bone (Yamada & Egusa, 2018). Another common procedure is the sinus lift or maxillary sinus floor augmentation, which is executed if the patient does not have enough upper jawbone for a dental implant. Here, a bone graft is placed to enable bone regeneration and later the implantation of a dental implant (Esposito *et al.,* 2010).

2.2 Properties of bone substitute materials

The aim of a bone substitute material is to promote bone tissue regeneration at the defect site and to degrade *in situ* to be replaced by newly produced bone tissue (Bharadwaz & Jaysuriya, 2020). For this, three-dimensional (3D) scaffolds from BSMs have been designed to support the tissue regeneration with specific requirements which are summarized in figure 2. Biocompatible materials are compatible with living tissue and do not present toxicity or carcinogenicity. The materials are also non-inflammatory and avoid immune rejection in the body. Good biocompatibility also builds the basis for a long-term tolerance of BSMs. Ideally, the BSM should be capable of osteoinduction, where undifferentiated cells are stimulated to develop into osteogenic. Moreover, in osteoconduction, bone cells begin to grow on the surface of the BSM which, in turn supports the ingrowth of the new bone (Kolk *et al*., 2012).

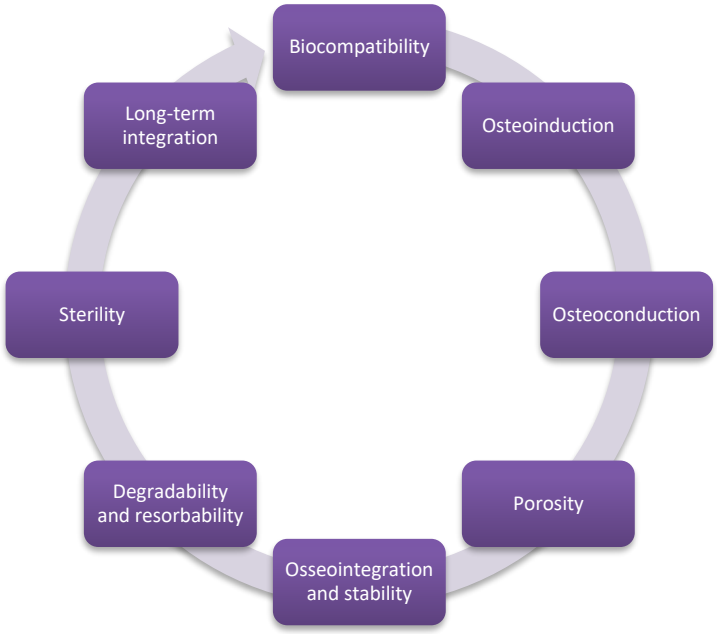

Figure 2. *Requirements for an ideal bone substitute material. (Kolk et al., 2012)*

Scaffolds with porous structures enhance the regeneration properties of the bone. Porosity allows cell migration and diffusion into the scaffold, but also broadens the surface for the cell-scaffold binding. The interconnected pores of BSMs enable the transportation of nutrients and vascular ingrowth. For this, it is crucial that the BSM provides osseointegration, a stable connection between the living bone tissue and the scaffold (Turnbull *et al.,* 2017). When porosity increases, the elastic modulus and flexural strength usually

decreases. This has been shown in a study where macropores were built on calcium phosphate cements (CPCs) by incorporating water-soluble mannitol crystals into CPC and removing the mannitol by water dissolution, resulting in an increase of pore size and a decrease in mechanical properties (Xu *et al.,* 2001). In addition to the porosity, the pore size plays a key role in the mechanical properties of bone substitute scaffolds. Pore size can be divided into microporous (<5 μm) and macroporous (>100 μm). With increasing pore size, the compressive modulus decreases (S.A. Park *et al.,* 2009). On the other hand, studies have shown that osteogenesis is better with bigger pore size (>300 μm), because bigger pores provide better vascularization and high oxygenation for osteogenesis. Properties of bone substitute scaffolds can be modified based on the wanted properties (Hannink & Arts, 2011).

Biodegradability refers to a controlled scaffold degradation through enzymatic or biological processes based on the influence of cells in the human body. The duration of biodegradability is a crucial property of a scaffold because too fast degradation may result in possible mechanical failure while too slow degradation can trigger an unwanted inflammatory response that can weaken the tissue regeneration. In an ideal situation, the tissue ingrowth is supported with controlled degradation of a BSM (Turnbull *et al.,* 2017). Furthermore, BSMs should withstand sterilization and be sterile. This can bring challenges to the sterilization process. For example, sterilization of scaffolds made from alginate-based hydrogels with γ-radiation results in degradation of the material. Bone tissue regeneration is a long-term process which requires the BSM to withstand the changes in the new environment and to support the formation of a new to maintain its functions (Chocholata *et al.,* 2019).

2.3 Overview on bone substitute materials

2.3.1 Natural bone substitute materials

BSMs can be divided into subcategories based on their origin: they are either natural or synthetic (alloplastic). BSM with natural origin include autografts, allografts, xenografts, and phytogenic materials (García-Gareta *et al.,* 2015). Autografts are the current gold standard in bone regeneration, and they are harvested from the patient's own body, usually from the region of the iliac crest. Autografts are ideal for bone reconstruction because they possess osteogenic, osteoinductive and osteoconductive properties, and they are non-immunogenic. Allografts, where bone tissue is obtained from living donors or cadaveric bone sources, are great alternatives to autografts. The issue with auto- and allografts is that they carry a potential risk for transmission of diseases, morbidity of the donor site,

the risk of surgical complications and lack of supply in graft materials. Xenografts are materials derived from a different species to humans (Bharadwaz & Jaysuriya*,* 2020). For example, natural hydroxyapatite can be obtained from animal bones and are used for their stable absorption properties. Xenografts made from bovine bone are commonly used in the dental surgery field. For example, Cerabone® (botiss biomaterials GmbH, Zossen, Germany) and BioOss® (Geistlich AG, Wolhusen, Switzerland) are both xenogenic bone replacement materials made from bovine bone. The disadvantage of xenografts is that they carry a high risk of disease transmission. Phytogenic materials are derived from marine origins, such as marine algae. They share the same issues as xenograft materials (Kolk *et al.,* 2012). An example of a commercially available phytogenic material is Symbios® Algipore® (Dentsply Sirona, York, Pennsylvania, United States), which has been derived from the red algae. It is naturally occurring hydroxyapatite that has a large surface area for protein binding, thus making it suitable as a protein carrier for the bone growth promoting factors (Dentsply Sirona, 2021).

2.3.2 Synthetic bone substitute materials

Alloplastic synthetic bone substitute materials (SBSM) have been developed to overcome the challenges of natural BSMs. Synthetic materials can be roughly divided into metals, polymers, composites, and ceramics. Metals are the first group of synthetic BSMs that are commonly used in load-bearing applications and in the need of stability and structural support because of their great mechanical properties and machinability. However, the challenge with metal BSMs is when comparing the properties of metals to bone, the value of Young's modulus in metals is much higher. Therefore, metallic implants can lead to the resorption of the surrounding bone tissues and affect the implantation process. The effect can be reduced by using metallic materials with porous structures, such as titanium-based alloys or stainless steel (Wu *et al*., 2014). Metals do not always have a good biocompatibility. Over the recent years, more approaches have focused on the controlling of biodegradability rates of metals, such as magnesium, iron and zinc-based biomaterials. These biodegradable metals aim to corrode gradually *in vivo* with an appropriate host response (Zheng *et al.,* 2014). Additionally, the bone integration of metal implants can be enhanced by hydroxyapatite coatings to increase the bone ingrowth and interface attachment strength (Agarwal *et al.,* 2015).

Metal alloys, such as zirconium and titanium, are commonly used in joint replacements and fracture fixation implants for their strength and biocompatibility. For example, Natix® (Tigran Technologies, Malmö, Sweden) is a BSM made from pure titanium granules and used in dental implants. It is used for its superior biocompatibility, osteoconductivity and

mechanical strength that provides support for the new bone formation (Sabet *et al.,* 2017). The use of composite metal scaffolds is increasing to overcome the limitations of metal biomaterials. For example, strontium has been combined with hydroxyapatite and chitosan via freeze-drying process to create composite nanohybrid scaffolds that can enhance cell proliferation and osteogenic differentiation (Lei *et al.,* 2017).

The second group of synthetic BSMs include polymers, that can be harvested from synthetic sources, e.g., poly-lactic acid and poly-glycolic acid or from natural sources, e.g., collagen, hyaluronic acid, and chitosan. Synthetic polymers offer a great variety of properties, including differences in degradation rate and pore size, in addition to their easy synthesis. A drawback of synthetic polymers is that they have a relatively low mechanical properties and can lack cell adhesion sites (Reddy *et al.,* 2021). An example of a synthetic polymer used in biomedical applications is poly(methyl methacrylate) (PMMA). It is commonly used as a bone cement in orthopedics for the primary fixation between the bone and the implant. For example, DePuy CMW™ (DePuy Synthes, Johnson & Johnson, New Brunswick, New Jersey, United States) is a commercially available PMMA bone substitute used as orthopedic bone cement (DePuy Synthes, 2016).

Natural polymers consist of long chains of nucleotides, monosaccharides, or amino acids. Their advantages include bioactivity, antigenicity, non-toxic byproducts and biodegradability. The most common disadvantages of natural polymers include risk for microbial contamination, immunogenic reaction and decreased tunability. Natural polymers are often combined with other materials in scaffolds, including calcium phosphate, hydroxyapatite and silk (Reddy *et al.,* 2021). For example, silk is a class of protein fibers spun by e.g., spiders and silkworms. Silk fibroins produced by *Bombyx mori* silkworms have been used to develop porous scaffolds in tissue engineering for its biocompatibility, tunable biodegradation and thermo-mechanical stability. They have shown to possess compression modulus comparable to the natural cancellous bone with interconnected pore architecture (Nisal *et al*., 2018). Additionally, a commercially available natural collagen membrane (Creos™, Nobel Biocare, Kloten, Switzerland) has been developed for dental use in guided bone regeneration and guided tissue regeneration. More examples of natural polymers and their properties, including collagen, hyaluronic acid, and chitosan are discussed in more detail in chapter 3 since they were used in the experimental part of the thesis.

Composite scaffolds have been developed to combine the best properties of different materials and to create materials with osteoconductive and osteoinductive properties. Commonly, composite scaffolds are constructed by using one type of matrix with dispersed phase, such as polymer/ceramics. For example, a polyester block copolymer with

the combination of a calcium phosphate layer has been developed with favorable handling properties and high rate of bone ingrowth (Polo-Corrales *et al.,* 2014). Furthermore, SmartBone® (Industrie Biomediche Insubri, Mezzovico-Vira, Switzerland) is a commercially available hybrid bioactive BSM that combines a bovine bone matrix with bioactive resorbable polymers and cell nutrients. SmartBone® provides integration and osteogenesis. It is used for bone regeneration in reconstructive surgery, such as sinus lift and socket preservation (SmartBone® 2021). Another example of a commercially available bone substitute composite is Infuse® (Medtronic, Minneapolis, Minnesota, United States), which consists of two parts including a recombinant human Bone Morphogenetic Protein-2 (rhBMP-2) and a collagen sponge. It has been developed to stimulate natural bone formation and remodeling, where the collagen sponge is used as a carrier for the engineered rhBMP-2 protein (Medtronic 2021).

The last group of synthetic bone substitute materials are ceramics, which are discussed more comprehensively because they were used in the experimental part of the thesis.

2.4 Ceramic bone substitute materials

Ceramic materials, such as calcium phosphates (CaP) and bioglass are widely used for bone regeneration applications. They are used for their similar chemical and crystallinity properties to bone mineral content. On the downside, ceramic materials are often brittle, lack osteoinductivity and have slow degradation rates (Polo-Corrales *et al.,* 2014). For several years, ceramic bone substitute materials have been extensively used in biomedical applications, for example in orthopedics and dentistry. This group of materials include ceramic composites, amorphous glasses, and crystalline ceramics (Turnbull *et al*., 2017). They can be retrieved from natural origin, such as coralline hydroxyapatite, or synthetic origin, such as synthetic hydroxyapatite or β-tricalcium phosphate (β-TCP) and synthesized into different forms. In BTE, the most common ceramics are calcium phosphate ceramics that possess excellent biocompatibility, osteoconductivity and biodegradability because of their resemblance to natural. CaPs cannot form bone without additional trigger but can contribute to the new bone formation in the defect area. However, CaP materials can possess osteoinductive properties when they present specific chemical compositions or surface structures. For example, CaP can regulate the amount of osteoinductive factors on the implant site (García-Gareta *et al.,* 2015).

HAp and β-TCP are the two most common CaPs. They can also be found as a composite material, which has been the focus of this thesis. HAp contributes most of the inorganic bone structure and builds connections with collagen fibers to create a harder and more

resistant bone. In CaP ceramics, the favorable component ratio is the same as in natural bone (Ca/P = 1.67). The ideal ratio causes HAp to release calcium and phosphate ions into the organism (Kolk *et al.,* 2012). The chemical formula and properties of synthetic HAp are nearly identical to the natural HAp in bone and teeth. Therefore, HAp can be used as bone substitute or replacement in filling bones, bone augmentation and as coatings in dental and orthopedic implants (Szczés *et al.,* 2017). Tricalcium phosphates (TCPs) can be found in two different forms: α-TCP and β-TCP that have a similar chemical composition but different crystallographic properties. β-TCP is more commonly used in a form of blocks or granules and is less soluble compared to α-TCP (Barrère *et al.,* 2006). β-TCP has good biocompatibility and has a faster degradation process compared to HAp. It has good microporosity which helps the material to be embedded into the tissue by the invasion of blood vessels (Kolk *et al.,* 2012).

CaPs can form biphasic, triphasic or polyphasic compositions by mixing the individual phases together into a homogeneous mixture. The most studied combination is made from HAp and β-TCP to create a biphasic calcium phosphate (BCP) (Eliaz *et al.,* 2017). BCP of HAp and β-TCP can be prepared through sintering which is a thermal process creating solid material from loose fine particles (Legeros *et al.,* 2003). They are available in the form of blocks, granules and custom-designed shapes for bone graft or bone substitute materials in orthopedic, maxillofacial, and dental applications. The idea of BCPs is to combine the osteoconductive properties of HAp with the solubility of β-TCP (Eliaz *et al*., 2017). During the degradation of BCP, calcium and phosphate ions are released, enhancing new bone formation. HAp has a slow degradation rate while β-TCP degrades fast. As the two different components have different solubility, the degradation kinetics of TCPs can be modified *in vitro* and *in vivo* (Turnbull *et al.,* 2017). Table 1 shows advantages and disadvantages of HAp and β-TCP that also reflect on the characteristics of their composite material.

Table 1*. Advantages and disadvantages of hydroxyapatite and β-tricalcium phosphate materials (Chocholata et al., 2019; Szczés et al., 2017).*

Material	Advantage	Disadvantage
Hydroxyapatite	Biocompatibility, osteoconductivity, non-inflammatory, non-toxicity, bioactivity	Brittle structure, not osteoinductive
β-Tricalcium phosphate	Osteogenic properties	Slow degradation, risk of inflammatory reaction

Bioceramics are an interesting group of bone substitute materials to repair or replace bone tissue. Calcium phosphate ceramics are focused on in this thesis because of their similar structure to the bone and natural properties that stimulate the bone regeneration. Commercially available synthetic CaPs include for example MBCP® (Biomatlante, Nantes, France) which is a biocompatible synthetic bone graft substitute material. Its advantage is the unique micro and microporous structure that is close to the human bone (MBCP® Synthetic Bone Substitute 2021). Another example is Vitoss® (Stryker, Malvern, United States), which is a highly porous calcium-phosphate with interconnected structure. It is available in foam, blocks or morsels and is commonly use as void filler in cancellous bone applications (Sinha *et al.,* 2009). Moreover, Biobase® (Biovision, Milpitas, United States) is a synthetic, inorganic and bioresorbable α-TCP (BioBASE 2020). The experimental part of this thesis has focused on synthetic bone substitute material, maxresorb® (botiss biomaterials GmbH, Zossen, Germany). Its unique production process creates homogeneously distributed material with the combination of HAp and β-TCP (maxresorb® 2021). Table 2 below compares the properties of these different CaP bone substitutes.

***Table 2**. Comparison of three different calcium phosphate bone substitute materials and their properties (maxresorb® 2021; Sinha et al., 2009, MBCP® 2021; Biobase® 2021).*

Product	Composition	Porosity	Structure	Form	Application
maxresorb®	60% HAp and 40% β-TCP	80%	Ultra-high interconnected porosity	Granula and block	Implantology, periodontology and oral surgery
Vitoss®	TCP	Up to 90%	Open-interconnected structure	Foam pack / strip, morsel, and block	Spinal applications
MBCP®	Mixture of either 60 or 20% HAp with 40 or 80 % βTCP	70%	Macropores of interconnected network and micropores as intercrystalline spaces	Block and granula	Bone graft fill or reconstruct osseous bone defects
Biobase®	α-TCP	65%	Micropores (< 5µm) and macropores (1mm)	Block	Temporarily fill for pathological, traumatic, and postoperative bone defects

3. FUNCTIONALIZATION OF SYNTHETIC BONE SUBSTITUTE MATERIALS

Functionalization, the process of adding new functions or properties to the bone substitute materials, aims to enhance the regenerative potential of BSMs. It can help to improve the material and the biological performances of a scaffold. The material performances are related to creating porous structures that mimic the environment of the native tissue with the ideal chemical, physical and mechanical properties. On the biological performance side, the scaffold should allow cell attachment and support the cell survival while they undergo proliferation, migration and differentiation. Functionalization can be used to modify various properties of the material from changing the roughness and topology all the way to enhancing the biocompatibility and bioactivity of the material. It can be done by adding new functional groups to the material or by functionalizing the surface of the material. Especially in the field of bone tissue engineering, surface functionalization by chemical or physical treatments or by applying functional coatings has been shown to tune the chemical composition, resorption behavior and release kinetics of BSMs (Rossi & van Griensven, 2014). Often, functionalization is achieved by combining materials of synthetic and natural polymers (Tian *et al*., 2012). As an example, a poly lactic-co-glycolic acid scaffold (synthetic polymer) has been combined with a natural polymer (collagen) to overcome the issues due to the low hydrophilicity and cell adhesion of the polyester (Chen *et al.,* 2012).

Different bone substitute material groups and their main characteristics have been presented in chapters 2.3 and 2.4. This chapter focuses on the different functionalization methods with a specific focus on calcium phosphate ceramics.

3.1 Functionalization methods

3.1.1 Copolymerization

Functionalization can be achieved by introducing new functional groups to the monomers of the polymers or by introducing new functional groups to the polymer chains. Copolymerization of monomers with functional groups or other monomers is widely used for the functionalization of synthetic polymers. Synthetic polymers have been widely used in bone tissue engineering for their excellent biocompatibility and mechanical properties. However, many synthetic polymers cannot provide sufficient signals for cell adhesion or

proliferation. To overcome the challenges and to improve the biocompatibility and cell adhesion of synthetic polymers, triblock copolymers of poly(glutamic acid)-b-poly(-lactide)-b-poly(glutamic acid) have been developed to exploit the hydrophobic and hydrophilic parts of the chains (Deng *et al.,* 2007).

Copolymerization has also been used for the chemical modifications of chitosan. Here, synthetic polymers have been graft polymerized onto chitosan to introduce new properties. The graft copolymers are composed of a linear backbone of one polymer and branches of another polymer. For example, aniline has been polymerized in the presence of chitosan, resulting in a graft copolymer that forms self-supporting materials (Enescu & Olteanu, 2008). Additionally, copolymerization can be used for the formation of aliphatic polyesters with reactive groups. The polyesters with aliphatic groups are interesting for the biomedical applications because of their tunable properties in hydrophilicity, biodegradation and bio adhesion (Tian *et al.,* 2012). In addition, natural polymers, such as alginates, can be modified into different copolymers for controlled drug delivery (Szabó *et al.,* 2020). For example, by creating graft copolymers of sodium alginates and cross-linking them with glutaraldehyde in acidic conditions, it is possible to create beads for the entrapment and release of the anti-inflammatory drug indomethacin (Nuran *et al*., 2008).

3.1.2 Surface functionalization

Various methods have been developed for the incorporation of bioactive molecules onto the scaffold. Surface functionalization includes tailoring of the surface chemistry and the surface structure via chemical, physical and biological strategies. Multiple functionalization methods can also be implemented at the same time to modify the same surface to enhance bone healing. One way to tailor the surface chemistry of a material is by adding coatings on scaffolds. These coatings can be based on the organic components of the extracellular matrix, such as collagen, gelatin or glycosaminoglycans, on the hydroxyapatite (HA) derived inorganic coatings or on hybrid coatings (Wu *et al.,* 2014). For example, hybrid coatings have been developed from poly(L-lysine)/polydopamine to functionalize porous hydroxyapatite scaffolds. These hybrid-coated scaffolds have showed better osteoinductive properties and promoted bone marrow stromal cell adhesion and differentiation (Han *et al.,* 2019).

The surface structure can be functionalized through chemical and physical treatments. Chemical modifications can be achieved between the biomaterial and the surrounding media, e.g., via anodization, hydrolysis or oxidation techniques. Additionally, chemical functionalization can be achieved by establishing coatings with controlled micro or nano-

architectures (Wu *et al*., 2014). An example of the chemical functionalization is for the natural polymers called alginates. Alginates consist of linear copolymers of (1→4) linked β-D-mannuronic acid and α-L-guluronic acid units with a backbone of hydroxyl and carboxyl groups. The hydroxyl and carboxyl groups in the backbone of alginates allow their chemical functionalization to modify the physical, chemical and biological properties. For example, the oxidation of alginate results in the opening of the polysaccharide backbone with highly reactive aldehyde moieties and derivates that are susceptible to hydrolytic degradation. Oxidation has been shown to help with controlled degradation of alginates and further allow the creation of cross-linked systems to tune the degradation for tissue engineering applications (Szabó *et al.,* 2020). Meanwhile, the surface functionalization through physical treatments does not alter the chemical composition of scaffolds and can be achieved from direct mechanical processes, for example with surface mechanical attrition treatment (SMAT). As an example, ultrasonic shot peening is a form of SMAT that can be used to enhance cell adhesion on titanium-based alloys (Wu *et al*., 2014).

Surface functionalization can be achieved by anchoring organic molecules to the surfaces. This results in controlled cell-material interactions and enhanced material biocompatibility. For example, ceramic materials are often functionalized with silanes to introduce surface functional groups. In silanization, the surface is covered with alkoxysilane molecules to modify materials with hydroxyl-rich groups, e.g., hydroxyapatite. In addition to anchoring molecules to the surfaces, biomolecules, such as proteins, peptides and carbohydrates, can be introduced to the surfaces of materials. This attachment of biomolecules is called immobilization, which relies on physical, covalent and bioaffinity of the biomolecules. Covalent immobilization enhances the attachment of biomolecules to the material surface. This method is commonly based on glutaraldehydes and carbodiimide chemistry. Physical immobilization is one of the simplest methods since it relays on dipping the material into a solution containing the target biomolecules. It can be based on electrostatic interactions between oppositely charged solutions, hydrogen bonds or van der Waals forces (Treccani *et al.,* 2013). An example of physical immobilization called polyelectrolyte multilayer deposition based on electrostatic interactions is described in chapter 3.2.4 for the functionalization of calcium phosphate ceramics.

3.2 Functionalization of calcium phosphate ceramics

The focus of the thesis has been on the functionalization of calcium phosphate ceramics. Composite calcium phosphates (CaP) have been developed from one or more CaP phase with better chance of improving the bioactivity, biodegradability, and mechanical

properties of CaPs (Eliaz *et al.,* 2017). In this thesis, the composite calcium phosphate was composed of synthetic hydroxyapatite (HAp) and beta-tricalcium phosphate (β-TCP). Synthetic HAp is the most used CaP for dental tissue engineering applications because of its great biocompatibility and bioactivity properties. When combined with β-TCP, the CaP provides a nanostructured surface for the adhesion of osteoblasts with slow resorption properties that enhance the formation of the new bone (Wei *et al*., 2020). Calcium phosphates are typically functionalized by the incorporation of organic and polymeric compounds and biological macromolecules. Functionalization can be achieved through various methods, such as by the creation of composites. For example, to improve the performance of a single bone substitute material, they can be combined with different materials to incorporate the desired properties of each material group. One way to do this is to combine synthetic polymers with natural polymers to create a composite material. Here, the synthetic polymer possesses tunable properties, such as degradation rate and mechanical composition, while natural polymers have unique compositions and are biocompatible (Rossi & van Griensven, 2014).

The next chapters will highlight the materials, including collagen and bioactive molecules, and their incorporation methods, that have been used for the functionalization of CaP ceramics in this thesis.

3.2.1 Collagen

CaP ceramics can be functionalized by the addition of a collagen network. (Fernandez-Yague *et al.,* 2015) Collagen is the most abundant protein in humans and the most widespread component of the extracellular matrix (ECM) and in the organic matter of bones. (Shoulders & Raines, 2009) It is composed of four levels composed of amino acid chains, α-chains, collagen fibrils and collagen fibers (figure 3).

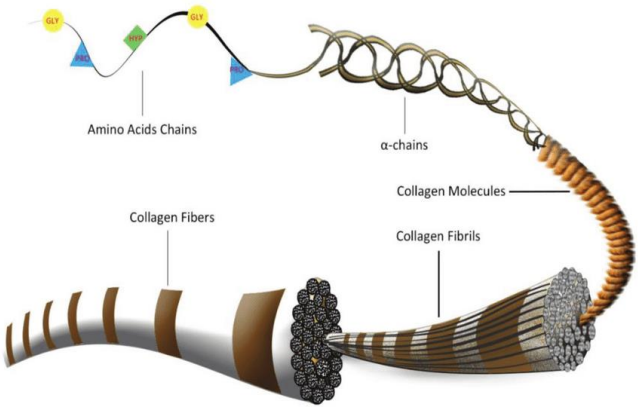

Figure 3. *Representation of the collagen structure. (Lin et al., 2019)*

The defining feature of collagen is that it consists of amino acids bound together to form a right-handed triple helix structure which has a triple helical region and two nonhelical regions in the ends of the helix. Collagen has a repeating sequence of $[Gly\text{-}X\text{-}Y]_n$, where Gly is glycine and X, and Y are commonly either proline or its hydroxylated form called hydroxyproline. This tripeptide sequence goes along the entire length of the collagen and is called the primary structure of collagen (Sorushanova *et al*., 2019). The secondary structure is composed of these tripeptides that are linked together forming α-chains. The tertiary structure is a triple helix which has a coiled rope-like structure that is composed of three parallel α polypeptide chains, more precisely of two identical α_1(I)- and α_1(II)-chains, wound around each other. The triple helix structure has approximately 1000 amino acids with length a of 300 nm and a diameter of 1.5 nm. The hydroxyl groups of hydroxyproline stabilizes the triple helix with hydrogen bonds (figure 4). The quaternary structure of collagen builds collagen fibrils from five triple-helical collagen molecules packed together into a supramolecular form (Ferreira *et al.,* 2012).

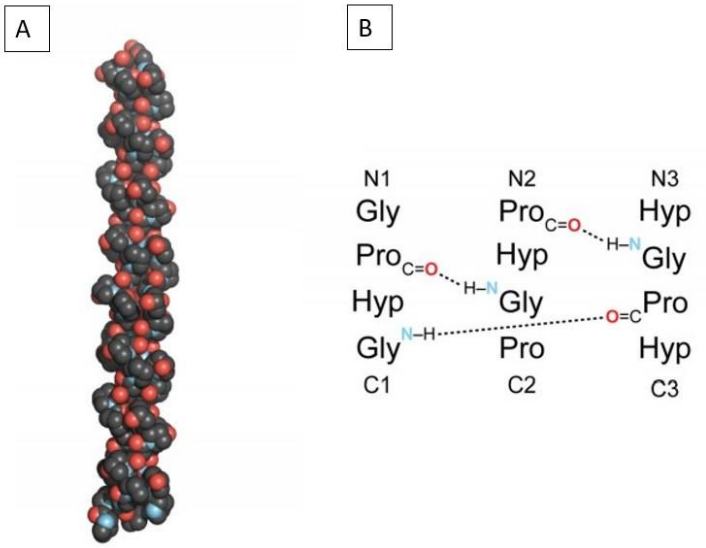

Figure 4. *A) Collagen triple helix structure and B) three strands of collagen with ladder of hydrogen bonds between amino acids. Modified from Shoulders et al, 2009.*

Collagen can be extracted from different sources, such as porcine skin or pericardium or from bovine tissue, respectively. Collagen can be processed by solely decellularizing the collagen to mimic the composition of native tissue by preserving the original shape of collagen tissue and ECM structure. Also, collagen can be extracted, purified, and polymerized to form a scaffold. It is widely used in biomedical applications for its biodegradability, biocompatibility, availability, and versatility (Parenteau-Bareil *et al.,* 2010). Collagen is degraded enzymatically in the body by collagenases and metalloproteinases,

and therefore possesses non-toxicity. In general, the drawback of collagen biomaterials are their weak mechanical properties. Despite the challenges, collagen has a lot of potential when combined with other biomaterials (Song *et al.,* 2018). For example, collagen sponges have been used to deliver bioactive proteins for bone reconstruction in alveolar ridge defects to prolong the release of these bioactive proteins (Jovanovic *et al.,* 2007). Additionally, a graft material of nano-hydroxyapatite-collagen-polylactic acid combined with autologous adipose-derived mesenchymal stem cells has been developed for posterolateral spinal fusion in rabbit model. The collagen and nano-hydroxyapatite components simulated the cancellous bone and osteoconductive capabilities (Tang *et al*., 2011).

3.2.2 Hyaluronic acid

The functionalization of CaP ceramics can be enhanced with the addition of hyaluronic acid (HA). HA is a polyanionic glycosaminoglycan, a major constituent of the ECM and contributes to cell proliferation, differentiation, and migration. It has been shown to possess good biocompatibility, biodegradability and bioactivity properties. Structurally, hyaluronic acid is composed of *N*-acetylglucosamine, and glucuronic acid and it has a backbone consisting of carboxyl and hydroxyl groups that can be beneficial in hyaluronic acid cross-linking (figure 5). HA can be found with various molecular weights up to 12,000,000 Da in animal tissue. It can retain water molecules and maintain a hydrated environment for cell infiltration, making it excellent for wound healing applications (Collins & Bircumshaw, 2013).

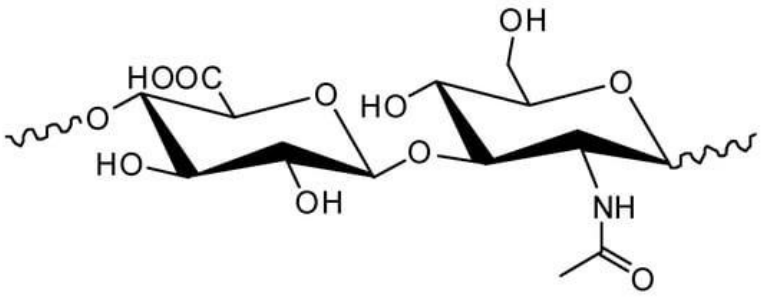

Figure 5. *Chemical structure of the hyaluronic acid repeating unit. (Sionkowska et al., 2020)*

The importance of hyaluronic acid in bone healing is related to its high concentrations found in early stages of bone fracture repair and in the cytoplasm of osteoprogenitor cells. Especially when combined with other osteoconductive molecules, HA has shown to support new bone growth. HA can be crosslinked into a hydrogel for the creation of

stable scaffolds through carbodiimide-mediated or photo crosslinking strategies (Patterson *et al*., 2010). The modification can also be achieved by means of chemical modifications of glucuronic acid, carboxylic acid, the *N*-acetyl group and hydroxyl groups of HA. With the versatile modification methods of hyaluronic acid, it is an important building block in the functionalization of bone substitute materials (Burdick & Prestwich, 2011). For the applications of hyaluronic acid, a poly(lactic-*co*-glycolic acid) grafted hyaluronic acid has been developed for periodontal barrier applications for bone regeneration (J.K. Park *et al.,* 2009).

3.2.3 Chitosan

Addition of a natural polymer, chitosan, can further functionalize a SBSM. Chitosan is a linear polysaccharide composed of β-(1→4)-linked D-glucosamine and N-acetyl-D-glucosamine (figure 6). It is obtained by the alkaline deacetylation process of chitin that is a mucopolysaccharide present in the exoskeleton of some crustaceans and insects. Chitosan is used in tissue engineering for its non-toxic, biodegradable, and antimicrobial properties that allow cell adherences, proliferation, and differentiation. Additionally, it can be molded in various forms to create porous scaffolds (Ahsan *et al.,* 2018). The antibacterial activity of chitosan against pathogenic bacteria, such as *Staphylococcus aureus* and *Escherichia coli* has been shown with immobilization of hyaluronic acid onto chitosan graft membranes (Hu *et al.,* 2003). Chitosan can be found with various molecular weights ranging from 300 to over 1000 kDa with deacetylation from 30% to 95%. Its cationic nature can be utilized for electrostatic interactions with anionic molecules, such as hyaluronic acid (Di Martino *et al.,* 2005).

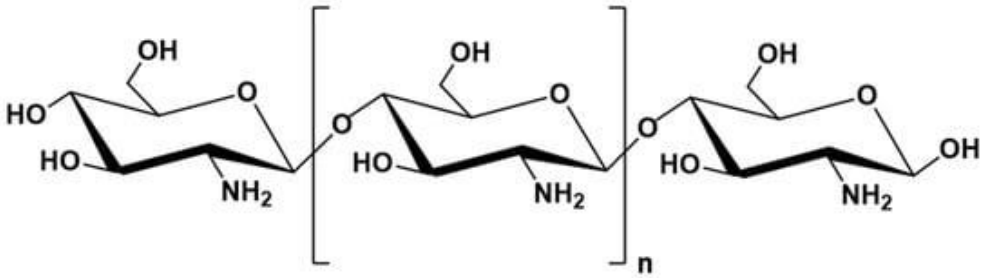

Figure 6. *Chemical structure of chitosan. (El-banna et al., 2019)*

Chitosan has been combined with CaPs, hyaluronic acid and synthetic polymers for bone tissue engineering applications. It has shown to promote growth and deposition of mineral rich matrix by osteoblasts. When chitosan has been added to CaP scaffolds, it has

provided stronger and biodegradable scaffolds (Khor & Lim, 2003). Additionally, chitosan microspheres have been combined with absorbable collagen sponge for controlled release of recombinant human bone morphogenetic protein-2 (rhBMP-2) in rabbits, which is known for its osteoconductive properties in bone regeneration. The results showed that composite chitosan-collagen scaffolds remarkably enhanced new bone formation and mechanical properties. Therefore, it could potentially be used as a carrier for BMP-2 for bone defect treatment (Hou *et al.,* 2012).

3.2.4 Methods for the incorporation of bioactive molecules

Hyaluronic acid and chitosan are incorporated into a BSM composite to enhance its properties, especially the antimicrobial ability. Both materials have shown self-healing properties that enable autonomous healing of the damage site. Furthermore, self-healing properties help during the implantation to improve the safety and lifetime of a BSM, in addition to helping the new bone to recover its original shape (Barroso *et al.,* 2019). The incorporation of bioactive molecules is desirable to induce new tissue formation and regulate cellular activities. One approach is to bind the bioactive molecules to the surface of the BSMs, e.g., polyelectrolyte multilayer (PEM deposition). Another approach is to deliver the bioactive molecules during the preparation process of scaffolds directly to the composite, e.g., by mixing materials together during fabrication process. Additionally, bioactive molecules can be loaded in carriers, such as micro- and nanoparticles for the sustained release of the molecules overtime (Singh *et al.,* 2013).

The first incorporation method of both hyaluronic acid and chitosan into a BSM can be executed by binding the molecules to the surface with a method called polyelectrolyte multilayer (PEM) deposition. Hyaluronic acid is a weak polyanion while chitosan is a weak polycation, and therefore have opposite electrical charges. This enables the utilization of their electrostatic interactions to create PEMs through alternate adsorption of polycation and polyanion on the surface of a BSM (Barroso *et al.,* 2019). PEM are commonly deposited with a layer-by-layer (LbL) assembly which allows an easy and reproducible way to modify the surfaces of BSMs. The layers are deposited by either dipping the BSM material in the polyelectrolyte (PE) solutions of hyaluronic acid and chitosan or pipetting the PE solutions in wells with the BSM. Because of the electrostatic interactions between polycation and polyanion, the layers increase in each deposition creating multilayers with a thick structure (Borges & Mano, 2014).

The pH and charge of the polyelectrolyte solutions has shown to influence the thickness of the formed PEMs. When the PEs are strongly charged, the thickness of the PEM is lower compared to PEs with weakly charged PEs (Bieker & Schönhoff, 2010). Especially

weak PEs are strongly pH-dependent and even small changes in pH and ionic strength of the environment can affect the thickness of PEM formation (Boudou *et al.,* 2010). Examples of the applications of PEM coatings include the usage of the polyelectrolytes as carriers to immobilize BMP-2, which has a key role in bone and cartilage development. This has been shown to induce osteoblast differentiation in bone cells, which is enhanced through the efficient attachment of cationic and anionic charges of PEs. Additionally, PEM deposition offers a great tool for the surface modification of BSMs (Nath, *et al.,* 2015).

These bioactive molecules can be incorporated into CaP ceramics during the fabrication process of CaP composites with collagen network. Some of the most common fabrication methods for scaffolds include freeze-drying, solvent casting, or gas foaming (Turnbull *et al.,* 2017). The focus on this thesis has been on the freeze-drying method. For the freeze-drying, a suspension of combined BSMs is first frozen and exposed to environment with lower pressure. Then, the ice crystals are removed through sublimation, a process where the substance goes directly from solid to gas state. In figure 7, the curve from A to B represents the solid-vapor curve, where ice and water vapor are in equilibrium. This results in the formation of a highly porous scaffolds. Also, the pore structure is heterogeneously distributed with large variation in pore diameter, orientations, and locations (O'Brien *et al*., 2004). One of the main advantages of freeze-drying is that the method does not use high temperatures which could potentially decrease the activity of biological factors in the scaffold. The limitation of freeze-drying comes from high energy consumption and long processing time (Roseti *et al.,* 2017).

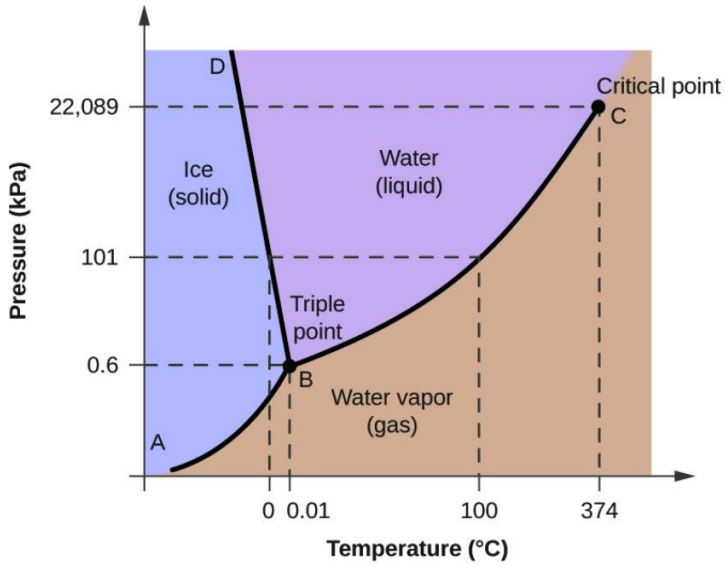

Figure 7. *Phase diagram of water. (OpenStax Chemistry, 2016)*

4. MATERIALS AND METHODS

4.1 Materials

In this thesis, a synthetic bone substitute material, maxresorb® (botiss biomaterials, Zossen, Germany) was functionalized. Figure 8 represents maxresorb® made from hydroxyapatite (HAp) and beta-tricalcium phosphate (β-TCP) which was used in a form of a block (1 cm x 1 cm x 0.5 cm) and granula (0.5 - 1.0 mm). It is composed of 60% slowly resorbing hydroxyapatite and 40% fast resorbing beta-tricalcium phosphate with ultra-high interconnected porosity and rough surface (maxresorb®, 2021).

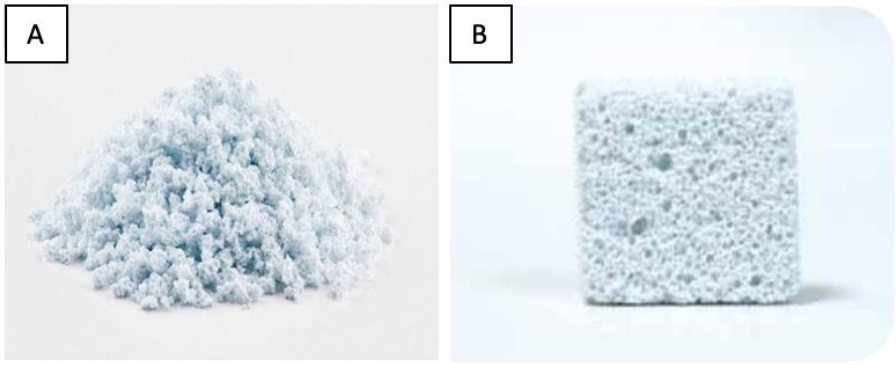

Figure 8. *SBSM, maxresorb®, in a form of A) granula and B) block (maxresorb® 2021).*

This SBSM was first functionalized with the incorporation of a collagen network (porcine dermis, biotrics bioimplants AG, Berlin, Germany). Later, different bioactive molecules, including hyaluronic acid, chitosan, kappa-carrageenan, and chondroitin sulphate, were incorporated to the structure. Hyaluronic acid was purchased from Sigma-Aldrich (sodium hyaluronate 95%, MW: 1400kD) and dissolved in DM-water at 2 mg/mL. Low molecular-weight chitosan (50-190kD, Sigma-Aldrich) was dissolved in 0.15M NaCl solution in DM-water at 2 mg/mL and filtered under vacuum through a porous membrane (Whatman® qualitative filter paper, 70 mm, 100/PK) into a Büchner flask. The pH value of the solution was adjusted to 4.0 with 0.1M hydrochloric acid (HCl). Chondroitin sulfate (sodium salt from bovine trachea, Sigma-Aldrich) and kappa-carrageenan (highly pure, from red algae (*Rhodophyceae*), Carl Roth GmbH) were dissolved in DM-water at 2 mg/mL, respectively.

4.2 Preparation of composite ceramics

The preparation of composite ceramics was done in two ways: my mixing the materials together or through a polyelectrolyte multilayer deposition (PEM) (4.3). The mixing method included the incorporation of the collagen network and bioactive molecules to the SBSM block or granula. For the granula with collagen network - samples, collagen suspension was mixed with granula to yield a 32:25 (w/w) mixture. The mixture was placed into a mold of 5 x 5 x 1 cm^3 as seen in figure 9.

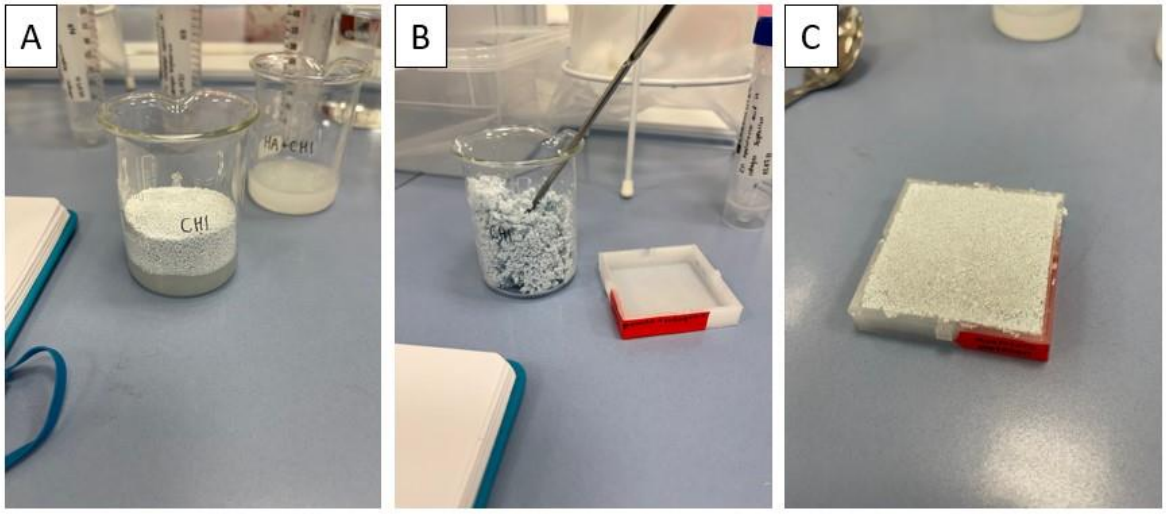

Figure 9. *Preparation of composite ceramics A) granula (top) and collagen suspension (bottom) B) granula and collagen mixed C) patted into a mould.*

Additionally, samples with different combinations of granula, collagen suspension (with different concentrations) and different bioactive molecules, including 2 mg/mL hyaluronic acid, 2 mg/mL chitosan, 2 mg/mL kappa-carrageenan, and 2 mg/mL chondroitin sulfate were prepared. The ratio of collagen and granula was always the same 32:25 (w/w) but the ratio between collagen and bioactive molecule differed, as shown in table 3, where collagen concentration is denoted as wt% (weight percent).

Table 3. *Combination SBSM granula, collagen and bioactive molecule.*

Sample	Ratio
3 wt% collagen + hyaluronic acid	Col:HA 51:1 (w/w)
3 wt% collagen + chitosan	Col:Chi 51:1 (w/w)
3 wt% collagen + hyaluronic acid + chitosan	Col:HA:Chi 102:1:1 (w/w)
3 wt% collagen + chondroitin sulfate	Col:CS 51:1 (w/w)
3 wt% collagen + kappa carrageenan	Col:KC 51:1 (w/w)
3 wt% collagen frozen with dry ice	-
5 wt% collagen (frozen with and without dry ice)	-
5 wt% collagen + hyaluronic acid (frozen with and without dry ice)	Col:HA 51:1 (w/w)
7 wt% collagen	-
7 wt% collagen + hyaluronic acid + chitosan	Col:HA:Chi 102:1:1 (w/w)

For the SBSMs in a form of a block with collagen network, samples were prepared by filling a 5 x 5 x 1 cm^3 mold to the half with collagen suspension. To better observe the penetration of collagen network later with the microscope, the collagen suspension was stained with 0.01% (w/v) riboflavin (riboflavin 5'monophosphate sodium salt hydrate, Cayman Chemicals) in DM-water. In each mold, 4 blocks were placed with collagen suspension and covered evenly. Each mold was treated differently (table 4) before freezing to potentially increase the penetration of the collagen network into the block. Additionally, samples with only collagen suspension were prepared for the characterization of the collagen network by pouring collagen suspension into a 5 x 5 x 1 cm^3 mold.

Table 4*. Pre-treatment of SBSM blocks before freezing.*

Sample / Condition	Treatment
1 / Room temperature	After placing the blocks on a mold with collage suspension, samples were left in room temperature for 1 h before putting in the freezer
2 / Hydration	Samples were hydrated on a 12-well plate with 2 ml of DM water for 5 min before placing in the mold with collagen suspension
3 / Ultrasonic bath	Samples were placed in ultrasonic bath for 2 min

Samples with granula and block were frozen in the freezer (GNH650BT, Gastro Hero, Dortmund-Holzwickede, Germany) at – 20 °C for at least 17 h. Some samples were first frozen on dry ice (- 78.5 °C) before storing them in at – 20 °C. After the samples were

completely frozen, they were freeze-dried with a freeze-drier (ModulyoD, Thermo Electron Corporation, Massachusetts, United States) at – 47 °C and vacuum (< 1.0 mbar) for at least 24 h for the samples frozen in the freezer, and at least 48h for the samples frozen with dry ice until they were completely dry. After freeze-drying, the granula samples were cut into 1 x 1 x 1 cm^3 cubes and block samples into 1 x 1 x 0.5 cm^3 following their original shape with a scalpel.

4.3 Polyelectrolyte multilayer

Polyelectrolyte multilayer (PEM) deposition was used as an alternative preparation method for the incorporation of bioactive molecules, including hyaluronic acid and chitosan, to the SBSM. The technique was based on the layer-by-layer deposition of oppositely charged polyelectrolytes, where hyaluronic acid was used as the polyanion and chitosan as the polycation. For the PEM deposition, 5mM sodium acetate buffer in DM-water was prepared from 98 % sodium acetate (MW: 82.03 g/mol, VWR) and the pH value was adjusted to 5.5 with 1 M acetic acid. Poly(ethyleneimine) (PEI) (50 wt% in H_2O) was purchased from Sigma-Aldrich, a solution at 5 mg/mL in DM-water was prepared and pH was adjusted to 5.5 with 1 M acetic acid. Polyelectrolyte solutions at 1 mg/mL in 5 mM sodium acetate buffer were prepared from hyaluronic acid (1.5 - 2.0 MDa, sodium hyaluronate, Kraeber & Co GmbH) and chitosan (50 - 190 kD, Sigma-Aldrich).

The aim was to deposit the polyelectrolyte multilayer on the SBSM. Before this, as a proof of principle, a protocol of PEM coating was established on glass coverslips (10 x 10 mm^2, Menzel-Gläser, Thermo Scientific) and Si-Wafers (provided by the project partner, Natural and Medical Sciences Institute, Tübingen, Germany). The deposition time was in total 200 min, where the procedure from table 5 was repeated five times.

Table 5. *Protocol for the deposition of polyelectrolyte multilayer.*

Polyelectrolyte / Na-acetate	Deposition time
PEI	10 min
Na-acetate (rinse)	3 x 2 min
Hyaluronic acid	10 min
Na-acetate (rinse)	3 x 2 min
Chitosan	10 - 20 min
Na-acetate (rinse)	3 x 2 min

The deposition was executed in the wells of a 12-well-plate by pipetting 2 mL of solutions next to the samples in the wells and let them immerse before pipetting the solution out of the wells. PEI was used as an anchoring network for the following layers being deposited. During the deposition, the 12-well-plates were placed on a rocker (Stuart^{TM} Gyratory rocker SSL3, Staffordshire, UK) at 20 rpm. The same protocol was then later implemented for the SBSM blocks (figure 10). During the deposition, the stability of SBSM blocks in the polyelectrolyte solution was analyzed by measuring the pH of polyelectrolyte solutions after 10, 20, 40, 60, and 80 min of deposition to ensure that the samples would not degrade during the coating process.

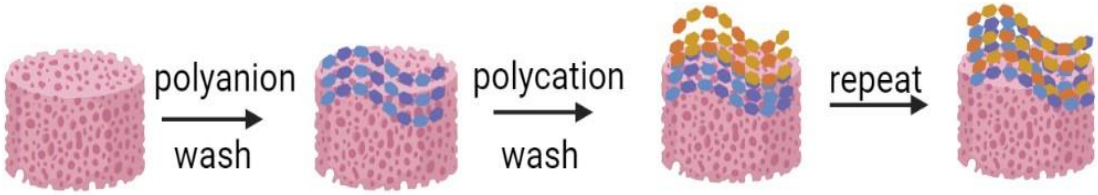

Figure 10. *Schematic representation of the polyelectrolyte multilayer deposition on SBSM blocks.*

4.3.1 Microscopic analysis of polyelectrolyte multilayers

For the microscopic analysis of PEM layers, hyaluronic acid solution was later labelled with fluoresceinamine (FL-NH_2, Acros 400770010) by dissolving it into a 2-(N-morpholino)ethanesulfonic acid (MES) buffer. This was done by mixing HA in MES buffer to yield solution of 1.2 mg/mL of HA and adding 1-Ethyl-3-(3-dimethylaminopropyl)carbodiimide (EDC) in with a final concentration of 1.1 mg/mL and N-hydroxy succinimide (NHS) with 0.68 mg/mL. Then, FL-NH_2 was dissolved in dimethyl sulfoxide (DMSO) at 2 mg/mL and 1.4 mL of this solution were added into the HA solution to be stirred overnight covered with aluminum foil. The FL-NH_2 solution was dialyzed in dialysis membranes (15 cm, 3500 MWCO, Carl Roth) for 5 days in DM-water by changing the dialysis solution twice per day. After 5 days, the solution was transferred into a metal plate which was frozen overnight (- 18 °C). The next day, the metal plate was covered with parafilm (with small holes) and freeze-dried for at least 24 h. From this, a 1 mg/mL HA solution was prepared in 5 mM Na-acetate buffer for the PEM coating.

4.4 Functionalization of a synthetic bone substitute material with collagen

4.4.1 Preparation of collagen suspension

A 7.4 wt% collagen paste was provided by biotrics bioimplants AG (Berlin, Germany). This paste had been processed from split porcine dermis through a sequence of treatments which included liming, splitting and deliming. In liming, hair of the porcine dermis was removed, fat content was reduced, and the raw dermis was swollen. In splitting, rawhide was horizontally cut in different skin depths, while in deliming, the fat content, germ reduction and preservation of split skins was carried out. The split dermis was treated chemically, resulting in swelling, to prepare it for the mechanical treatment where the dermis was minced. The resulting collagen paste was further processed into 5 wt% collagen suspension (equation 1) in DM-water by mixing with UltraTurrax dispersing instrument (T25 easy clean digital, IKA, Staufen, Germany) for 5 min. The pH was measured always using the same pH meter (SevenExcellenceTM S470 pH/conductivity benchtop meter, Mettler Toledo, Giessen, Germany) and adjusted slowly with 0.4M TNP buffer (pH 10.48, M = 380.12 g/mol, PanReacAppliChem) in DM-water to 7.0-7.4.

$$m_{H2O} = \frac{m_p(c_p - c_s)}{c_s} \quad (1)$$

where m_{H2O} denotes the mass of water, m_p means the mass of collagen paste, c_p means the concentration of collagen paste, and c_s means concentration of collagen suspension.

4.4.2 Optimization of collagen dry mass

The concentration of the prepared collagen suspension was verified through dry weight analysis. Single glass dishes were placed in drying and heating chamber (Binder, Fisher Scientific GmbH, Schwerte, Germany) for at least 3h at 102°C to remove inherent water of the glass surface. The collagen samples were only used for the dry weight measurements and were not further used for the applications due to degradation during the heating and drying process. The dish was taken out and placed into a vacuum desiccator (Duran®, DWK Life Sciences GmbH, Mainz, Germany) to cool down with active silica gel for 30 min. After cooling, argon (Ar) was added into the desiccator for another 10 min. The dishes were taken out from the desiccator and weighed with an analytical balance (EG 620-3 NM, KERN & Sohn GmbG, Balingen, Germany), 5 g of collagen suspension was added into each single glass dish and they were placed back into the drying

and heating chamber. The mass of samples was measured after 4 h, 5 h and 6 h of drying and the experiment was performed with three parallel samples (figure 11).

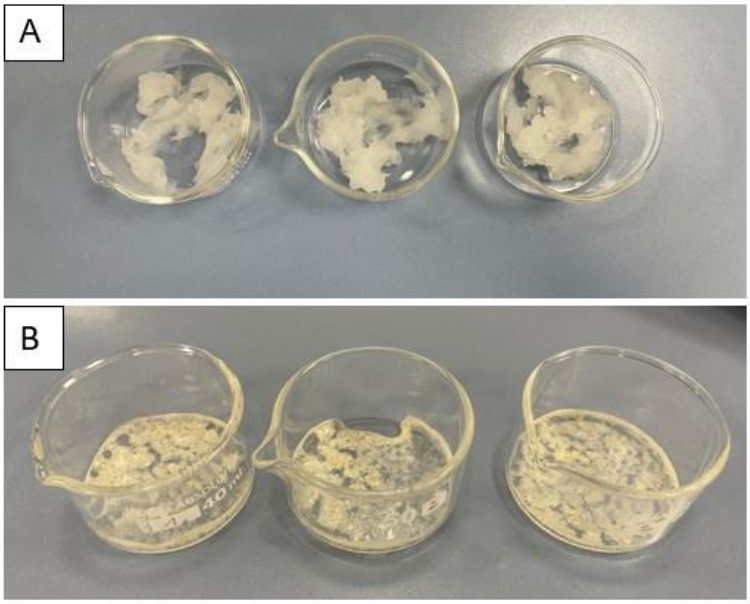

Figure 11. *A 5 wt% collagen suspension A) before and B) after drying in the drying and heating chamber for 6 h.*

The collagen concentration was used to be calculated with the following equation *2.*

$$Collagen\ concentration\ (\mathrm{wt\%}) = \frac{(m_s + m_{ca}) - m_s}{m_{cb}} * 100 \qquad (2)$$

where m_s denotes to mass of single glass dish, m_{ca} was the mass of collagen after drying, and m_{cb} was the mass of collagen before drying.

4.4.3 Collagenase assay

The collagenase assay was used as a characterization method for the collagen network to evaluate the resistance of collagen against enzymatic degradation by collagenase *in vitro*. As the collagen network was analyzed separately from the SBSM, it is called collagen fleece because of its fluffy and fleece-like shape. Table 6 represents the samples that were evaluated in the collagenase assay. These samples were chosen for the evaluation of the difference in degradation with samples with different collagen concentration and freezing method.

***Table 6**. Collagen fleece samples for the collagenase assay.*

Sample	Collagen concentration
1	3 wt% collagen fleece
2	5 wt% collagen fleece
3	5 wt% collagen fleece frozen with dry ice
4	7 wt% collagen fleece

The evaluation was based on the mass loss of the freeze-dried collagen fleece samples due to the digestion by collagenase. The collagenase assay consisted of different steps, which were sample preparation, digestion, washing process and weight analysis (figure 12).

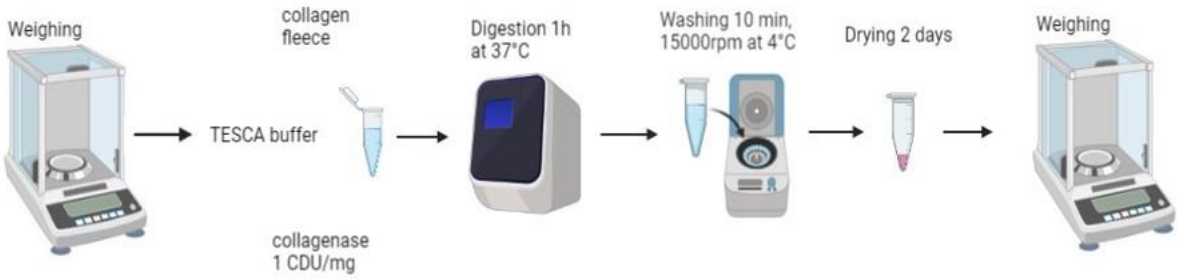

***Figure 12.** Summary of the collagenase assay steps.*

For the preparation step, TESCA buffer (50 mM TES, 0.36 mM $CaCl_2$, pH 7.4) was prepared. For each measurement, three repeats per condition with collagenase (+) and three repeats without collagenase (-) were used as a reference to evaluate the degradation solely by TESCA buffer. Only collagen samples with collagenase (+) were evaluated for better characterization of the collagen network. The samples were cut into pieces (<10mg) and weighed into Eppendorf tubes. Based on the mass of the collagen in each Eppendorf tube, the amount of collagenase was added to yield 1 collagen digestion unit (CDU)/mg. A stock solution at 1 mg/mL of collagenase was prepared in TESCA buffer. For the digestion, TESCA buffer was added to the Eppendorf tubes and the collagenase stock solution at 1 mg/mL was added into each (+) tube. Samples were put into the thermo cycler (ThermoMixer C, Eppendorf AG, Wesseling-Berzdorf, Germany) and incubated for digestion time of 1 h at 37 °C.

The digestion was stopped by placing the tubes into the centrifuge (Centrifuge 5424 R, Eppendorf AG, Hamburg, Germany) for 10 min at 15000 rpm and 4°C. The reaction buffer was pipetted out of the tubes without collecting the pellet in the bottom. Washing

was started by adding 1 mL of DM-water into the tubes, mixed with Vortex (Vortex-Genie™ 2, Scientific Industries Inc., New York, United States) for 2 s and let wash in room temperature for 5 min. The tubes were placed back to the centrifuge for 10 min at 15000 rpm and 4°C. Washing solution was again pipetted out from the tubes without collecting the pellet in the bottom. Tubes were dried with the lid open for 2 days, after which the samples were weighed, and the mass loss was calculated based on the equation 3.

$$mass\ loss\ (\%) = \frac{m_0 - m_1}{m_0} \times 100\% \quad (3)$$

where m_o denotes the mass before immersion, and m_1 after immersion.

4.4.4 Differential Scanning Calorimetry

Differential Scanning Calorimetry (DSC) was used to evaluate the thermal stability of collagen separately from the SBSM. The samples were prepared from collagen fleece with a hole punch (KNIPEX-Werk C. Gustav Putsch KG, Wuppertal, Germany) by cutting out samples from the freeze-dried collagen fleece. The samples were weighed and sealed inside a pan and a lid (both from Concavus®, Netzsch GmbH, Selb, Germany) with a galling press and weighed with an analytical balance (ACJ/ACS, KERN & Sohn GmbH, Balingen, Germany). The sample mass was in the range of 1-6 mg. The samples were heated at a constant rate of 10K/min from 25 °C to 150 °C with an empty sample as the reference with the DSC device (DSC 214 Polyma, Netzsch GmbH, Selb, Germany).

The tested samples for DSC included a 5 wt% collagen fleece, 5 wt% collagen fleece frozen with dry ice (both in pH 7.0), 1 wt% collagen fleece (pH 2.5), 1 wt% collagen fleece (pH 7.0), 7 wt% collagen fleece with hyaluronic acid and 7 wt% collagen fleece without hyaluronic acid. These samples were chosen to analyze the effect of collagen concentration, pH and freezing method in the thermal stability of collagen.

The reaction enthalpy for the samples is positive, representing an endothermic process, which can be seen in the figure 13 with peak going upwards. The surface represents the reaction enthalpy which is calculated by integrating the area of peak and the interpolate baseline between the onset temperature and the end of the peak.

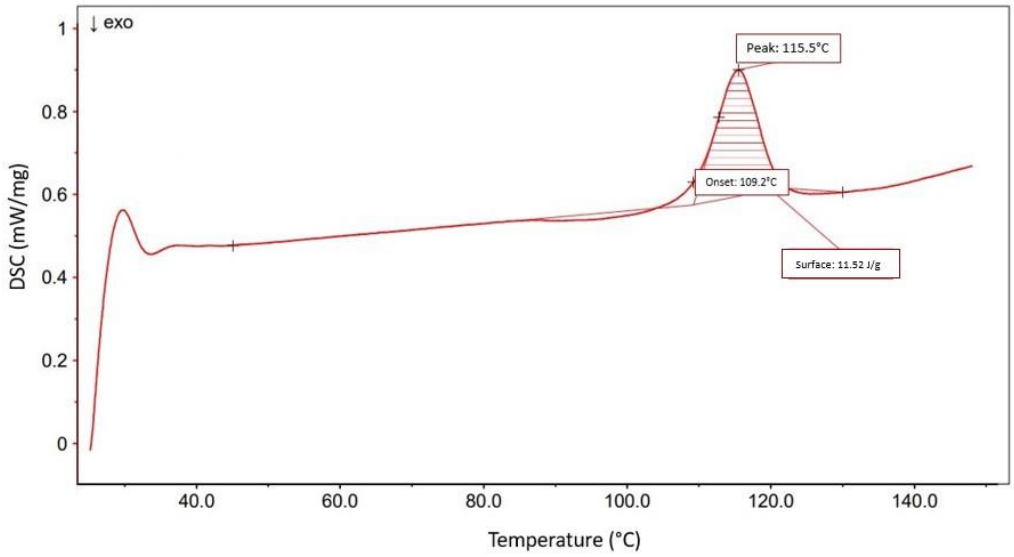

Figure 13. *Example of a DSC curve for 5 wt% collagen sample, where the peak represents the denaturation temperature of the collagen fleece.*

4.5 *In vitro* degradation studies

In vitro degradation studies were conducted in 5 mM sodium acetate buffer and in Hanks' Balanced Salt Solution (HBSS) to compare the degradation of different combinations of SBSM, collagen and bioactive molecules (table 7).

Table 7*. Sample combinations used for the in vitro degradation studies.*

Sample	Combination
1	SBSM block
2	SBSM block with 7 wt% collagen network
3	SBSM granula with 7 wt% collagen network
4	SBSM granula with 7 wt% collagen network, hyaluronic acid and chitosan
5	SBSM granula with 3 wt% collagen network (frozen with dry ice)
6	SBSM granula with 3 wt% collagen network and hyaluronic acid
7	7 wt% collagen fleece

The degradation studies were first conducted in 5 mM sodium acetate buffer to simulate the conditions during PEM coating process (4.3) and to analyze the stability of the SBSM blocks in sodium acetate buffer during this process. The stability of the SBSM blocks with and without collagen network was analyzed by filling Falcon tubes with 8 mL of Na-acetate buffer and 4 SBSM blocks with and without collagen to keep the ratio of buffer and SBSM block the same as during the PEM coating (ratio of buffer:block, 2:1). The samples were immersed for 200 min on a rocker (PS-3D Sunflower Mini-Shaker, BioSan,

Riga, Latvia) with 60 rpm. To analyze the stability of SBSM in Na-acetate, pH and conductivity were measured at different time points: 0, 10, 20, 60, 120 and 200 min but the focus was on the first 10 – 20 min of the deposition which was the most crucial for the stability of SBSM blocks considering the deposition times of polyelectrolyte solutions during PEM coating. Before and after immersion, light microscopy (SteREO Discovery.V12, ZEISS, Oberkochen, Germany) was used to take pictures of the samples to visualize the degradation of the samples. Additionally, the mass loss of samples was measured based on equation 3 (chapter 4.4.3.).

In vitro degradation studies for different combinations of SBSM granula with collagen network, a separate collagen fleece and bioactive molecules were also performed in Hanks' Balanced Salts Solution to evaluate the degradation of samples regarding changes in pH-value, conductivity, and mass loss. The study was used to simulate degradation processes *in vitro* with physiological ion concentration and 37 °C. HBSS was prepared from a powdered salt mixture (without $NaHCO_3$ and phenol red) from Sigma-Aldrich based on the instructions by Hanks, J (1976). The specific details about HBSS preparation are presented in Appendix A.

Before the immersion, the mass of the samples was measured with an analytical balance (ABT120-5DNM, Kern & Sohn, Balingen, Germany). Samples were placed in separate 15 mL Falcon tubes (Centrifuge tubes, Falcon®, VWR, Radnor, Pennsylvania, United States), and the tubes were filled with 7 mL of HBSS. The samples were kept in an incubator (BBD 6220, Thermo Electron Corporation, Langenselbold, Germany) at 37 °C for 28 days. During incubation, pH-value and conductivity were measured at timepoints 0 min, 30 min, 1 h, 3 h, 6 h, 2 d, 7 d, 14 d, 21 d and 28 d. Additionally, the mass loss of the samples was analyzed at timepoints 6 h, 2 d, 7 d, 14 d, 21 d and 28 d after they had been drying at room temperature for at least 48 h and calculated with the equation 3 (chapter 4.4.3).

4.6 Usability studies

The usability studies were performed to analyze the differences in performance in regards of stability, handling, and usability of SBSM functionalized with a collagen network and bioactive molecules (table 8). All samples were compared to a SBSM sample that already existed on the market (maxresorb® flexbone, botiss biomaterials GmbH, Zossen, Germany). This study aimed to simulate the performance of the materials during the indicated application. The study had five participants: three participants had at least 2 years' experience in Research and Development of bone substitutes, one had at least

2 years' experience in Product Management, and one was a student in Material Science and Engineering. All participants were given instruction sheets and a questionnaire to answer (appendix B). For the creation of the usability study, a proof-of-concept experiment was first executed with SBSM composite samples that had been prepared throughout the thesis project.

***Table 8**. Summary of the evaluated samples with evaluation criteria below.*

Sample	Material combination
Reference	5 wt% collagen with SBSM granula (maxresorb® flexbone)
Sample 1	5 wt% collagen with SBSM granula
Sample 2	5 wt% collagen with SBSM granula, hyaluronic acid frozen with dry ice
Sample 3	3 wt% collagen with SBSM granula and chitosan
Sample 4	5 wt% collagen with SBSM granula frozen with dry ice
Sample 5	3 wt% collagen with SBSM granula
Sample 6	7 wt% collagen with SBSM granula

In general, the participants were asked to place the samples in separate wells into a 12-well-plate, to hydrate the samples with approximately 2 mL of DM-water for 2 min. Then, the samples were to be lifted from the wells with tweezers and performance of the samples were to be analyzed. Additionally, the participants were asked to place the samples back into DM-water for a "2nd hydration" to analyze its performance by lifting the sample immediately from the DM-water after placing the sample there. Each sample was rated from 1 – 5, where 1 = poor, 2 = fair, 3 = average, 4 = good and 5 = excellent, based on performance criteria in table 9.

***Table 9.** Evaluation criteria for the usability study.*

Criteria	Explanation
Appearance	Appearance of the sample in dry state. Is it consistent and compact or already broken down?
Applied pressure	After hydration, how much pressure is applied to the sample regarding the softness of the sample?
Moldability	How well can the sample be molded into a ball?
Consistency	Does the ball hold its shape when molding it with fingers?
Coherency	Are the granules sticking together or separating?
2nd hydration	After placing the sample back to DM-water, does it hold together or break apart?

5. RESULTS

5.1 Functionalization of a synthetic bone substitute material with collagen network

5.1.1 Optimization of collagen dry weight

Based on the collagen dry mass, the collagen concentration was used to be calculated with the equation 2 (chapter 4.4.2). However, the equation 2 does not represent the actual collagen concentration because the dry weight includes the dry mass from the TNP buffer which was used for the adjustment of the pH-value. To calculate the actual dry weight and collagen concentration, the dry mass of the TNP buffer was measured, resulting that approximately 10 wt% of the TNP buffer is the dry weight of salts. This information was used to calculate the percentage of TNP salts in the mass of the collagen suspension (equation 3).

$$Percentage\ of\ TNP\ salts\ (\%) = \frac{m_{TNP}*0.1}{m_{TNP+col+H2O}} * 100 \quad (3)$$

where m_{TNP} denotes the mass of TNP buffer, and $m_{TNP+col+H2O}$ was the mass of the collagen suspension, including the mass of TNP buffer, collagen paste and DM-water.

From equation 3, the actual collagen concentration was then calculated by taking into consideration the dry weight of the TNP salts. Equation 4 represents the final collagen concentration.

$$Actual\ collagen\ concentration\ (\mathrm{wt\%}) = \frac{(m_{ca}+m_{TNP})*c_{TNPd}}{m_{cb}} * 100 \quad (4)$$

where m_{ca} denotes the mass of collagen after drying, m_{TNP} was the percentage of TNP salts, C_{TNPd} was the dry weight of collagen from equation 2, and m_{cb} was the mass of collagen before drying.

5.1.2 Analysis of the collagen network penetration

The functionalization of a synthetic bone substitute material with collagen network aims for the penetration of the collagen network throughout the SBSM material. The following pictures from the microscopic analysis were taken to evaluate and compare the penetration of the collagen network inside the SBSM block and granula to find out which form of the SBSM should be further functionalized with bioactive molecules.

Figure 14 represents two different freeze-dried SBSM block samples with riboflavin labeled and non-labeled collagen network. The riboflavin-labeled collagen network can be more easily distinguished from the pictures with the yellow color, and therefore was further used to analyze the penetration of the collagen network inside the SBSM blocks.

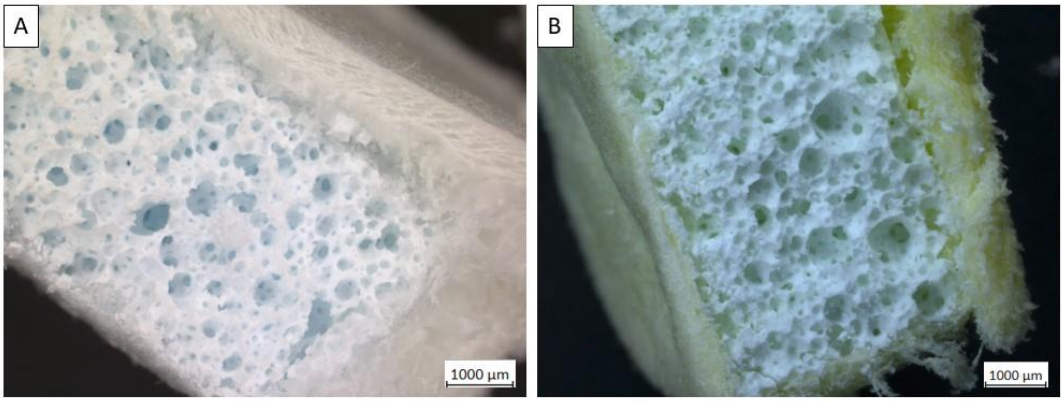

Figure 14. *SBSM blocks with A) non-labeled collagen network and B) 0.01 %(w/v) riboflavin labeled collagen network with 12.5x magnification.*

Microscopic analysis was also done for SBSM block samples with different pre-treatments, including 2 min in ultrasonic bath, 2 min hydration in DM-water or left in room temperature for 45 min before the freeze-drying. Figure 15 represents a freeze-dried SBSM with riboflavin-stained collagen left in room temperature before freeze-drying. When comparing the sample to the figure 14B, there is no detectable difference in the penetration of the collagen network inside to the SBSM block.

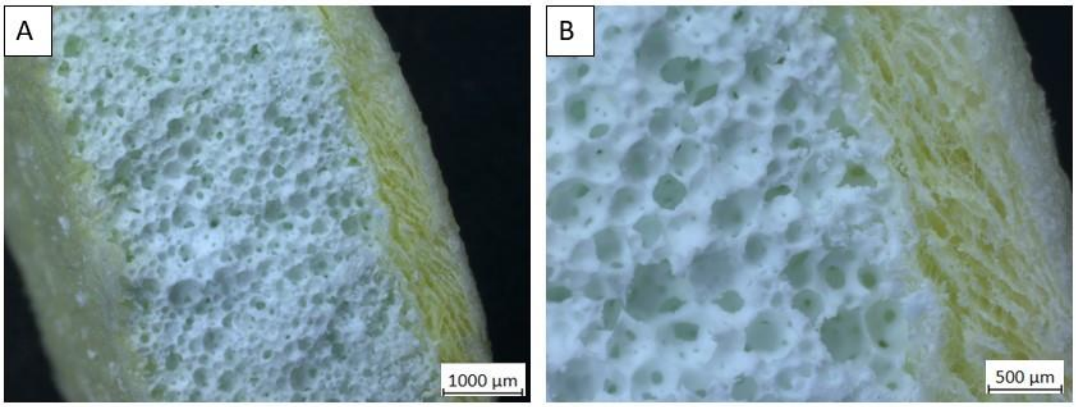

Figure 15. *Microscopic pictures of freeze-dried SBSM block with 0.01 % (w/v) riboflavin-stained collagen network left in room temperature for 45 min before freeze-drying with A)12.5x magnification and B) 22x magnification.*

Figure 16 represents a freeze-dried SBSM with riboflavin-stained collagen network that was pre-treated by hydrating in DM-water for 2 min. When comparing to the reference

sample in figure 14, there is a small change in the edge of the SBSM: it looks more dense and less porous on the right side of the block. Additionally, the collagen network has penetrated inside the SBSM block slightly towards the inner parts of the block which can be seen as a yellow color.

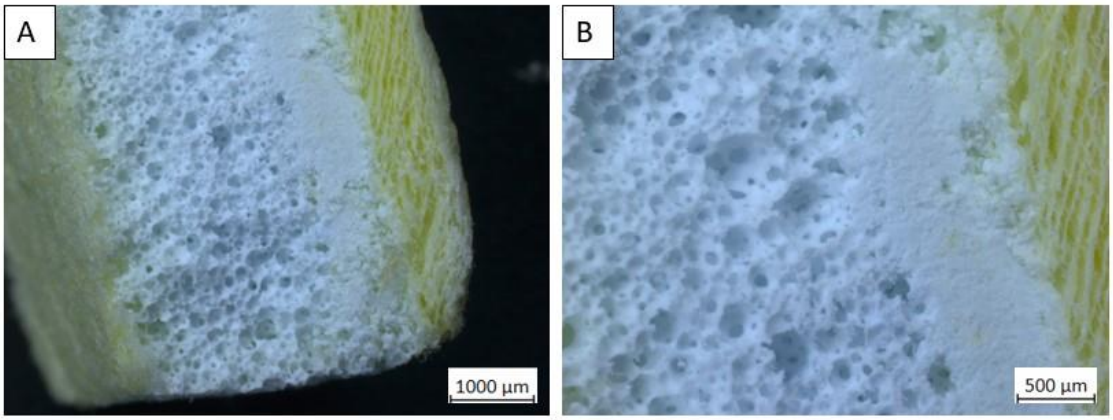

Figure 16. *Microscopic pictures of freeze-dried SBSM with 0.01 % (w/v) riboflavin-stained collagen network pre-treated with hydration in DM-water with A) 12.5x magnification and B) 22x magnification.*

Figure 17 represents freeze-dried SBSM block with riboflavin-stained collagen network that was pre-treated in ultrasonic bath for 2 min before freeze-drying. When comparing the SBSM to the reference, there are bigger pores filled with collagen (yellow). However, the collagen network has penetrated only to some parts of the SBSM block and not throughout the whole structure.

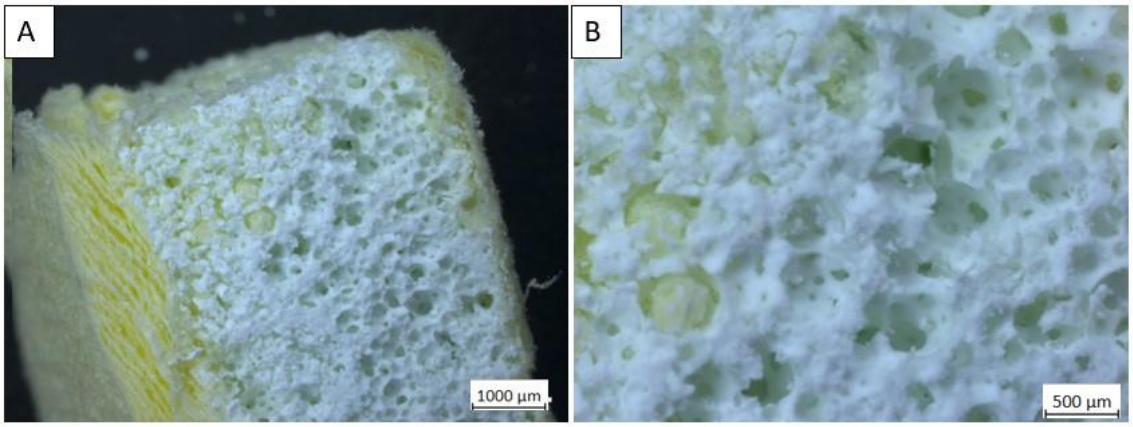

Figure 17. *Microscopic pictures of freeze-dried SBSM with 0.01 % (w/v) riboflavin-stained collagen network pre-treated in ultrasonic bath with A) 12.5x magnification and B) 22x magnification.*

When comparing the penetration of the collagen network into the SBSM block and granula, there is a clear difference. Figure 18 represents SBSM granula samples where collagen network can be seen as shiny and gel-like structure inside the material. The collagen network has penetrated inside the SBSM granula better compared to the SBSM block, where the collagen network is mostly on the outer parts of the SBSM.

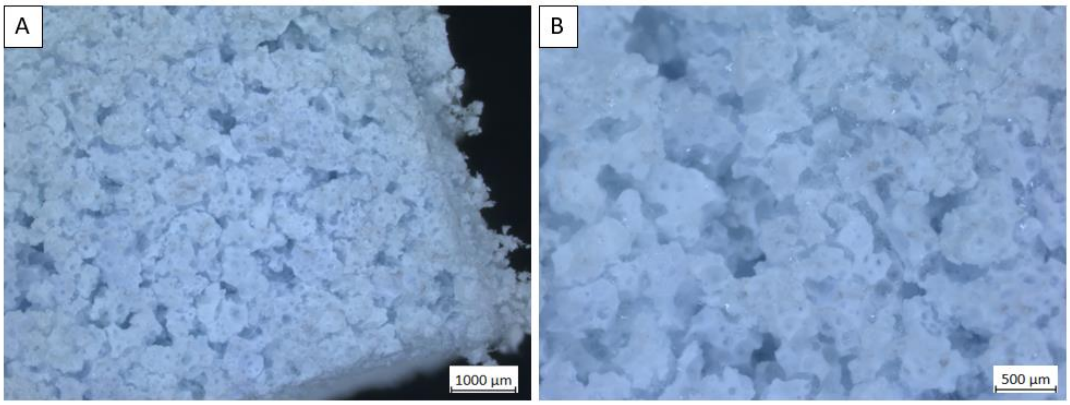

Figure 18. *Microscopic pictures of SBSM granula with 3 wt% collagen network penetrated inside, where A) 12x magnification and B) 22.5x magnification.*

Figure 19 represents a close-up picture of the successfully developed SBSM granula with collagen and bioactive molecule. The penetration of the collagen network has been successful into the SBSM granula. This supports the findings from the microscopic pictures where collagen network was shown to have a better penetration inside SBSM granula compared to the block. However, there are differences in the prepared SBSM samples. Sample with chitosan (left A) has bigger pore size compared to the reference sample without chitosan (right A). Additionally, the structure is less compact, and granules are starting to disintegrate when moving the sample. Sample frozen with dry ice (left B) has a more similar structure to the reference sample (right B).

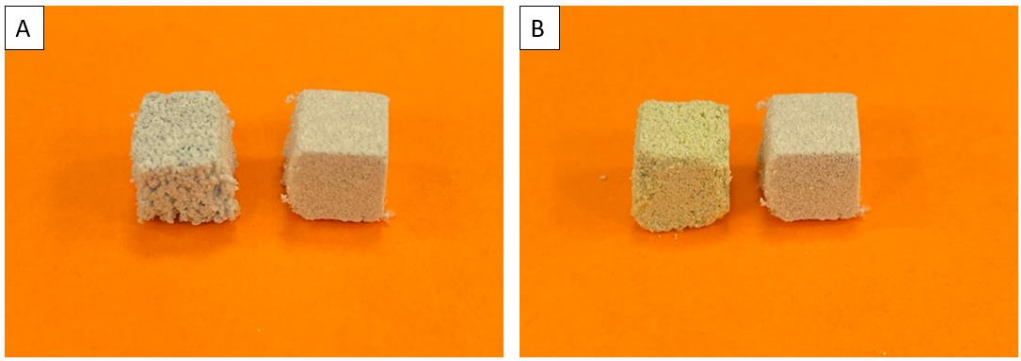

Figure 19. *A) SBSM granula with 3 wt% collagen and chitosan (left) in comparison to a reference sample with SBSM with 5 wt% collagen frozen with dry ice. B) SBSM granula with 3 wt% collagen frozen with dry ice compared to the same reference sample as in A).*

5.1.3 Collagenase assay for the evaluation of the resistance of collagen against enzymatic degradation

Functionalization of the SBSM included the addition of a collagen network. The collagenase assay was used to as a characterization method for the collagen network to evaluate the resistance of collagen against enzymatic degradation by collagenase *in vitro* and to find out the most suitable collagen concentration for the application. The properties of the collagen network were analyzed separately from the SBSM composite, thus referring to it as collagen fleece in the text. Differences in the enzymatic degradation with different concentrations and freezing methods of collagen were compared and those parameters thereby optimized. This was done through the evaluation of the mass loss of the samples due to the digestion of collagenase. Figure 20 represents the mean and standard deviation of the mass loss of the collagen fleece samples due to collagenase (n=3) and due to TESCA buffer (n=3).

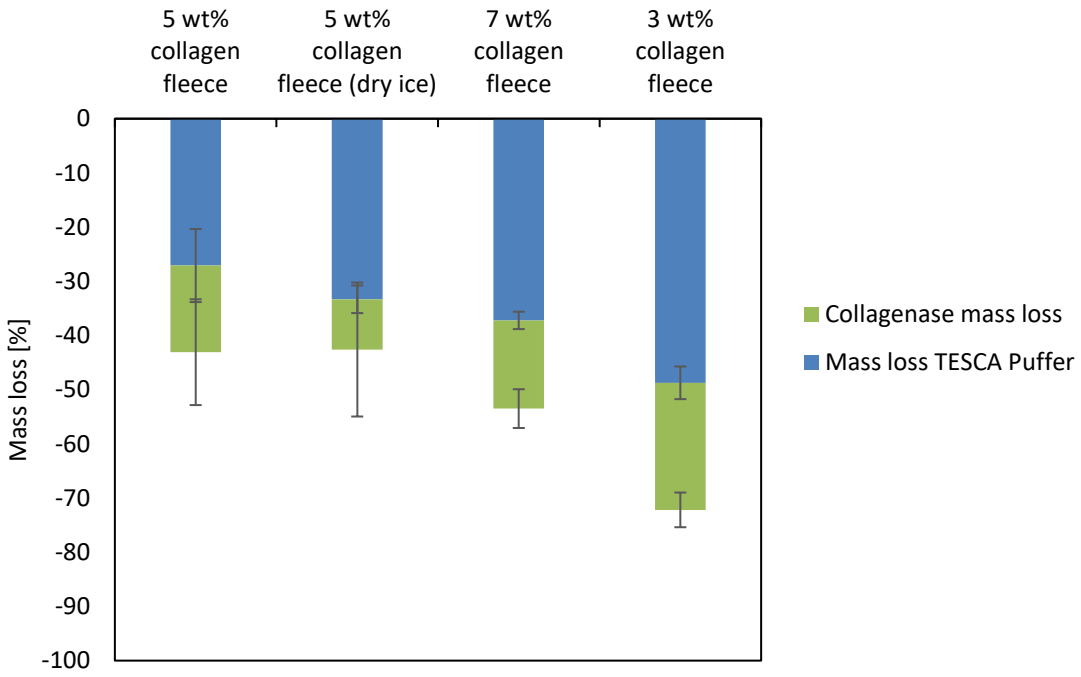

Figure 20. *Mass loss of collagen fleece samples during enzymatic degradation by collagenase in vitro.*

The mass loss values for each mean with standard deviations are shown in table 10. The highest mass loss due to collagenase was seen for the sample with 3 wt% collagen concentration (mass loss 23.4% ± 3.2) and the lowest mass loss for the sample with 5 wt% collagen frozen with dry ice (mass loss only 9.3% ± 2.4). There was a clear difference in mass loss between samples with same concentration (5 wt%) but with different

freezing methods: the sample frozen with dry ice had noticeably smaller mass loss. There was only a small difference between mass loss of samples with collagen concentrations of 5 wt% (mass loss 16.0 %) and 7 wt% (mass loss 16.3 %) due to collagenase.

Table 10. *Mean values of collagen fleece mass loss due to collagenase and TESCA buffer with standard deviations.*

Sample	5 wt% collagen	5 wt% collagen dry ice	7 wt% collagen	3 wt% collagen
Total mass loss (%)	-43.37	-42.59	-49.31	-72.18
Mass loss TESCA buffer (%)	-27.09	-33.32	-37.22	-48.74
Mass loss collagenase (%)	-15.99	-9.27	-16.28	-23.45
Standard deviation (collagenase)	9.76	2.36	5.34	3.20
Standard deviation (TESCA buffer)	6.74	2.55	1.60	3.01

5.1.4 Differential Scanning Calorimetry

Differential Scanning Calorimetry (DSC) was used to evaluate the denaturation temperature of collagen and to characterize the collagen network further. This was done for the collagen fleece samples without the SBSM. Denaturation temperatures were measured for six different samples seen in figure 21. The difference in denaturation temperatures between 5 wt% collagen suspension frozen with or without dry ice was small or not detectable (0.5 °C). Meanwhile, the difference between 1 wt% collagen fleece samples with pH-value of 1.0 and 7.0 is different. The sample with pH 2.5 has a lower denaturation temperature (106.7 °C) compared to the sample in neutral pH (111.6 °C). When hyaluronic acid was added to 7 wt% collagen sample, the denaturation was slightly higher (122.8 °C) compared to 7 wt% collagen sample without hyaluronic acid (119.6 °C).

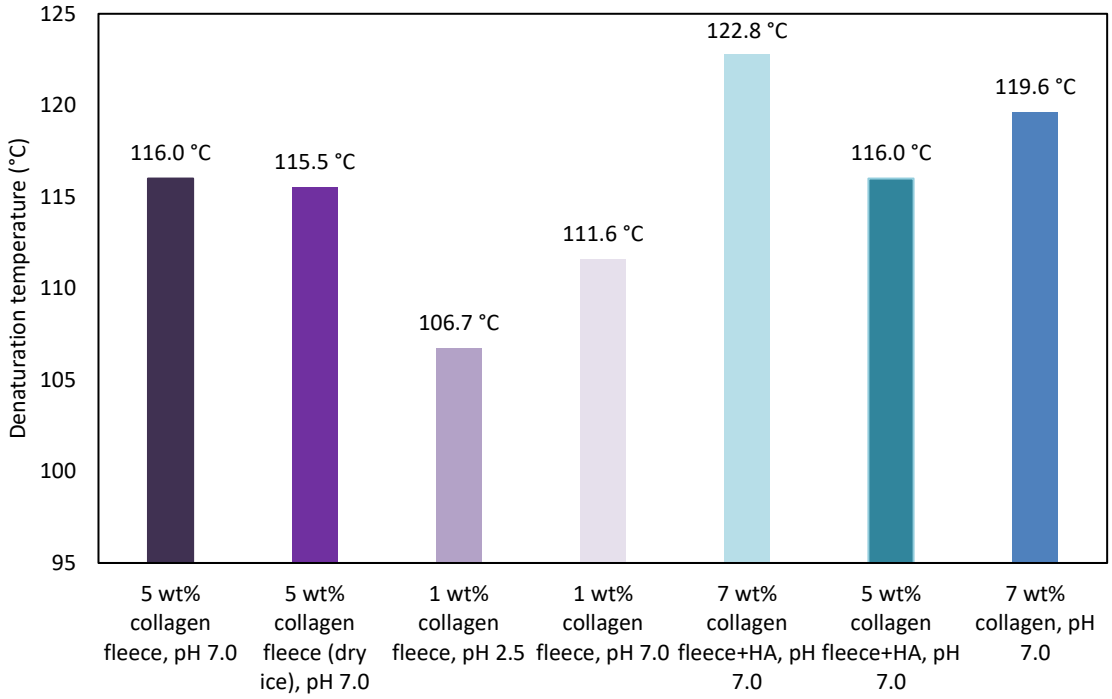

Figure 21. *Denaturation temperatures (°C) of different collagen fleece samples measured with the DSC.*

5.2 Functionalization of a synthetic bone substitute material with bioactive molecules

5.2.1 Polyelectrolyte multilayer deposition

Polyelectrolyte multilayer (PEM) deposition was used as a method to incorporate bioactive molecules, including hyaluronic acid and chitosan to the synthetic bone substitute material. The method utilized an alternative pipetting of the negatively charged (hyaluronic acid) and positively charged (chitosan) polyelectrolyte solutions, resulting in the adsorption of the solutions to the SBSM due to their electrostatic interactions because of their opposite charges. As a proof-of-concept, the PEM deposition was first conducted on Si-Wafers with and without activation layer of PEI before the deposition on the SBSM. The samples were analyzed by the project partner (NMI) by ellipsometry with a spectral range of 450 - 850 nm to detect the thickness of the PEM layers (table 12). The effect of PEI activation layer was seen with the noticeably thicker PEM layer deposition (18.1 nm ± 7.4) with PEI compared to the thickness without PEI (10.9 nm ± 3.8). The standard deviation was high, especially for the sample with PEI activation layer. The PEM deposition on Si-Wafers as a proof-of-concept showed that activation layer with PEI increases the thickness of the PEM film and the amount of polymer adsorbed in the film.

Table 11. *Thickness of the deposited PEM on Si-Wafer with and without PEI activation layer.*

Sample	Thickness (average)	Standard deviation
Si-Wafer without PEI	10.9 nm	3.8
Si-Wafer with PEI	18.1 nm	7.3

After the proof of concept and successful deposition of polyelectrolytes on the Si-Wafers, the PEM deposition was conducted on the SBSM granula with fluorescein labeled hyaluronic acid as one of the polyelectrolyte solutions. The aim was to confirm the success of the PEM deposition on the SBSM. Figure 22 represents fluorescence microscope pictures of SBSM granula with fluorescein labeled hyaluronic acid as one of the deposited polyelectrolytes. The pictures were taken by the project partner at the NMI. Fluorescence microscope utilizes the light emission by materials and molecules that have absorbed light. The PEM deposition on the SBSM was successful which is seen as the light green color on the pictures. The difference between SBSM samples with and without activation layer of PEI is small. The sample without PEI seems slightly darker, with less fluorescein labeled hyaluronic acid, and therefore not as much fluorescence.

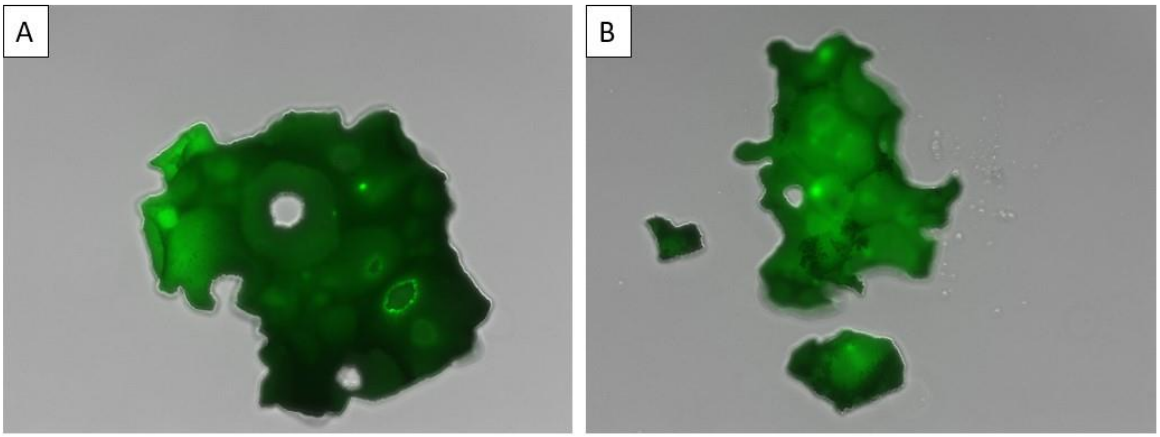

Figure 22. *Fluorescence microscope pictures (5 x, 40 ms, 100 ms) of SBSM after polyelectrolyte multilayer deposition with chitosan and fluorescein labeled hyaluronic acid polyelectrolyte solutions A) without activation layer of PEI and B) with activation layer of PEI.*

5.2.2 Stability of a synthetic bone substitute material during polyelectrolyte multilayer deposition

Stability studies were conducted in Na-acetate buffer to simulate the conditions during PEM coating process. The aim was to analyze the possible changes in pH and conductivity by immersing samples in Na-acetate buffer. High rise in pH could potentially affect the conformity of the polyelectrolyte layers. Further the stability of the materials during the PEM coating process should be assessed. The pH-values of the buffer were measured (figure 23), where conditions are shown as mean values (n=3) with error bars as standard deviation for SBSM blocks (experiment 1 and 2) and as mean values (n=3) with error bars as standard deviation for other samples. The highest increase in pH was for the samples with only SBSM blocks (experiments 1 and 2). Samples with collagen had a sharp increase in pH already during the first 10 min but stayed rather stable until the rest of the experiment. There was no difference between samples with SBSM block or granula.

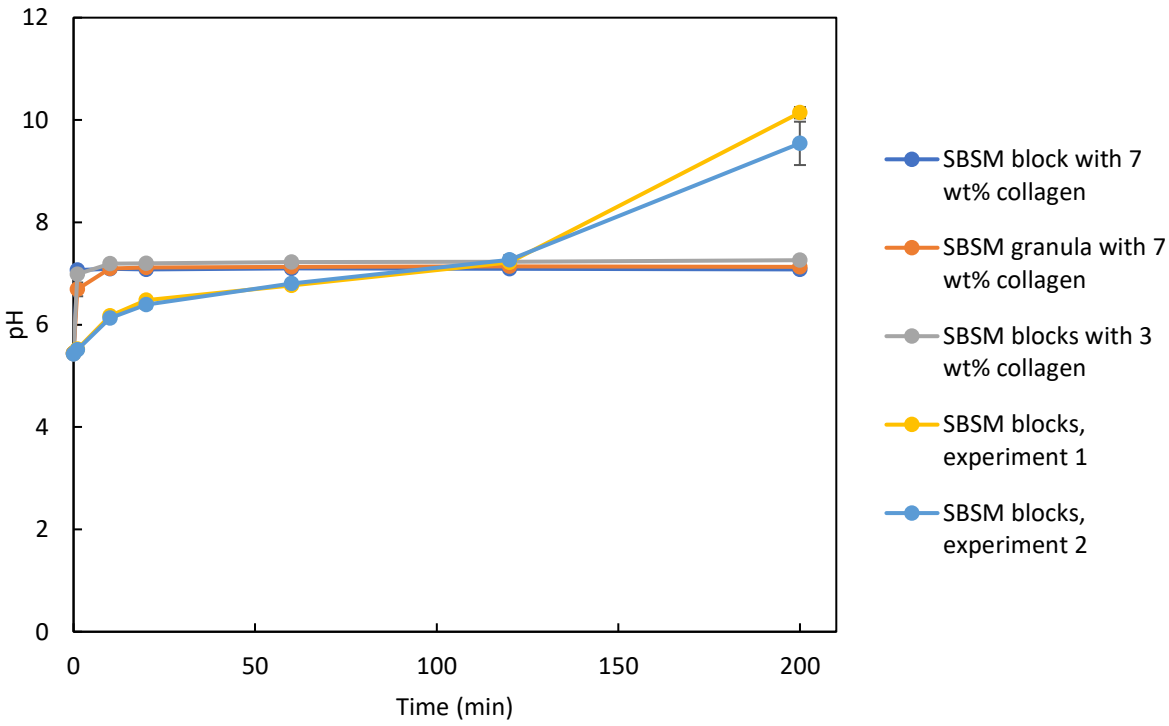

Figure 23. *Changes in pH of Na-acetate buffer during a 200 min immersion of SBSM blocks from two parallel experiments, SBSM blocks with 7 wt% collagen, SBSM granula with 7 wt% collagen and SBSM blocks with 3 wt% collagen.*

Beside the pH-value, also the conductivity of the Na-acetate buffer was measured, (figure 24), where conditions are shown as mean values (n=3) with error bars as standard

deviation for SBSM blocks (experiment 1 and 2) and as mean values (n=3) with error bars as standard deviation for other samples. There was a clear rise in the conductivity of the buffer with SBSM block or granula with collagen network already during the first 10 min of immersion while the conductivity of the buffer stays more stable the whole time for the tubes with only SBSM blocks. When comparing the conductivity changes, there was a clear difference between the conductivity of SBSM blocks with 3 wt% collagen (< 3500 µS/cm) and SBSM blocks with 7 wt% collagen (< 6500 µS/cm). Also, the difference between the conductivity in tube with SBSM block with collagen compared to the tubes with only SBSM blocks was big in the end of the immersion (> 6000 µS/cm vs. < 1000 µS/cm). The SBSM granula with 7 wt% collagen had a slower increase in conductivity compared to the SBSM block with 7 wt% collagen. There was also a noticeable difference in conductivity between the SBSM block with collagen and with the SBSM granula with collagen (over 6000 µS/cm vs 4000 µS/cm). The small change in the conductivity for the SBSM blocks (experiment 1 and 2) was within 10 min from the beginning of the immersion.

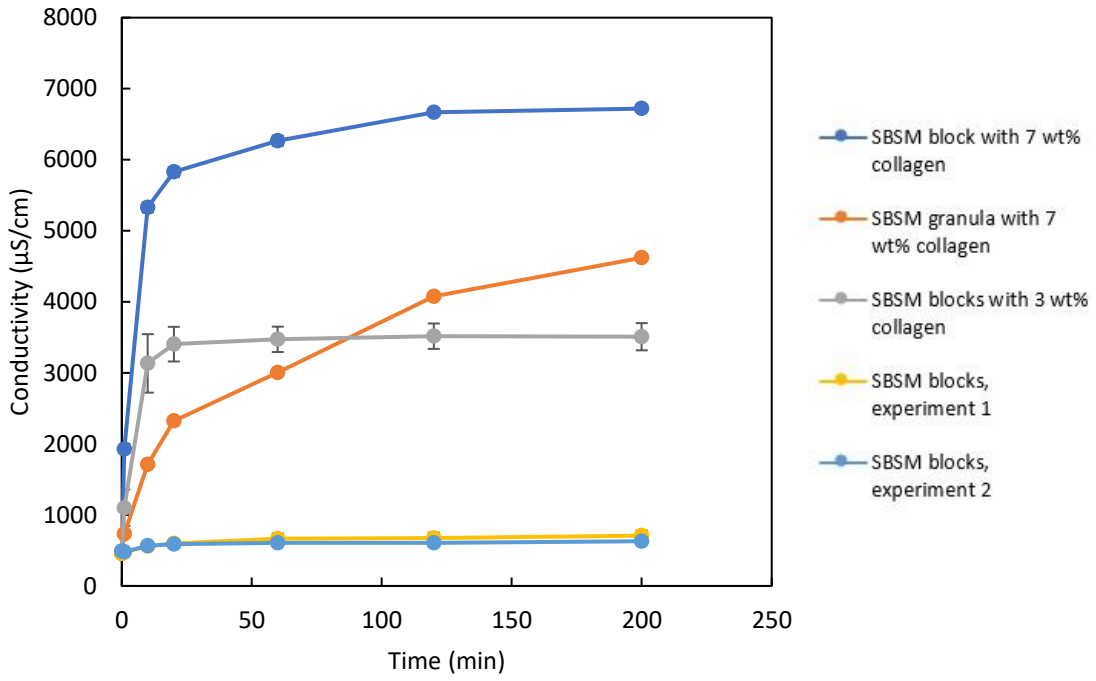

Figure 24. *Changes in conductivity of the Na-acetate buffer during a 200 min immersion of SBS blocks from two different experiments, SBS blocks with 7 wt% collagen, SBS granula with 7 wt% collagen and SBS blocks with 3 wt% collagen.*

Mass loss of samples are summarized in appendix C. In general, the mass loss of SBSM blocks during a 200 min of immersion was small or not detectable (less than 1%). On the other hand, the mass loss for the SBSM blocks with 7 wt% collagen suspension was

slightly higher (4 – 8 %) and for SBSM granula with 7 wt% collagen too (4 – 5 %). There was no big difference between the mass loss of SBSM block with collagen compared to the SBSM granula with collagen. The changes in the collagen network of the SBSM block and granula were also analyzed with a microscope.

5.3 *In vitro* degradation in Hanks' Balanced Salt Solution

In vitro degradation studies for different combinations of SBSM, collagen and bioactive molecule was performed in Hanks' Balanced Salts Solution (HBSS). The complete data from the degradation study can be found in appendix D. Changes in the pH-values of HBSS were measured (figure 25). Each condition was performed with three parallel samples (n=3), in the diagram the mean value and the error are stated as the standard deviation of these parallel samples. The highest increase in pH was for SBSM blocks (up to 8.64 ± 0.04) while all the other samples included collagen network and experienced a slow decrease of the pH-values. For the samples with SBSM granula + collagen (dry ice) and SBSM granula + collagen + the change in pH was smaller for the first seven days compared to the other samples. The lowest pH in the end was for the samples with hyaluronic acid.

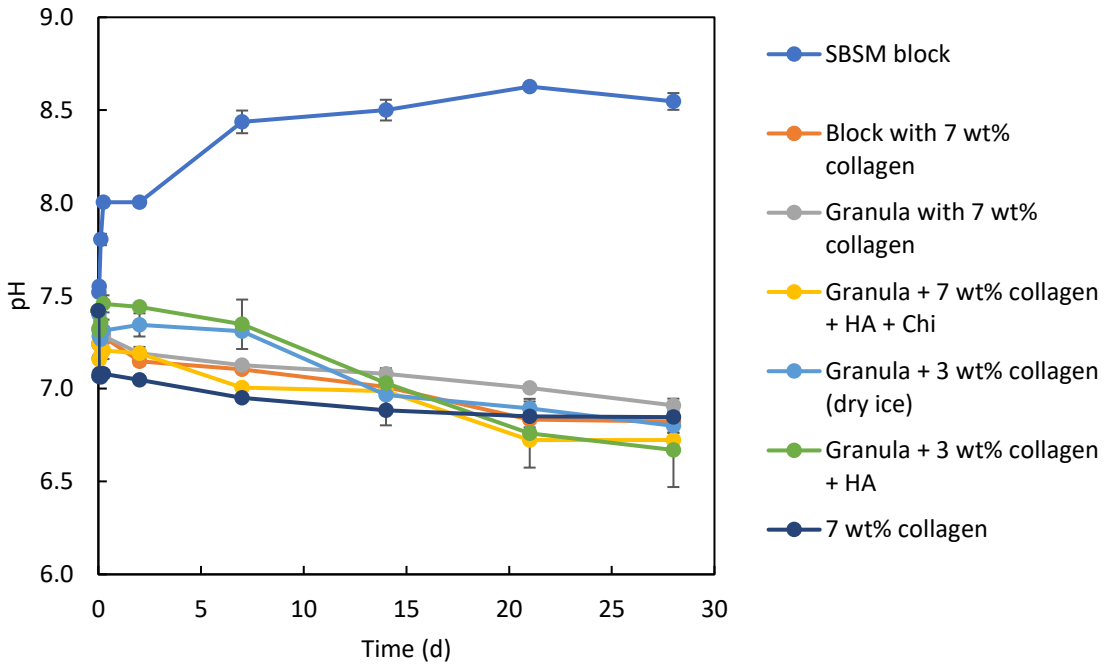

Figure 25. *Changes in pH for 28 days immersion of SBSM in HBSS.*

To get a better understanding of what happens directly after the samples are put in HBSS, figure 26 represents the first seven hours of immersion. There was a big drop in pH for collagen fleece already within the first 30 min (from 7.42 ± 0.0 to 7.07 ± 0.01). The smallest change in pH during the first 7 hours was for the sample with SBSM + collagen + hyaluronic acid (from 7.42 to 7.46). Samples with 3 wt% collagen with hyaluronic acid or dry ice have the steadiest pH throughout the first seven hours of immersion.

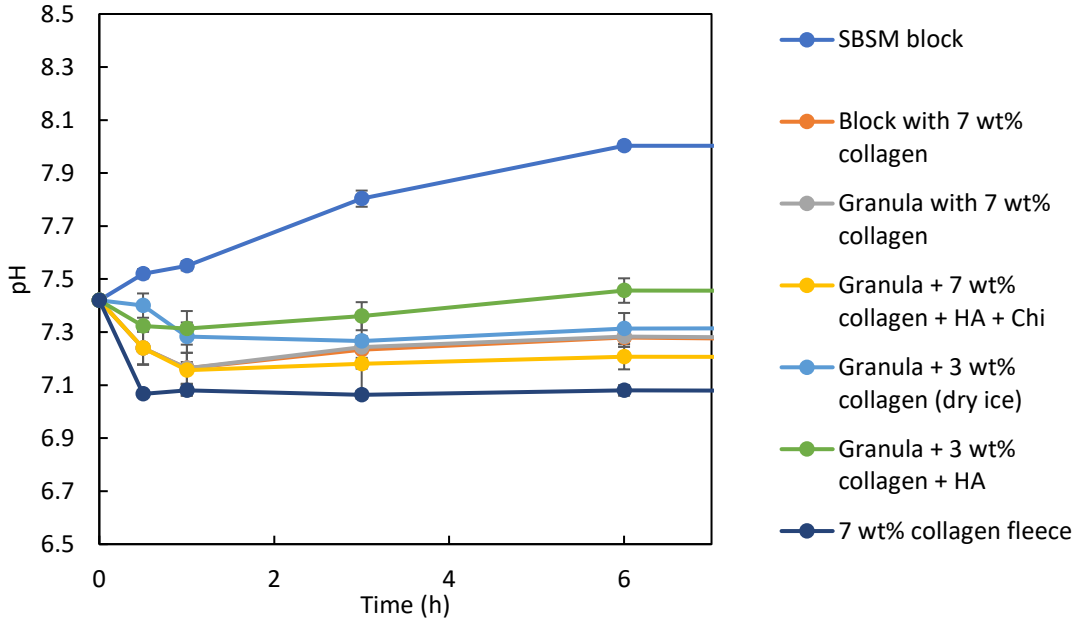

Figure 26. *Changes in pH for 7 hours immersion of SBSM in HBSS.*

Changes of the conductivity of HBSS were measured (figure 27). The highest increase in conductivity was shown for the solution with only collagen fleece sample. The standard deviation was also high for these samples. The conductivity was shown to be higher for the samples with higher collagen concentrations compared to the lower concentrations. The lowest conductivity was shown for the SBSM block sample with no collagen network.

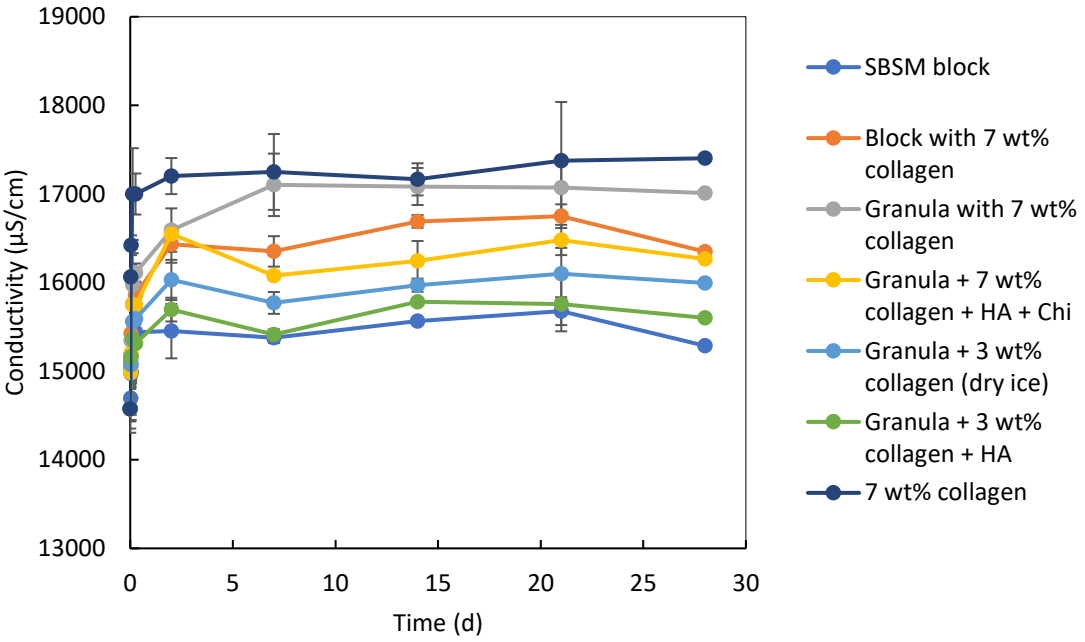

Figure 27. *Changes in conductivity for 28 days immersion of SBSM in HBSS.*

To better observe what happens when the samples are put in HBSS, figure 28 represents the first seven hours of immersion. Collagen fleece samples had a fast increase of the conductivity from 14 600 µS/cm ± 0.0 to 16 900 µS/cm ± 111 (+2 420 µS/cm) compared to sample with SBSM + collagen + HA from 14 600 µS/cm ± 0.0 to 15 300 µS/cm ± 379 (+738 µS/cm) during that time.

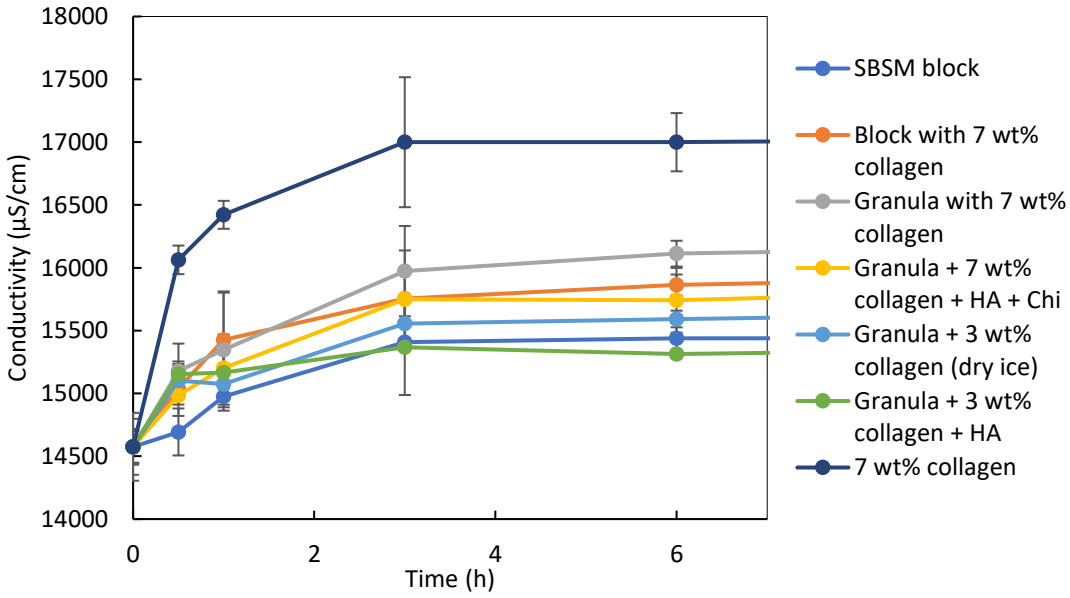

Figure 28. *Changes in conductivity for 7 hours immersion of SBSM in HBSS.*

The mass loss of samples with different combinations was analyzed and then the mean values (n = 3) were displayed (figure 29). The standard deviation of the samples is very high. The biggest mass loss was seen for collagen fleece samples, which had degraded fully in the solution already after 7 days of immersion. The smallest mass loss was seen for the SBSM block sample with collagen (-11.8 % ± 0.72).

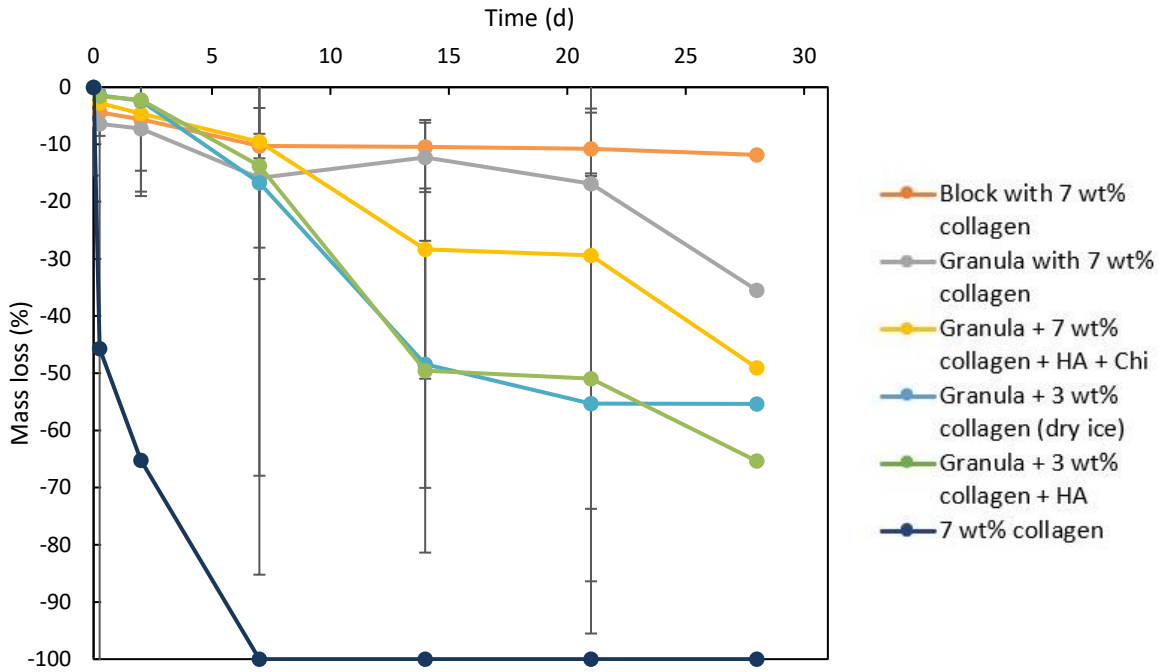

Figure 29. *Mass loss (%) of SBSM for 28 days immersion in HBSS.*

5.3.1 Microscopic analysis of the *in vitro* degradation samples

Microscopic analysis was done for the HBSS samples to observe changes in the shape before and after the immersion. Additionally, to observe the disintegration of the collagen network from the SBSM. Figure 30 represents the collagen fleece stained with riboflavin before and after of 6 h immersion in HBSS. The collagen fleece has lost its porosity and has shrunk into a dense and stiff material.

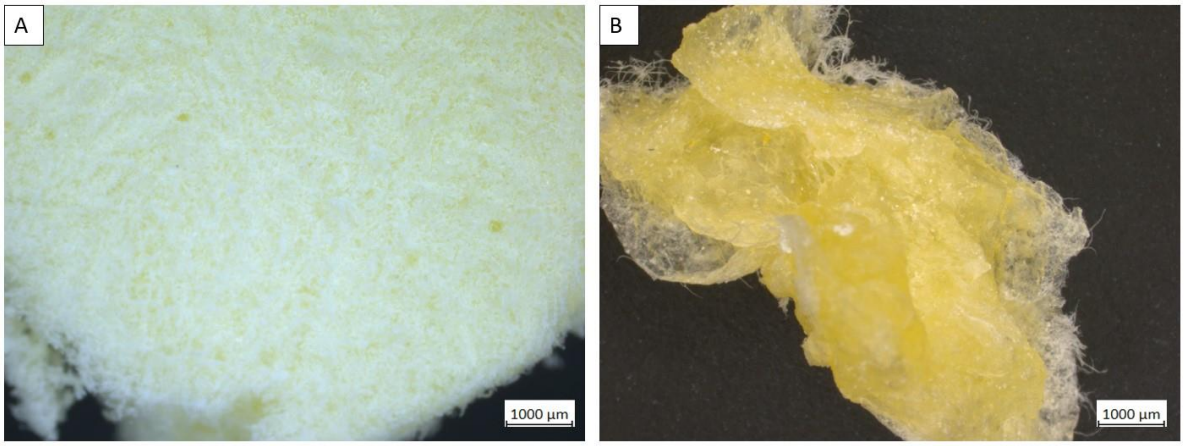

Figure 30. *Microscopic pictures of collagen fleece labelled with riboflavin A) before and B) after 6h of immersion in HBSS with 12x magnification.*

Figure 31 represents a freeze-dried SBSM block with collagen network labelled with riboflavin before and after 7 days immersion in HBSS. The collagen network around the SBSM has disintegrated into the HBSS solution and there is only a small layer visible in the corner of the SBSM block.

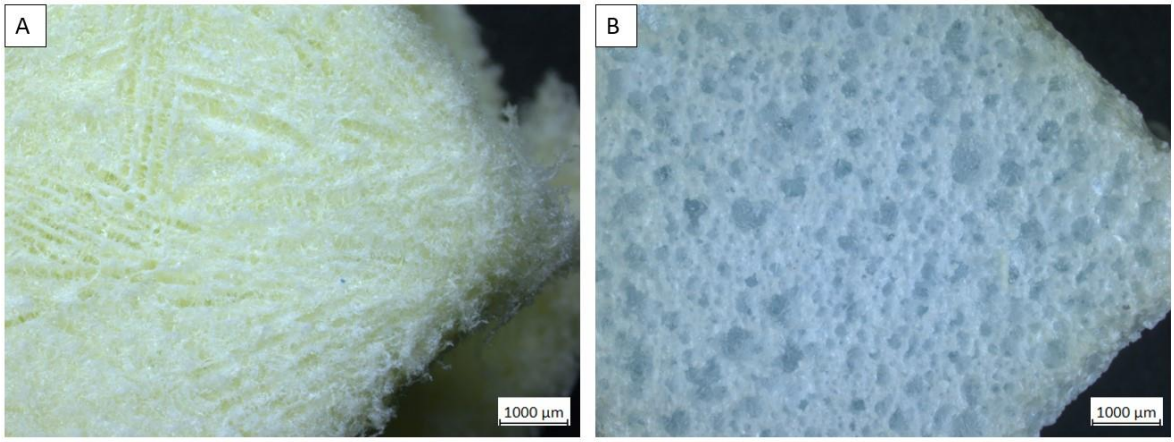

Figure 31. *Microscopic pictures of SBSM block with collagen network A) before and B) after 7 d of immersion in HBSS with 12x magnification.*

Figure 32 represents a freeze-dried SBSM granula sample with collagen network before and after 7 days of immersion in HBSS. The SBSM sample is still sticking together and the collagen has not completely disintegrated from the structure, because this would lead to the breakage of the structure.

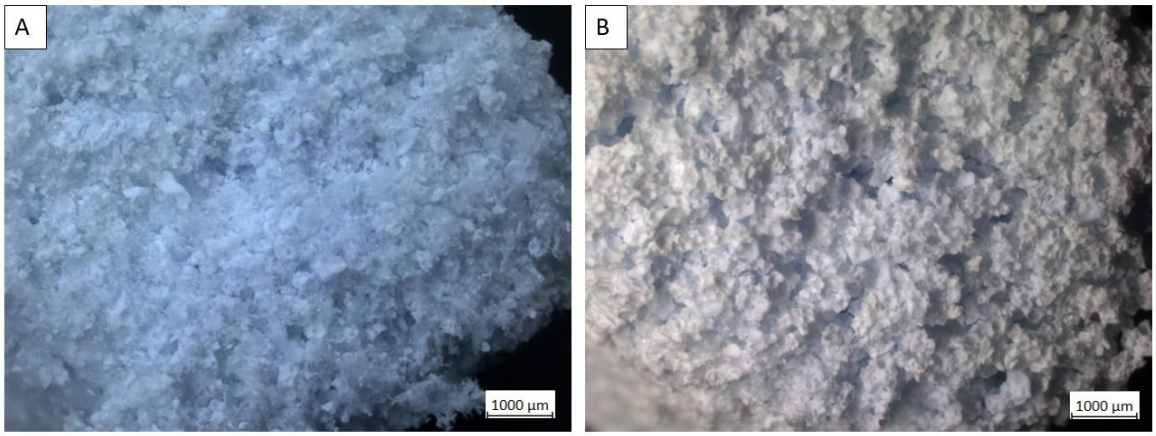

Figure 32. *Microscopic pictures of the SBSM granula with collagen network A) before and B) after 7d of immersion in HBSS with 12x magnification.*

5.4 Usability studies

A pretrial experiment was conducted for samples before conducting a usability study for participants. The results from the pretrial (n = 1) are shown in table 13. From the results of the proof-of concept, samples were picked for the usability study. The highest grades were given to sample 1 with SBSM, 5 wt% collagen and sample 7 with SBSM, 5 wt% collagen and hyaluronic acid frozen with dry ice. The lowest score was given to sample 3 with SBSM 3 wt% collagen and kappa carrageenan and sample 5 with SBSM and 3 wt% collagen. They were both particularly unstable during the 2nd hydration.

Table 12*. Results from pretrial of usability study, where col. = collagen, CS = chondroitin sulfate, KC = kappa carrageenan, HA = hyaluronic acid, Chi = chitosan and DI = dry ice freezing.*

	Sample 1	Sample 2	Sample 3	Sample 4	Sample 5	Sample 6	Sample 7
Sample	**SBSM + 5 wt% col.**	**SBSM + 3 wt% col. + CS**	**SBSM + 3 wt% col. + KC**	**SBSM + 5 wt% col. (DI)**	**SBSM + 5 wt% col.**	**SBSM + 7 wt% col.**	**SBSM + 5 wt% col. + HA (DI)**
Appearance	4	3	3	5	3	3	5
Pressure	4	3	3	4	2	2	5
Moldability	4	4	2	5	2	3	5
Con-sistency	5	2	2	5	2	4	5
Coherency	5	2	3	4	2	3	5
2nd hydra-tion	4	0	0	5	2	3	4
Overall experience	4	2	2	4	2	3	5
Average	4.29	2.28	2.14	4.57	2.14	3.0	4.86

Usability study for the performance of different combinations of SBSM granula, collagen and bioactive molecules was conducted in dry and hydrated stage. The results are presented as a mean value with standard deviation as error from 5 participants in table 14.

***Table 13**. Results of usability study given as average from five participants, where reference sample is a commercial SBSM, col. = collagen, HA = hyaluronic acid, Chi = chitosan and DI = dry ice freezing. The variation is shown as standard deviation (±).*

	Reference	Sample 1	Sample 2	Sample 3	Sample 4	Sample 5	Sample 6
Sample	SBSM + 5 wt% col. (commercial)	SBSM + 5 wt% col.	SBSM + 5 wt% col. + HA (DI)	SBSM + 3 wt% col. + Chi	SBSM + 5 wt% col. (DI)	SBSM + 3 wt% col.	SBSM + 7 wt% col.
Appearance	5	4	4.2	3.2	4.6	2.8	3.2
Pressure	4	3.4	3.6	3.6	3.6	2.6	2.25
Moldability	3	3.8	4.2	2.4	4.2	2.2	3
Consistency	2.6	4.4	4.2	2.6	4.6	2.2	3.6
Coherency	3.2	4.2	4.4	2.4	4.2	1.8	3.4
2nd hydration	3	4	3.6	3	4.6	2.4	2.25
Overall experience	3.2	3.8	4.2	3	4.2	2.0	2.8
Average	3.43 (± 0.99)	3.94 (± 0.37)	4.06 (± 0.41)	2.89 (± 0.72)	4.29 (± 0.81)	2.29 (± 0.77)	2.96 (± 0.44)

The highest grades were given to sample 2 with SBSM, 5 wt% collagen and hyaluronic acid frozen with dry ice and sample 4 with SBSM, 5 wt% collagen frozen with dry ice. Both samples had an average higher than 4. Especially in the sample 2, the standard deviation was seen to be rather small. When comparing sample 2 and 4 to the reference sample, they have a much higher grading regarding consistency and coherency. Also, the moldability was better for samples 2 and 4 compared to the reference sample. In general, the lowest grade was given to sample 3 with SBSM, 3 wt% collagen and chitosan and sample 5 with SBSM and 3 wt% collagen. Both had an average lower than 3. Especially moldability and coherency of these two samples was relatively lower than the reference sample. The highest variation was shown to be with the reference sample (3.43/5 ±0.99).

Figure 33 represents the analyzed samples before and after hydration in DM-water for 2 min. Reference sample has kept its shape and became stickier and moldable after hydration (B reference). Samples 1, 2 and 4 are comparable to the properties of reference sample, and especially 2 and 4 had excellent handling properties after hydration. Both

were sticky and held together nicely. Samples 3 and 6 had the least consistent shape after hydration and did not hold their shape as well as other samples. In sample 6, there were some visible collagen “granules” disintegrating from the SBSM structure.

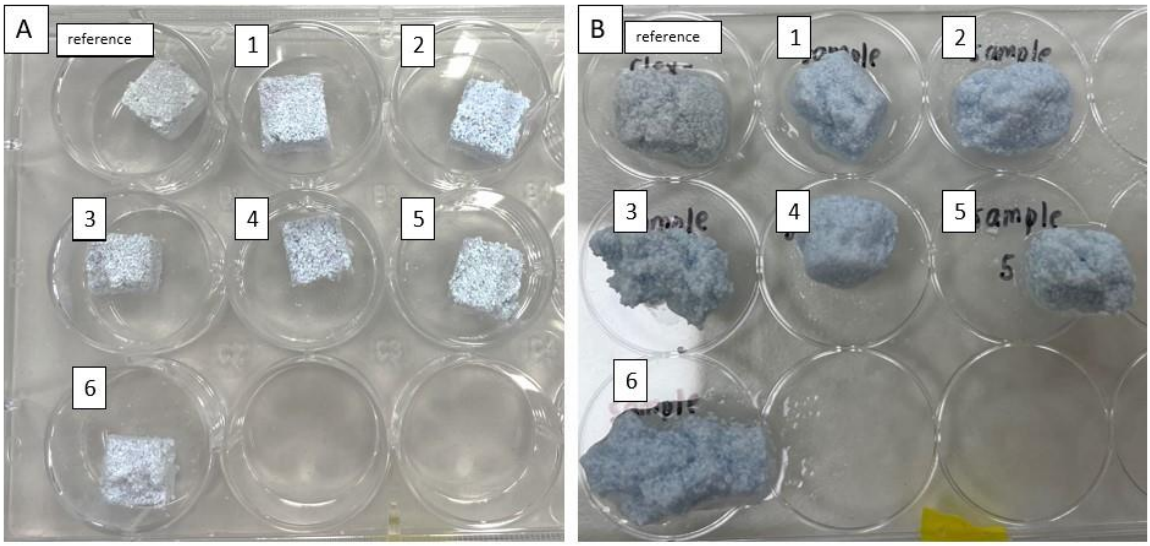

Figure 33. *SBSM samples A) before B) after hydration in DM-water for 2 min, where reference sample is made from SBSM granula and 5% collagen, 1) 5 wt% collagen and SBSM granula, 2) 5 wt% collagen, SBSM granula and hyaluronic acid frozen with dry ice, 3) 3 wt% collagen, SBSM granula and chitosan, 4) 5 wt% collagen and SBSM granula frozen with dry ice, 5) 5 wt% collagen with SBSM granula and 6) 7 wt% collagen with SBSM granula.*

6. DISCUSSION

6.1 Functionalization of a synthetic bone substitute material with collagen network

6.1.1 Optimization of collagen dry weight

The challenge to aim a specific collagen concentration was due to the adjustment of the pH of collagen suspension with TNP buffer. The initial calculations for collagen concentrations were based on collagen suspension which included only collagen paste and DM-water, but no TNP buffer. TNP buffer is composed of Na^+ and PO_4^{3-} salts that are left as part of the dry weight of collagen after the drying and heating chamber. Therefore, before modifying the calculations, the collagen concentration was lower than the equation gave as a result. When optimizing the protocol to yield a 5 wt% collagen suspension, the actual dry weight of collagen was calculated by removing the mass of TNP salts.

The matter of optimizing the collagen dry weight (concentration) is important to have reliable results during the preparation process to know how much collagen is in the suspension. For example, in the collagenase assay, the knowledge of exact amount of collagen is important as the amount of added collagenase is based on the weight of collagen fleece. If one sample were to contain a higher concentration of collagen, it would have also more TNP salts, thus a higher weight. Therefore, more collagenase would be added even though the amount of collagen has not changed. This might result in higher degradation due to collagenase. Additionally, the collagen concentration affects the release of TNP salts into HBSS and Na-acetate buffer, which has shown to influence the stability of SBSMs (chapter 5.3). The importance of the actual collagen concentration is also related to having a reproducible method to prepare collagen solutions with specific amounts of collagen. If the weight of TNP salts is not removed from the dry weight, the actual collagen concentration is smaller. In the future, the possible mass production of SBSM with collagen network could experience issues if the collagen concentration calculations are not reproducible. Meeting specifications in the technical documentation of eventual developed products could be a challenge. Also, it is crucial for the future customers to be aware of the materials and their concentrations in the product.

The new optimized method to calculate the collagen concentration by considering the mass of the TNP buffer enables the preparation of collagen suspensions with desired

concentration without the need to confirm the dry weight of collagen after each preparation. Furthermore, with the optimized method, there is no risk of preparing collagen suspensions of too high or low concentrations which might not be suitable for the desired properties of scaffolds. For example, SBSM with low collagen concentrations (3 wt%) have shown less stability in hydrated stage compared to SBSMs with higher concentrations (4 wt%) (chapter 5.4). Collagen content and concentration could potentially be analyzed through colorimetric-based hydroxyproline assay which uses a spectrophotometric technique to estimate the total amount of collagen based on the hydroxyproline content in tissues (Samuel, 2009).

6.1.2 Microscopic analysis

Microscopic analysis was conducted for the freeze-dried SBSM block and granula with collagen network. When the collagen was stained with riboflavin, it was easier to observe the collagen network on the SBSM blocks because of the yellow color of riboflavin. By pre-treating the SBSM blocks in ultrasonic bath or hydration in DM-water, the collagen network penetrated slightly inside the blocks compared to the non-treated blocks. Especially with the ultrasonic bath treatment, it was visible that there were pores filled with riboflavin-stained collagen. During the ultrasonic bath treatment, the air in the pores is removed and allows the collagen suspension to fill the pores. Later, during the freeze-drying process, the collagen network is created.

Despite the pre-treatment of SBSM blocks, the penetration of collagen network was weak and the collagen was seen mostly only on the surface of the SBSM block. In comparison, the SBSM granula with collagen network showed more penetration of collagen inside the SBSM composite. Therefore, samples with SBSM granula have greater potential to be combined with collagen network because the collagen network penetrates better and is thus released more steadily from the SBSM granula samples during degradation in the defect site (chapter 5.3). The SBSM granula composites would also be better for the indication of the product. For the application of SBSM with collagen network, samples made from SBSM granula are softer and easily moldable because of the distribution of collagen network inside the SBSM. In comparison, the SBSM block is hard, thus inconvenient in the application to a defect site in mouth (chapter 5.4).

6.1.3 Collagenase assay

Collagenase assay was used to evaluate the resistance of collagen against enzymatic degradation by collagenase *in vitro.* The specialty of collagenase is that it cleaves the

triple helix of collagen and hydrolyzes the peptide bonds of collagen into small fragments. Collagenase has an important role in tissue remodeling, where it can influence the endothelial cell function positively (Cui *et al.,* 2017). In the collagenase assay experiment, the highest degradation, thus mass loss, was seen for the sample with the lowest collagen concentration. This could potentially be due to the structural difference (less dense), leaving collagen more accessible for the collagenase to digest.

The mass loss for sample frozen fast with dry ice down to -80°C was almost half compared to the sample frozen slowly with freezer down to -18°C. This would indicate that the freezing method affects the stability of collagen against enzymatic degradation. This could be because the fast-freezing method affects the macrostructure of the collagen, especially to the hydrogen bonds. When the macrostructure is altered, the pore size changes and makes the collagen more accessible. Collagen is a heterogeneous molecule where the different sequences control the local conformation around the twisting axis of collagen. The conformations of collagen can vary and have different biological functions. Therefore, the low temperature associated with freezing with dry ice can affect the conformations of collagen by changing the ratios of different collagen conformations and potentially making the stable conformations more abundant (Fields *et al.,* 2017).

The collagenase assay was only done for four different samples and more experiments would need to be executed to establish a protocol for the enzymatic degradation experiments. The assay was done in TESCA buffer which meant that a big part of the mass loss was due to the degradation in TESCA buffer. The challenge came also from the light weight of samples (less than 10 mg), which required precise scale and working methods. Overall, the collagenase assay showed great potential in evaluating the enzymatic degradation of collagen *in vitro*. It gave indications to further use dry ice as the freezing method and supported the results from usability study, where samples with dry ice showed the best performance.

6.1.4 Differential Scanning Calorimetry

Differential Scanning Calorimetry (DSC) was used as a characterization method to evaluate the denaturation temperature of collagen and to compare the effect of different collagen concentrations, added bioactive molecules, pH, and freezing methods for the stability of collagen. The denaturation temperature is associated with atomic and molecular motions of collagen, in addition to the energy related to bonds keeping the bond in folded conformation. Therefore, when the energy or heat is high enough, the transition from triple helix to a randomly coiled formation happens, the protein unfolds and denaturates (Davidenko *et al.,* 2010).

There was only a small difference in the denaturation temperature of collagen samples with and without dry ice. This would indicate that the fast-freezing method with dry ice does not affect the thermal stability of collagen neither positively nor negatively. This is beneficial information because the dry iced samples have shown better stability related to the enzymatic degradation by collagenase, in the degradation studies in HBSS and in the usability study. When comparing the samples with different pH, the collagen samples in acidic environment seem to have lower denaturation temperatures. This is because the internal interactions between amino acids in collagen molecule are altered in acidic environment, thus reshaping the overall structure and stability of collagen (Changdao *et al.,* 2007). Therefore, collagen samples with neutral pH are more stable and potential for this application. This also confirms that the pH adjustments of collagen suspension are necessary to create more stable samples.

Addition of bioactive molecule, hyaluronic acid, increases the denaturation temperature compared to the unmodified collagen samples. The carboxyl group of HA reacts with both amino groups and hydroxyl groups of collagens which results in formation of ester linkages and making collagen more stable. To further increase the thermal stability of collagen, a method to cross-link HA with EDC/NHS to collagen could be investigated. It has been shown that EDC/NHS cross-linking makes collagen stiffer and increases the thermal stability (Pietrucha, 2005).

Even if there were no major differences in the denaturation temperatures, the results from DSC measurements indicate that the dry ice freezing-method does not break the collagen structure nor does the addition of hyaluronic acid. Therefore, these methods of functionalization can be safely used to enhance the regenerative properties of SBSMs. For this thesis project, the DSC measurements were done with dry samples. Some scientific papers suggest that the denaturation temperatures and enthalpy of dry samples are much higher than samples in aqueous solution. This could be explained by the dry collagen molecules having more closely packed structure, which means that higher amount of crystallization is needed to unfold the collagen molecules (Friess & Lee, 1996). This information could be used for future studies to compare the denaturation temperatures of dry and hydrated collagen fleeces. The possible source of error during the measurement can rise from the preparation of collagen fleece samples inside the pan and lid. Especially with the higher concentration samples, it was difficult to press the samples evenly inside the pan and lid. This could lead to uneven distribution of heat flow inside the samples, thus the results of denaturation temperature.

6.2 Functionalization of a synthetic bone substitute material with bioactive molecules

6.2.1 Polyelectrolyte multilayer deposition

PEM coating is a simple and efficient way to modify the surfaces of SBSM. It is important to simulate the conditions of PEM coating to ensure that the SBSM can withstand the environment it is exposed to during the deposition process. The pH plays a key role in the stability because even small changes in pH can affect the growth mechanism, thickness, and surface wettability of PE layers (Borges & Mano, 2014). Therefore, the sodium acetate buffer was adjusted to pH 5.5. The increase in pH was smaller for SBSM blocks or granula samples with collagen compared to only SBSM samples. When the SBSM block or granula starts to degrade, it releases Ca^{2+}, PO_4^{3-} and OH^- ions, of which especially OH- ions increase the pH. The smaller increase in pH with SBSM blocks and collagen could be because the collagen network around the SBSM block inhibits the contact of the block with Na-acetate and the degradation of the block.

However, during the PEM deposition, the SBSM is not exposed to the sodium acetate environment continuously for 200min but instead also exposed to hyaluronic acid and chitosan PE solutions. The pH of PE solutions did not change during the PEM coating, indicating that the SBSM is stable during the deposition. During the PEM coating, electrostatic interactions between the carboxylate group ($-COO^-$) of hyaluronic acid and the amine group ($-NH_3^+$) of chitosan are the strongest at pH 5 because the ionization is at their maximum. Therefore, the steady pH of 5.5 was crucial for the best results in PEM deposition.

When analyzing the conductivity changes of sodium acetate buffer, there is a difference between SBSM blocks with collagen and SBSM granula with collagen. This could be because more collagen network is in contact with the sodium acetate buffer in the blocks (outside of the block) than in the granula (distributed everywhere in the sample). There was a clear rise in the conductivity of the buffer with SBSM block or granula with collagen network in the beginning of immersion compared to only SBSM blocks. This could be because in the preparation of the collagen suspension, more TNP buffer (thus, more salts) was used to adjust the pH to 7. Therefore, during the immersion, there are more ions in the buffer increasing the conductivity. This would also explain why the conductivity is higher for higher collagen concentration samples.

In addition to changes in pH and conductivity, the adsorption time can affect the success of deposition. However, this is dependent on the PE solutions. For example, the thickness of the bilayers was shown to be significantly higher when the deposition time was increased from 5s to 300s for polyethylenimine and laponite clay, while the deposition time had little or no affect for polyethylenimine and montmorillonite PEs (Yang *et al.,* 2010). Moreover, the activation layer of PEI can have an effect on the layer thickness. The PEM deposition on Si-Wafers as a proof-of-concept showed that activation layer with PEI increases the thickness of the PEM film and the amount of polymer adsorbed in the film. PEI acts as an anchoring network for the following layers being deposited. (Trybala *et al.,* 2009) This could give reasoning to add PEI activation layer for the deposition on SBSM.

PEM deposition is time-consuming and detailed work. Additionally, the lack of stability of the collagen network during the PEM deposition creates challenges for the method. The collagen structure collapses and dissolves to the solutions during the stability study in sodium acetate buffer to simulate the PEM deposition environment (chapter 5.2.2). Therefore, alternative pathway to incorporate hyaluronic acid and chitosan to the SBSM was created by mixing the bioactive molecules directly into the collagen suspension during the production steps. This will also reduce the manufacturing steps in the later production of the prototype compared to the PEM coating process. For the possible future production of the SBSM, it is important to create an efficient and easy way to combine materials to create the product. PEM deposition might be more difficult to incorporate in a big production site compared to mixing materials.

6.3 *In vitro* degradation in Hanks' Balanced Salt Solution

Degradation studies in HBSS were conducted to analyze the stability of SBSM combinations and to simulate how they would behave in the defect site. HBSS is an isotonic solution that is used to maintain the osmolality and pH, and it contains essential salts to simulate the physiological conditions of body fluids with pH 7.4.

It is important to know the changes for pH to determine whether the SBSM provides an ideal environment for cells in the defect site. Also, because the SBSM composite samples are further studied for their biocompatibility and osteoblast growth. Overall, the pH changed in all the solutions with SBSMs. The samples with only SBSM began to degrade fast in the solution and release Ca^{2+}, PO_4^{3-} and OH^- ions, of which especially OH^- ions increased the pH. Other samples had been added with a collagen network and had a rather stable decrease in pH. This would indicate that the addition of collagen network

can be used to stabilize the SBSM. The samples with hyaluronic acid had the lowest pH in the end of the experiment. This is because hyaluronic acid is acidic and decreases the pH of HBSS. Also, the addition of hyaluronic acid seemed to increase the stability of SBSM. HA can bind and retain water molecules and creates interconnected porous structures when freeze-dried. This property of HA seems to fight against the degradation HBSS. Based on the changes in pH, freezing method with dry ice in addition to hyaluronic acid can help to stabilize the SBSM and overcome the challenges of CaP ceramics of their too fast degradation.

Conductivity changed in all SBSM samples. The samples with only collagen fleece increased the conductivity of HBSS the most. This could be because during the preparation process of collagen suspension, the pH was adjusted with TNP buffer, which includes Na^+ and PO_4^{3-} salts. When the collagen fleece is exposed to the liquid environment of HBSS, the degradation begins and the ions are released into the solution, thus increasing the conductivity rapidly. The same reason would explain why the conductivity was higher for the samples with higher collagen concentration: the higher the collagen concentration, the more buffer was used to adjust the pH in the processing steps. Additionally, conductivity is higher for SBSM block with collagen than for SBSM granula with collagen. This could be because the collagen network was only on the outer parts of the SBSM block and is in direct contact with HBSS compared to the SBSM granula that had collagen network inside its structure. Based on the changes in conductivity, SBSM in a form of granula possesses more stable characteristics than the block because the collagen network has not penetrated inside the block but is only on the outer parts.

Mass loss of the samples was analyzed throughout the 28-day immersion. After 7 days, the collagen fleece was completely degraded into HBSS which would indicate that it is not stable alone in the fluidic environment. The smallest mass loss was experienced for SBSM block with collagen which could be because the collagen network gets disintegrated fast, but the block is rather stable until the end. Higher mass loss was shown for samples with granula than block. However, the mass loss study was not completely reliable because when the samples started to degrade, it was hard to take out all the remaining sample and weigh it because the sample was distributed into the solution. High standard deviation indicated that the samples were spread out.

The penetration of collagen network is an important aspect that can affect the stability of the samples. The microscopic analysis (chapter 5.1.2) showed how the collagen network penetrated better inside the SBSM granula samples compared to SBSM blocks. Therefore, granula was shown to have a steadier disintegration of collagen compared to SBSM

block. This could be because the collagen network was able to penetrate inside the pores and deeper into the sample.

6.4 Usability studies

The usability study simulated a real-life situation where the dentist would hydrate the SBSM composite in the patient's own blood or 0.9% saline solution before applying to the defect area in mouth. The SBSM composites with collagen network and kappa-carrageenan or chondroitin sulfate were ruled out from the usability studies during the pre-trial. Kappa-carrageenan is a water-soluble polysaccharide that is often used in biomedical industry as an additive and stabilizer for its gelling properties (Khan *et al.,* 2020). Chondroitin sulfate is a natural polysaccharide in ECM of cartilage. It is commonly used in bone tissue engineering for its anti-inflammatory properties (Li *et al.,* 2021). For the functionalization of SBSM, neither kappa-carrageenan nor chondroitin sulfate, showed enough potential to be further investigated during the thesis. The problem with chondroitin sulfate is that it possesses rapid degradation rates that were not ideal in terms of performance. Since neither of the samples showed to improve the performance of the samples, they were ruled out for further studies.

The combination of SBSM with 5 wt% collagen frozen with dry ice was on average rated to have the best performance. This would indicate that the functionalization of a SBSM with collagen network and bioactive molecule increases its performance in dry and hydrated stage. Being one of the most hydroscopic bioactive molecules, hyaluronic acid can store liquid and create viscous and sticky structures when it is hydrated in DM-water. SBSM with hyaluronic acid are more easily moldable which helps the insertion to the defect site because the material can evenly fill the whole area. However, for the future production and delivery of the product, it is important to investigate the effect of sterilization in the SBSM, especially in hyaluronic acid. Hyaluronic acid is sensitive to gamma-irradiation and can experience decrease in surface hydrophilicity, structural weakening, and lower swelling capacity. (Srinivas & Ramamurthi, 2007). Furthermore, the freezing method with dry ice increased the properties of SBSM with or without hyaluronic acid. This could be because of the effect of dry ice in decreasing the size of macropores in SBSM that play a crucial role in the stability of the material. On average, the worst grade was given to SBSM sample with 3 wt% collagen and no bioactive molecules. This would indicate that higher collagen concentration is needed to create SBSM with better performance. Even in the dry state it was visible that the sample was not coherent or dense and the granules were not holding together as well as with higher collagen concentration.

The study did not completely simulate the real-life situation because normally the dentist would hydrate the sample in either the patient blood or saline solution. Also, the hydration time of 2 min can easily be too short if the dentist is for example talking to the patient, thus making the hydration time longer. What was noticed in the study is that the SBSM samples were disintegrated into the DM-water after 10 min, which means that it would be difficult for the dentist to use the sample afterwards. For future studies, it would be beneficial to test the performance of SBSM in saline solution instead of DM-water to see the effect of salts in the hydration of the product. Additionally, the dentist is most likely not going to have enough blood from the patient to hydrate the whole sample which could potentially make it harder to mold. Therefore, it would be crucial to further improve the performance of the sample to make it moldable and sticky even with smaller amount of liquid. A solution for this could be to create a packaging for the SBSM which could be used to pour saline solution in for hydrating the sample sufficiently. The first impression of product is crucial and if the appearance or handling of the SBSM is difficult, it might result in lower interest to purchase the product again.

Possible sources of error during the stability studies start from the preparation of different samples. As an example, throughout the thesis work, the preparation of SBSM with collagen improved as the methods evolved. In the beginning, the pressure used to create SBSM and collagen samples in molds was smaller until the realization to use more pressure and additional tools to create more dense samples. Also, the participants had different backgrounds that can affect the way to analyze the samples. There is always a risk to misunderstand instructions given in the questionnaire. One aspect that was different to a real-life case was the molding. In the study it was done with fingers but in real life, the dentist is more likely to use a spatula or a specific spoon for the molding. Maybe that could influence the moldability of the product. Additionally, if the defect is very small, the dentist would be likely to cut the SBSM product in half, which is why it is important to create homogeneous samples that does not break apart when cutting with surgical knife.

The usability study showed that the performance of SBSM composites is affected by multiple things. When looking at the scope of the thesis, the aim was to enhance the performance of SBSMs by functionalization. Even this early in the research stage, there were already differences in the performance of SBSM composite samples. To support the findings from the usability study, it would be beneficial to examine the regenerative properties by means of a co-culture of osteoblasts and endothelial cells on the developed composites.

7. CONCLUSIONS

Bone tissue remains as the second most common transplant type in the world. To address the need for bone grafts, new methods have been established to develop safe solutions to patients. The advantage of synthetic materials lies on their osteoconductive properties and cost-effectiveness, which makes them attractive alternatives to autografts. The development of biomimetic structures could be improved through functionalization of SBSMs.

In this thesis, the functionalization of SBSM was shown to be an efficient way to improve the performance of SBSM for BTE applications. Functionalization of calcium phosphate ceramics with both, collagen, and hyaluronic acid, has shown to play a key role in the formation of stable scaffolds to support bone tissue regeneration. Successful development of two separate methods for the preparation of SBSM with collagen were established. The mixing of collagen and bioactive molecules into the SBSM was shown to be more efficient compared to the polyelectrolyte multilayer deposition. Additionally, the use of SBSM granula over SBSM block was proven through microscopic studies that showed greater penetration of the collagen network inside the SBSM granula compared to the SBSM block. The SBSM granula created moldable products that fulfilled the requirements for the handling in dental applications, while the SBSM block did not.

The degradation studies in HBSS and the usability study showed that SBSM composites with collagen and hyaluronic acid frozen with dry ice, seemed to have the steadiest degradation rates and the best performance in dry and hydrated stage regarding handling, usability and stability of the samples. Moreover, the characterization of the collagen network supported that the best resistance against enzymatic degradation in vitro by collagenase was seen for the collagen samples frozen with the dry ice. All together, these materials could create a biocompatible material with better osteoconductivity and enhanced regenerative properties that offer new opportunities in the field of bone tissue engineering.

The most promising method for the functionalization of a SBSM included a 5 wt% collagen network, hyaluronic acid and dry ice – freezing. Additionally, the usability studies showed that the combination of a SBSM with 5 wt% collagen network frozen with dry ice had similar performance to the sample with the additional hyaluronic acid. Through usability study, the most promising prototypes could be selected for further biocompatibility studies.

REFERENCES

Agarwal, R. & García A.J. (2015). Biomaterial strategies for engineering implants for enhanced osseointegration and bone repair. Advanced Drug Delivery Reviews. Vol.1(94), pp. 53-62.

Ahsan, S.M., Thomas, M., Reddy, K.K., Sooraparaju, S.G., Asthana, A. & Bhatnagar, I. (2018). Chitosan as biomaterial in drug delivery and tissue engineering. International Journal of Biological Macromolecules. Vol.110, pp. 97-109.

Amini, A.R., Laurencin, C.T. & Nukavarapu, S.P. (2012). Bone tissue engineering: Recent advances and challenges. Critical Reviews in Biomedical Engineering. Vol.40(5), pp. 363-408.

Barrère, F., van Blitterswijk, C.A. & de Groot, K. (2006). Bone regeneration: molecular and cellular interactions with calcium phosphate ceramics. International Journal of Nanomedicine. Vol.1(3), pp. 317-332.

Barroso, N., Guaresti, O., Péréz-Álvarez, L., Ruiz-Rubio, L., Gabilondo, N. & Vilas-Vilela, J.L. (2019). Self-healable hyaluronic acid/chitosan polyelectrolyte complex hydrogels and multilayers. European Polymer Journal. Vol.120.

Beger, B., Blatt, S., Pabst, A.M., Hansen, T., Goetz, H., Al-Nawas, B. & Ziebart, T. (2018). Biofunctionalization of synthetic bone substitutes with angiogenic stem cells: influence on regeneration of critical-size bone defects in an in vivo murine model. Journal of Cranio-Maxillofacial Surgery. Vol.46(9), pp. 1601-1608.

Bharadwaz, A. & Jayasuriya, A.C. (2020). Recent trends in the application of widely used natural and synthetic polymer nanocomposites in bone tissue regeneration. Materials Science & Engineering C. Vol.110.

Bieker, P. & Schönhoff, M. (2010). Linear and exponential growth regimes of multilayers of weak polyelectrolytes in dependence on pH. Macromolecules. Vol.43, pp. 5052-5059.

BioBASE, *Biovision Biomaterial*, viewed on 1 June 2021, <https://www.biovision.de/en/products/biobase>

Borges, J. & Mano, J.F. (2014). Molecular interactions driving the layer-by-layer assembly of multilayers. Chemical reviews. Vol.114, pp. 8883-8942.

Boudou, T., Crouzier, T., Ren, K., Blin, G. & Picart, C. (2010). Multiple functionalities of polyelectrolyte multilayer films: new biomedical applications. Advanced Materials. Vol.22, pp. 441-467.

Chang, G., Boone, S., Martel, D., Rajapakse, C.S., Hallyburton, R.S., Valko, M., Honig, S. & Regatte R.R. (2017). MRI assessment of bone structure and microarchitecture. Journal of Magnetic Resonance Imaging. Vol.46(2), pp. 323-337.

Changdao, M., Defu, L., Wei, L., Yanwei, D. & Guangzhao, Z. (2007). Temperature induced denaturation of collagen in acidic solution. Biopolymers. Vol.86(4), pp. 282-287.

Chen, G., Xia, Y., Lu, X., Zhou, X., Zhang, F. & Gu, N. (2012). Effects of surface functionalization of PLGA membranes for guided regeneration of proliferation and behavior of osteoblasts. Journal of Biomedical Materials Research. Vol.101A(1), pp.44-53.

Chocholata, P., Kulda., V. & Babuska., V. (2019). Fabrication of scaffolds for bone-tissue regeneration. Materials. Vol.12(568).

Collins, M.N. & Birkinshaw, C. (2013). Hyaluronic acid based scaffolds for tissue engineering A review. Vol.92(2), pp. 1262-1279.

Cui, N., Hu, M. & Khalil, R.A. (2017). Biochemical and biological attributes of matrix metalloproteinases. Progress in Molecular Biology and Translational Science. Vol.147, pp. 1-73.

Davidenko, N., Campbell, J.J., Thian, E.S., Watson, C.J. & Cameron, R.E. (2010). Collagen-hyaluronic acid scaffolds for adipose tissue engineering. Acta Biomaterialia. Vol.6(10), pp. 3957-3968.

Deng, C., Chen, X.S., Sun, J., Lu, T.C., Wang, W.S., Jing, X.B. (2007). RGD peptide grafted biodegradable amphiphilic triblock copolymer poly(glutamic acid)-b-poly(L-lactide)-b-poly(glutamic acid): synthesis and self-assembly. Journal of Polymer Science Part A Polymer Chemistry. Vol.45, pp. 3218-3230.

Dentsply Sirona 2021, *Symbios Algipore*, viewed on 11 June 2021, <https://www.dentsplysirona.com/en-gb/shop/implants/regenerative-solutions/symbios.html/Implants/Regenerative-solutions/Symbios/Bone-graft-materials/Symbios-Algipore/p/IMP-32311400-1000122001/c/3000101.html>.

DePuy Synthes 2016, *DePuy CMW™ Heritage Bone Cements Product Information,* viewed 11 June 2021, < http://synthes.vo.llnwd.net/o16/LLNWMB8/INT%20Mobile/Synthes%20International/Product%20Support%20Material/legacy_Synthes_PDF/DSEM-BIO-0516-0054_LR.pdf>.

Di Martino, A., Sittinger, M. & Risbud, M.V. (2005). Chitosan: a versatile biopolymer for orthopedic tissue-engineering. Biomaterials. Vol.26(30), pp. 5983-5990.

Dimitriou, R., Jones, E., McGonagle, D. & Giannoudis, P.V. (2011). Bone regeneration: current concepts and future directions. BMC Medicine. Vol.9(66).

El-banna, F.S., Mahfouz, M.E., Leporatti, S., El-Kemary, M. & Hanafy, N.A. (2020). Chitosan as a natural copolymer with unique properties for the development of hydrogels. Applied Science. Vol.9(11).

Eliaz, N. & Metoki, N. (2017). Calcium phosphate bioceramics: A review of their history, structure, properties, coating technologies and biomedical applications. Materials. Vol.10(4), p. 334.

Enescu, D. & Olteanu, C.E. (2008). Functionalized chitosan and its use in pharmaceutical, biomedical, and biotechnological research. Chemical Engineering Communications. Vol.195(10).

Esposito, M., Grusovin, M.G., Rees, J., Karasoulos, D., Felice, P., Alissa, R., Worthington, H. & Coulthard, P. (2010). Effectiveness of sinus lift for dental implant rehabilitation: a Cochrane systematic review. European Journal of Oral Implantology. Vol.3(1), pp. 7-26.

Fernandez-Yague, M.A., Abbah, S.A., McNamara, L., Zeugolis, D.I., Pandit, A. & Biggs, M.J. (2015). Biomimetic approaches in bone tissue engineering: integrating biological and physicomechanical strategies. Advanced Drug Delivery Reviews. Vol.84, pp. 1-29.

Ferreira, A.M., Gentile, P., Chiono, V. & Ciardelli, G. (2012). Collagen for bone tissue regeneration. Acta Biomaterialia. Vol.8, pp. 3191-3200.

Fields, M., Spencer, N., Dudhia, J. & McMillan, P. (2017). Structural changes in cartilage and collagen by high temperature Raman spectroscopy. Biopolymers. Vol.107(6).

Florencio-Silva, R., Rodrigues da Silva Sasso, G., Sasso-Cerri, E., Simões, M.J. & Cerri, P.S. (2015). BioMed Research International. Vol.2015.

Friess, W. & Lee, G. (1996). Basic thermoanalytical studies of insoluble collagen matrices. Biomaterials. Vol.17, pp. 2289-2294.

García-Gareta, E., Coathup, M.J. & Blunn, G.W. (2015). Osteoinduction of bone grafting materials for bone repair and regeneration. Bone. Vol.81, pp. 112-121.

Han, L., Jiang, Y., Lv, C., Gan, D., Wang, K., Ge, X. & Lu, X. (2019). Mussel-inspired hybrid coating functionalized porous hydroxyapatite scaffolds for bone tissue regeneration. Colloids and Surfaces B: Biointerfaces. Vol.179, pp. 470-478.

Hanks, J. (1976). Hanks' balanced salt solution and pH control. Tissue Culture Association Manual. 3, 3.

Hannink, G. & Arts J.J.C. (2011). Bioresorbability, porosity and mechanical strength of bone substitutes: What is optimal for bone regeneration? Injury. Vol.42(2), pp. 22-25.

Hou, J., Wang, J., Cao, L., Qian, X., Xing, W., Lu, J. & Liu, C. (2012). Segmental bone regeneration using rhBMP-2-loaded collagen/chitosan microspheres composite scaffold in a rabbit model. Biomedical Materials. Vol.7(3).

Hu, S-G., Jou, C-H. & Yang, M.C. (2003). Protein adsorption, fibroblast activity and antibacterial properties of poly(3-hydroxybutyric acid-co-3-hydroxyvaleric acid) grafted with chitosan and chitooligosaccharide after immobilized with hyaluronic acid. Biomaterials. Vol.24(16), pp. 2685-2693.

Jovanovic, S.A., Hunt, D.R., Bernard, G.W., Spiekermann, H., Wozney, J.M. & Wikesjö, U.M.E. (2007). Bone reconstruction following implantation of rhBMP-2 and guided bone regeneration in canine alveolar ridge defects. Clinical Oral Implants Research. Vol.18(2), pp. 224-230.

Khan, M.U.A., Raza, M.A., Mehboob, H., Kadir, M.R.A., Razak, S.I.A., Shah, S.A., Iqbal, M.Z. & Amin, R. (2020). Development and *in vitro* evaluation of κ-carrageenan based polymeric hybrid nanocomposite scaffolds for bone tissue engineering. Royal Society of Chemistry. Vol.10.

Khor, E. & Lim, L.Y. (2003). Implantable applications of chitin and chitosan. Biomaterials. Vol.24(13), pp. 2339-2349.

Kim, J.H. & Lee, S.J. (2016). 'A biomimetic strategy to design biomaterials for in situ tissue regeneration' in Lee, S.J., Yoo, J.J., Atala, A., In Situ Tissue Regeneration, ed 1, Academic Press. pp.185-201.

Kolk, A., Handschel, J., Drescher, W., Rothamel, D., Kloss, F., Blessmann, M., Heiland, M., Wolff, K-D. & Smeets, R. (2012). Current trends and future perspectives of bone substitute materials – From space holders to innovative biomaterials. Journal of Cranio-Maxillo-Facial Surgery. Vol.40, pp. 706-718.

Kuwaja, P., Moraille, P., Sanchez, J., Badia, A. & Winnik, F.M. (2005). Effect of molecular weight on the exponential growth and morphology of hyaluronan/chitosan multilayers: a surface plasmon resonance spectroscopy and atomic force microscopy investigation. Journal of the American Chemical Society. Vol.127(25), pp. 9224-9234.

Legeros, R.Z., Lin, S., Rohanizadeh, R., Mijares, D. & Legeros, J.P. (2003). Biphasic calcium phosphate bioceramics: preparation, properties and applications. Journal of Materials Science: Materials in Medicine. Vol.14, pp. 201-209.

Lei, Y., Xu, Z., Ke, Q., Yin, W., Chen, Y., Zhang, C. & Guo, Y. (2017). Strontium hydroxyapatite/chitosan nanohybrid scaffolds with enhanced osteoconductivity for bone tissue engineering. Materials Science and Engineering: C. Vol.72, pp. 134-142.

Li, X., Xu, Q., Johnson, M., Wang, X., Lyu, J., Li, Y., McMahon, S., Greiser, U., Sigen, A. & Wang, W. (2021). A chondroitin sulfate based injectable hydrogel for delivery of stem cells in cartilage regeneration. Biomaterial Science. Vol.9, pp. 4139-4148.

Lin, K., Zhang, D., Macedo, M.H., Cui, W., Sarmento, B. & Shen, G. (2019). Advanced collagen-based biomaterials for tissue regeneration and their clinical translation. Pharmaceutics. Vol.12(7).

Lutzweiler, G., Halili, A.N. & Vrana, N.E. (2020). The overview of porous, bioactive scaffolds as instructive biomaterials for tissue regeneration and their clinical translation. Pharmaceutics. Vol.12(7).

Maxresorb®, botiss biomaterials / dental, viewed on 2 June 2021, <https://botiss-dental.com/products/maxresorb/>

MBCP® synthetic bone graft substitute bioactive calcium phosphate, Biomatlante, viewed 2 June 2021, < https://biomatlante.com/en/products/mbcp-synthetic-bone-graft-substitute>.

Medtronic 2021, Infuse® bone graft, Medtronic, viewed on 15 June 2021, <https://www.medtronic.com/us-en/healthcare-professionals/products/spinal-orthopaedic/bone-grafting/infuse-bone-graft.html>.

Nair, A.K., Gautieri, A., Chang, S-W. & Buehler, M.J. (2013). Molecular mechanics of mineralized collagen fibrils in bone. Nature Communications. Vol.4(1724).

Nath, S.D., Abueva, C., Kim, B. & Lee, B.T. (2015). Chitosa-hyaluronic acid polyelectrolyte complex scaffold crosslinked with genipin for immobilization and controlled release of BMP-2. Carbohydrate Polymers. Vol.115, pp. 160-169.

Nisal, A., Sayyad, R., Dhavale, P., Khude, B., Deshpande, R., Mapare, V., Shukla, S. & Venugopalan, P. (2018). Silk fibroin micro-particle scaffolds with superior compression modulus and slow bioresorption for effective bone regeneration. Scientific Reports. Vol.8

Nuran I., Murat, I. & Mustafa, Y. (2008). Synthesis and charactertization of poly(N-vinyl-2-pyrrolidone) gradted sodium alginate hydrogel beads for the controlled release of indomethacin. Journal of Applied Polymer Science. Vol.110, pp. 481-493.

O'Brien, F.J., Harley, B.A., Yannas, I.V. & Gibson, L. (2004) Influence of freezing rate on pore structure in freeze-dried collagen-GAG scaffolds. Biomaterials. Vol.25(6), pp. 1077-1086.

OpenStax, Chemistry. OpenStax CNX. Jun 20, 2016, >http://cnx.org/contents/85abf193-2bd2-4908-8563-90b8a7ac8df6@9.311>.

Oryan, A., Alidadi, S., Moshiri, A. & Maffulli, N. (2014). Bone regenerative medicine: classic options, novel strategies, and future directions. Journal of Orthopaedic Surgery and Research. Vol.9(18).

Oryan, A., Monazzah, S. & Bigham-Sadegh, A. (2015). Bone injury and fracture healing biology. Biomedical Environment Science. Vol.28(1), pp. 57-71.

Parenteau-Bareil, R., Gauvin, R. & Berthod, F. (2010). Collagen-based biomaterials for tissue engineering applications. Materials. Vol.3, pp. 1863-1887.

Park, J.K., Yeom, J., Oh, E.J., Reddy, M., Kim, J.Y., Cho, D-W., Lim, H.P., Kim, N.S., Park, S.W., Shin, H-I., Yang, D.J., Park, K.B. & Hahn, S.K. (2009). Guided bone regeneration by poly(lactic-co-glycolic acid) grafted hyaluronic acid bi-layer films for periodontal barrier applications. Acta Biomaterialia. Vol.5(9), pp. 3394-3403).

Park, S.A., Kim, G., Jeon, Y.C., Koh, Y. & Kim, W. (2009). 3D polycaprolactone scaffolds with controlled pore structure using a rapid prototyping system. Journal of Material Science: Materials in Medicine. Vol.20(1), pp. 229-234.

Patterson, J., Siew, R., Herring, S.W., Lin, A.S.P., Guldberg, R. & Stayton, P.S. (2010). Hyaluronic acid hydrogels with controlled degradation properties for oriented bone regeneration. Biomaterials. Vol.31(26), pp. 6772-6781.

Pietrucha, K. (2005). Changes in denaturation and rheological properies of collagen-hyaluronic acid scaffolds as a result of temperature dependencies. International Journal of Biological Macromolecules. Vol.36, pp. 399-304.

Polo-Corrales, L., Latorre-Esteves, M. & Ramirez-Vick, J.E. (2014). Scaffold design for bone regeneration. Journal of Nanoscience and Nanotechnology. Vol.14(1), pp. 15-56.

Reddy, M.S.B., Ponnamma, D., Choudhary, R. & Sadasivuni, K.K. (2021). A comparative review of natural and synthetic biopolymer composite scaffolds. Polymers. Vol.13.

Roseti, L., Parisi, V., Petretta, M., Cavallo, C., Desando, G., Bartolotti, I. & Grigolo, B. (2017). Scaffolds for bone tissue engineering: state of the art and new perspectives. Materials Science and Engineering. Vol.78, pp. 1246-1262.

Rossi, F. & van Griensven, M. (2014). Polymer functionalization as a power tool to improve scaffold performance. Tissue Engineering Part A. Vol.20(15&16).

Sabet, J.M., Amoian, B. & Seyedmajidi, M. (2017). Histological and histomorphometric evaluation of the synthetic biomaterial Natix® in horizontal reconstruction of alveolar ridge. Dental Research Journal. Vol.14(2), pp. 97-103.

Samuel, C.S. (2009) Determination of collagen content, concentration and sub-types in kidney tissue. Methods in Molecular Biology. Vol.466, pp.223-235.

Shoulders, M.D. & Raines, R.T. (2009). Collagen structure and stability. Annual Review Biochemistry. Vol.78, pp. 929-958.

Singh, M., Kasper, K., Mikos, A.G. (2013). Biomaterials Science. 3rd edn. Academic Press.

Sinha, R., Menon, P.S. & Chakranarayan, A. (2009). Vitoss synthetic cancellous bone (void filler). Medical Journal Armed Forces India. Vol.65(2).

Sionkowska, A., Gadomska, M., Musial, K. & Piatek, J. (2020). Hyaluronic acid as a component of natural polymer blends for biomedical applications: a review. Molecules. Vol.25(18).

SmartBone® 2021, *SmartBone® the next frontier of bone regeneration,* viewed 15 June 2021, <http://puredent.dk/pdf/Smartbone%20Brochure.pdf>.

Song, R., Murphy, M., Li, C., Ting, K. & Soo, C. (2018). Current development of biodegradable polymeric materials for biomedical applications. Drug Design, Development and Therapy. Vol.12, pp. 3117-3145.

Sorushanova, A., Delgado, L.M., Wu, Z., Shologu, N., Kshirsagar, A., Raghunath R., Mullen, A.M., Bayon, Y., Pandit, Y., Raghunath, M. & Zeugolis, D.I. (2019). The collagen suprafamily: from biosynthesis to advanced biomaterial development. Advanced materials. Vol.31(1).

Srinivas, A. & Ramamurthi, A. (2007). Effects of gamma-irradiation on physical and biologic properties of crosslinked hyaluronan tissue engineering scaffolds. Tissue Engineering. Vol.13(3), pp. 447-459.

Szabó, L., Gerber-Lemaire, S. & Wandrey, C. (2020). Strategies to functionalize the anionic biopolymer Na-alginate without restricting its polyelectrolyte properties. Polymers. Vol.20.

Szczés, A., Holysz, L. & Chibowski, E. (2017). Synthesis of hydroxyapatite for biomedical applications. Advances in Colloid and Interface Science. Vol.249, pp. 321-330.

Tang, Z-B., Cao, J-K., Wen, N., Wang, H-B., Zhang, Z-W., Liu, Z-Q., Zhou, J., Duan, C-M., Cui, F-Z. & Wang, C-Y. (2011). Posterolateral spinal fusion with nano-hydroxyapatite–collagen/PLA composite and autologous adipose-derived mesenchymal stem cells in a rabbit model. Tissue Engineering and Regenerative Medicine. Vol.6(4), pp. 325-336.

Tian, H., Tang, Z., Zhuang, Z., Chen, X. & Jing, X. (2012). Biodegradable synthetic polymers: preparation, functionalization and biomedical application. Progress in Polymer Science. Vol.37, pp. 237-280.

Titsinides, S., Agrogiannis, G. & Karatzas, T. (2019) Bone grafting materials for dentoalveolar reconstruction: a comprehensive review. Japanese Dental Science Review. Vol.55, pp. 26-32.

Treccani, L., Klein, T.Y., Meder, F., Pardun, K. & Rezwan, K. (2013). Funtionalized ceramics for biomedical, biotechnological and environmental applications. Acta Biomaterialia. Vol.9(7), pp. 7115-7150.

Trybala, A., Szyk-Warszýnska, L. & Warszynski, P. (2009). The effect of anchoring PEI layer on the build-up of polyelectrolyte multilayer films at homogeneous and heterogeneous surfaces. Colloids and Surfaces A: Physicochemical and Engineering aspects. Vol.343, pp. 127-132.

Turnbull, G., Clarke, J., Picard, Frédéric, P., Riches, P., Jia, L., Han, F., Li, B. & Shu, W. (2017). 3D bioactive composite scaffolds for bone tissue engineering. Bioactive Materials. Vol.3(3), pp. 278-314.

Wei, S., Ma, J.-X., Xu, L., Gu, X.-S. & Ma, X.-L. (2020). Biodegradable materials for bone defect repair. Military Medical Research. Vol.7(54).

Wu, S., Liu, X., Yeung, K.W.K., Liu, C. & Yang, X. (2014). Biomimetic porous scaffolds for bone tissue engineering. Materials Science and Engineering R. Vol.80, pp. 1-36.

Xu, H.H., Quinn, J.B., Takagi, S., Chow, L.C. & Eichmiller, F.C. (2001). Strong and microporous calcium phosphate cement: effects of porosity and fiber reinforcement on mechanical properties. Journal of Biomedical Materials Research. Vol.5(57), pp. 457-466.

Yamada, M. & Egusa, H. (2018). Current bone substitutes for implant dentristry. Journal of Prosthodontic Research. Vol.62, pp. 152-161.

Yang, Y-H., Malek, F.A. & Grunlan, J.C. (2010). Influence of deposition time on layer-by-layer growth of clay-based thin films.

Zheng, Y.F., Gu, X.N. & Witte, F. (2014). Biodegradable metals. Materials Science and Engineering: R: Reports. Vol.77, pp.1-34.

APPENDIX A: PROTOCOL FOR THE PREPARATION OF HANKS' BALANCED SALT SOLUTION

Preparation of HBSS is based on preparation instructions by Sigma-Aldrich (Hanks, 1976). In total, 1 L of solution was prepared by first measuring 90% of the final required volume of DM-water (temperature 15-20°C) into a beaker and adding one package of powdered Hanks' salt medium (table 15) while stirring on a magnetic stirrer. After, 0.35g of sodium bicarbonate was added and the pH was measured to be 7.39 (desired range 7.0-7.4). Differing from the instructions, the solution was not filtered because it did not have to be sterile for the experiment. Remaining DM-water was added to bring the solution to final volume. HBSS was stored in the fridge at 2-8 °C in blue cap bottle for 1 day before using it.

Table 14. *Components of Hanks' Balanced Salt Solution.*

Component	$CaCl_2$	$MgSO_4$	KCl	KH_2PO_4	NaCl	Na_2HPO_4	D-Glucose
Concentration	0.1396 g/L	0.09767 g/L	0.4 g/L	0.06 g/L	8.0 g/L	0.04788 g/L	1.0 g/L

APPENDIX B: USABILITY STUDY QUESTIONNAIRE

Performance of combination of maxresorb® granula, collagen and bi-oactive molecule in hydrated stage

Noora Haapalainen

27.05.2021

Consent Form

Name of the participant _____

Experience

At least 2 years of experience in Clinical Application

At least 2 years of experience in R&D for bone substitute materials

At least 2 years of experience in Product Management

Other: _____

Signature

I confirm with my signature that I have filled the form and performed the test independently and without any influence by third parties.

_____

Date / Place / Signature

Instructions:

You are given 6 samples composed of different combinations of maxresorb® granula, collagen and bioactive molecules. Additionally, you are given a flexbone sample, composed of maxresorb® granula and 5 wt% collagen suspension, as reference. The samples are placed in separate wells on 12-well-plate and hydrated with DM-water for 2min. This is to simulate the application of the product when a dentist would hydrate the sample in saline solution or patient's blood before applying to the defect site.

Your task is to evaluate the samples based on criteria ranging from 1-5 in comparison to the flexbone sample. Additional feedback can be left on the "comments" - section below the grading system.

- 5 Excellent
- 4 Good
- 3 Average
- 2 Fair
- 1 Poor

Study begins here.

1. Appearance. Before hydrating the sample, how would you analyze the appearance of the sample in dry state? Is the sample consistent and compact or is it already broken / are the granules separating from the sample? Rate from 1-5, where 5 = consistent, homogeneous, and compact structure while 1 = completely broken and/or separating granules.

Sample	Grade	Comments
Flexbone	1 2 3 4 5 ☐ ☐ ☐ ☐ ☐	
Sample 1	1 2 3 4 5 ☐ ☐ ☐ ☐ ☐	
Sample 2	1 2 3 4 5 ☐ ☐ ☐ ☐ ☐	
Sample 3	1 2 3 4 5 ☐ ☐ ☐ ☐ ☐	
Sample 4	1 2 3 4 5 ☐ ☐ ☐ ☐ ☐	
Sample 5	1 2 3 4 5 ☐ ☐ ☐ ☐ ☐	
Sample 6	1 2 3 4 5 ☐ ☐ ☐ ☐ ☐	

2. Applied pressure. After hydrating the sample, try lifting the samples from the wells with a pair of tweezers. How much pressure is applied to the sample regarding the softness / toughness of the sample? Rate from 1-5, where 5 = high pressure → the sample does not compress from the force applied and 1 = no pressure → the sample is soft and compresses without additional force applied with tweezers.

Sample	Grade 1 no pressure - 5 high pressure	Comments
Flexbone	1 2 3 4 5 ☐ ☐ ☐ ☐ ☐	
Sample 1	1 2 3 4 5 ☐ ☐ ☐ ☐ ☐	
Sample 2	1 2 3 4 5 ☐ ☐ ☐ ☐ ☐	
Sample 3	1 2 3 4 5 ☐ ☐ ☐ ☐ ☐	
Sample 4	1 2 3 4 5 ☐ ☐ ☐ ☐ ☐	
Sample 5	1 2 3 4 5 ☐ ☐ ☐ ☐ ☐	
Sample 6	1 2 3 4 5 ☐ ☐ ☐ ☐ ☐	

3. Moldability. Shape the sample into “ball-shape” with your fingers. How is the moldability?

Sample	Grade 1 poor 5 excellent	Comments
Flexbone	1 2 3 4 5 ☐ ☐ ☐ ☐ ☐	
Sample 1	1 2 3 4 5 ☐ ☐ ☐ ☐ ☐	
Sample 2	1 2 3 4 5 ☐ ☐ ☐ ☐ ☐	
Sample 3	1 2 3 4 5 ☐ ☐ ☐ ☐ ☐	
Sample 4	1 2 3 4 5 ☐ ☐ ☐ ☐ ☐	
Sample 5	1 2 3 4 5 ☐ ☐ ☐ ☐ ☐	
Sample 6	1 2 3 4 5 ☐ ☐ ☐ ☐ ☐	

4. Consistency. When the sample has been molded into a ball-shape, how would you evaluate the consistency, i.e., does the ball shape hold its shape well when moving the structure with fingers?

Sample	Grade 1 poor 5 excellent	Comments
Flexbone	1 2 3 4 5 ☐ ☐ ☐ ☐ ☐	
Sample 1	1 2 3 4 5 ☐ ☐ ☐ ☐ ☐	
Sample 2	1 2 3 4 5 ☐ ☐ ☐ ☐ ☐	
Sample 3	1 2 3 4 5 ☐ ☐ ☐ ☐ ☐	
Sample 4	1 2 3 4 5 ☐ ☐ ☐ ☐ ☐	
Sample 5	1 2 3 4 5 ☐ ☐ ☐ ☐ ☐	
Sample 6	1 2 3 4 5 ☐ ☐ ☐ ☐ ☐	

5. Coherency. When the sample has been molded into a ball-shape, how would you evaluate the coherency, i.e., how well are the granules sticking together?

Sample	Grade 1 poor 5 excellent	Comments
Flexbone	1 2 3 4 5 ☐ ☐ ☐ ☐ ☐	
Sample 1	1 2 3 4 5 ☐ ☐ ☐ ☐ ☐	
Sample 2	1 2 3 4 5 ☐ ☐ ☐ ☐ ☐	
Sample 3	1 2 3 4 5 ☐ ☐ ☐ ☐ ☐	
Sample 4	1 2 3 4 5 ☐ ☐ ☐ ☐ ☐	
Sample 5	1 2 3 4 5 ☐ ☐ ☐ ☐ ☐	
Sample 6	1 2 3 4 5 ☐ ☐ ☐ ☐ ☐	

6. Second hydration. Place the samples one by one back to the wells with DM-water and try to immediately lift the samples up with tweezers. How well is the sample holding together?

Sample	Grade 1 poor 5 excellent	Comments
Flexbone	1 2 3 4 5 ☐ ☐ ☐ ☐ ☐	
Sample 1	1 2 3 4 5 ☐ ☐ ☐ ☐ ☐	
Sample 2	1 2 3 4 5 ☐ ☐ ☐ ☐ ☐	
Sample 3	1 2 3 4 5 ☐ ☐ ☐ ☐ ☐	
Sample 4	1 2 3 4 5 ☐ ☐ ☐ ☐ ☐	
Sample 5	1 2 3 4 5 ☐ ☐ ☐ ☐ ☐	
Sample 6	1 2 3 4 5 ☐ ☐ ☐ ☐ ☐	

7. Overall experience. How satisfied are you with handling of the sample in general? What would you change to give one grade better for the samples? You can leave comments to the comments section.

- 5 Very satisfied
- 4 Satisfied
- 3 Fair
- 2 Dissatisfied
- 1 Very dissatisfied

Sample	Grade	Comments
Flexbone	1 2 3 4 5 ☐ ☐ ☐ ☐ ☐	
Sample 1	1 2 3 4 5 ☐ ☐ ☐ ☐ ☐	
Sample 2	1 2 3 4 5 ☐ ☐ ☐ ☐ ☐	
Sample 3	1 2 3 4 5 ☐ ☐ ☐ ☐ ☐	
Sample 4	1 2 3 4 5 ☐ ☐ ☐ ☐ ☐	
Sample 5	1 2 3 4 5 ☐ ☐ ☐ ☐ ☐	
Sample 6	1 2 3 4 5 ☐ ☐ ☐ ☐ ☐	

7. Additional thoughts. Did anything particular stand out in any of the samples? Please share your thoughts or ideas in the comment box below.

Sample	Comments
Flexbone	
Sample 1	
Sample 2	
Sample 3	
Sample 4	
Sample 5	
Sample 6	

The study ends here.

Thank you for your participation!

APPENDIX C: RESULTS FROM THE STABILITY STUDIES IN SODIUM ACETATE BUFFER

Table 15. *Summary of the mass loss of samples during immersion in Na-acetate buffer for 200 min.*

Sample	Mass before immersion (mg)	Mass after immersion (mg)	Mass loss (%)
SBSM block 1 (experiment 1)	238.9	237.7	0.50
SBSM block 2 (experiment 1)	240.5	238.5	0.83
SBSM block 3 (experiment 1)	283.3	282	0.46
SBSM block 4 (experiment 1)	259.6	257.8	0.69
SBSM block 5 (experiment 1)	272.8	271.7	0.40
SBSM block 6 (experiment 1)	237.7	236.2	0.63
SBSM block 7 (experiment 2)	286.1	284.7	0.49
SBSM block 8 (experiment 2)	257.3	256.9	0.16
SBSM block 9 (experiment 2)	231.1	230.2	0.39
SBSM block 10 (experiment 2)	250.6	249.9	0.28
SBSM block 11 (experiment 2)	198.6	197.4	0.60
SBSM block 12 (experiment 2)	266.1	265.2	0.34
SBSM block 13, 7 wt% col.	285.9	272.3	4.76
SBSM block 14, 7 wt% col.	292.7	280.5	4.16
SBSM block 15, 3 wt% col.	299.7	282.4	5.77
SBSM block 16, 3 wt% col.	309.9	285.7	7.81
SBSM granula, 7 wt% col.	525	500	4.76
SBSM granula, 7 wt% col.	472	452.2	4.19

Table 16. *Summary of changes in conductivity of Na-acetate buffer during 200 min immersion as mean (n=3) for SBSM blocks (experiments 1 and 2) and mean (n=2) for other samples with standard deviation as error.*

Time (min)	SBSM blocks, experiment 1	SBSM blocks, experiment 2	SBSM granula with 7 wt% collagen	SBSM blocks with 7 wt% collagen	SBSM blocks with 3 wt% collagen
0	458.76 ± 6.96	490.40 ± 0	463.76 ± 7.07	453.756 ± 7.07	490.40 ± 0
1	472.32 ± 10.55	480.27 ± 6.04	737.16 ± 10.72	1915.78 ± 14.14	1099.70 ± 257.22
10	559.75 ± 14.11	564.20 ± 8.53	1727.80 ± 121.11	5278.17 ± 70.71	3132.46 ± 411.71
20	598.32 ± 22.15	590.34 ± 9.55	2320.57 ± 89.72	5777.54 ± 72.54	3403.60 ± 243.89
60	663.51 ± 75.22	607.67 ± 2.24	3003.18 ± 72.11	6217.09 ± 64.82	3471.45 ± 178.63
120	675.89 ± 73.51	607.67 ± 5.70	4077.96 ± 100.22	6666.98 ± 62.4	3516.04 ± 178.65
200	708.06 ± 72.61	629.42 ± 11.69	4623.27 ± 4.23	6744.54 ± 32.35	3508.31 ± 191.72

Table 17. *Summary of changes in pH of Na-acetate buffer during 200 min immersion shown as mean (n=3) for SBSM blocks (experiments 1 and 2) and mean (n=2) for other samples with standard deviation as error.*

Time (min)	SBSM blocks, experiment 1	SBSM blocks, experiment 2	SBSM granula with 7 wt% collagen	SBSM blocks with 7 wt% collagen	SBSM blocks with 3 wt% collagen
0	5.44 ± 0	5.44 ± 0	5.44 ± 0	5.44 ± 0	5.44 ± 0
1	5.52 ± 0.01	5.51 ± 0.02	6.88 ± 0.13	7.07 ± 0.02	6.99 ± 0.05
10	6.17 ± 0.04	6.13 ± 0.03	7.09 ± 0.00	7.09 ± 0.05	7.19 ± 0.02
20	6.48 ± 0.05	6.39 ± 0.08	7.1 ± 0.01	7.08 ± 0.02	7.2 ± 0.04
60	6.77 ± 0.04	6.80 ± 0.07	7.12 ± 0.09	7.1 ± 0.01	7.23 ± 0.05
120	7.22 ± 0.03	7.27 ± 0.09	7.13 ± 0.08	7.09 ± 0.02	7.23 ± 0.01
200	10.14 ± 0.11	9.54 ± 0.42	7.1 ± 0.02	7.08 ± 0.08	7.26 ± 0.03

APPENDIX D: RESULTS FROM DEGRADATION STUDIES IN HBSS

***Table 18**. Changes in conductivity during the degradation studies in HBSS shown as average (n=3) and standard deviation.*

Time (h) / conduc-tivity (µS/cm)	SBSM block	SBSM block + 7 wt% col	SBSM granula + 7 wt% col.	SBSM granula + 7 wt% col. + HA + Chi	SBSM granula + 3 wt% col. (DI)	SBSM granula + 3 wt% col. + HA	7 wt% col.
0	14575.3	14575.3	14575.3	14575.3	14575.3	14575.3	14575.3
0.5	14693.5	15037.8	15178.2	14984.0	15101.2	15154.1	16063.1
1	14974.4	15425.0	15346.1	15200.6	15073.3	15166.1	16421.6
3	15407.6	15755.6	15973.2	15750.0	15557.0	15366.3	16999.4
6	15438.1	15863.5	16112.5	15741.2	15592.4	15313.9	16999.4
48	15451.9	16365.0	16592.6	16316.5	16029.8	15661.6	17201.9
168	15378.9	16268.7	17103.1	16093.3	15770.3	15538.3	17248.9
336	15564.2	16690.5	17084.5	16245.7	15970.4	15783.9	17164.9
504	15677.6	16749.1	17070.9	16481.0	16099.9	15756.1	17376.5
672	15286.2	16248.0	17010.6	16266.6	15997.0	15600.2	17402.7
Standard deviation							
0.5	222.97	270.06	127.51	130.13	132.23	127.29	142.51
1	186.87	216.80	56.09	28.71	121.15	242.75	113.78
3	28.32	387.15	456.48	134.32	162.73	303.21	111.30
6	22.44	382.38	359.16	203.96	185.49	378.82	517.26
48	128.57	82.98	102.70	257.40	66.16	34.33	231.73
168	306.81	207.91	245.07	79.54	226.83	133.81	203.64
336	62.16	171.85	352.60	36.80	123.06	60.30	428.29
504	13.70	71.52	208.99	223.23	74.29	39.66	181.46
672	157.11	133.87	299.72	170.78	291.44	305.93	661.26

***Table 19**. Changes in pH-value during the degradation studies in HBSS shown as average (n=3) and standard deviation.*

Time (h) / pH	SBSM block	SBSM block + 7 wt% col	SBSM granula + 7 wt% col.	SBSM granula + 7 wt% col. + HA + Chi	SBSM granula + 3 wt% col. (DI)	SBSM granula + 3 wt% col. + HA	7 wt% col.
0	7.42	7.42	7.42	7.42	7.42	7.42	7.42
0.5	7.52	7.24	7.24	7.24	7.40	7.32	7.07
1	7.55	7.16	7.16	7.16	7.28	7.31	7.08
3	7.80	7.23	7.24	7.18	7.27	7.36	7.06
6	8.00	7.28	7.28	7.21	7.31	7.46	7.08
48	8.00	7.15	7.19	7.19	7.34	7.44	7.05
168	8.44	7.10	7.13	7.01	7.31	7.35	6.95
336	8.50	7.01	7.08	6.99	6.97	7.03	6.88
504	8.63	6.83	7.00	6.72	6.89	6.76	6.85
672	8.55	6.82	6.91	6.72	6.80	6.67	6.85
Time (h) / Standard deviation							
0.5	0.01	0.06	0.06	0.06	0.04	0.01	0.01
1	0.01	0.05	0.05	0.09	0.09	0.02	0.02
3	0.03	0.03	0.01	0.10	0.10	0.05	0.015
6	0.01	0.03	0.01	0.04	0.05	0.04	0.02
48	0.02	0.02	0	0.03	0.06	0.01	0.01
168	0.06	0.01	0.01	0.01	0.01	0.13	0
336	0.05	0.01	0.03	0	0.01	0.02	0.08
504	0.01	0.04	0.01	0.01	0.03	0.18	0.02
672	0.04	0.05	0.03	0.04	0.11	0.19	0.01

Table 20. *Mass loss (%) during the degradation studies in HBSS shown as average (n=3) and standard deviation.*

Time (h) / mass loss (%)	SBSM block + 7 wt% col	SBSM granula + 7 wt% col.	SBSM granula + 7 wt% col. + HA + Chi	SBSM granula + 3 wt% col. (DI)	SBSM granula + 3 wt% col. + HA	7 wt% col.
6	4.37	6.38	2.75	1.43	1.60	45.68
48	5.62	7.26	4.61	2.37	2.22	65.24
168	10.29	15.85	9.55	16.68	13.71	100.00
336	10.44	12.27	28.35	47.31	56.12	100.00
504	10.78	16.87	29.42	79.48	46.25	100.00
672	11.83	35.49	49.07	55.36	65.36	100.00
Time (h) /Standard deviation						
6	1.20	3.80	1.32	0.57	0.26	4.60
48	0.43	1.83	0.87	0.85	0.70	14.20
168	1.92	7.98	2.55	11.56	8.74	0.00
336	1.73	9.83	13.36	18.04	7.26	0.00
504	0.57	4.11	11.32	17.90	4.25	0.00
672	1.54	6.22	13.42	19.22	4.22	0.00